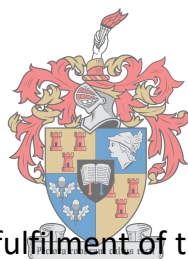


Development of a Multiple Fractionation Protocol for the Comprehensive Analysis of Low Density Polyethylene

by

Paul Severin Eselem Bungu



Dissertation presented in partial fulfilment of the requirements for the degree of
Doctor of Philosophy (PhD) in Polymer Science

UNIVERSITEIT
iYUNIVESITHI
STELLENBOSCH
UNIVERSITY

at the

100
1918 · 2018

University of Stellenbosch

Promoter: Prof. Harald Pasch

December 2018

DECLARATION

By submitting this thesis electronically, I, Paul Severin Eselem Bungu declare that the entirety of the work contained therein is my own, original work, that I am the authorship owner thereof (unless to the extent explicitly otherwise stated) and that I have not previously in its entirety or in part submitted it for obtaining any qualification.

Date: December 2018

Signature of Candidate:.....

Copyright © 2018 Stellenbosch University

All rights reserved

Declaration for the Publications

I, Paul Severin Eselem Bungu further declare that the research papers titled:

1. Comprehensive Analysis of Branched Polyethylene: The Multiple Preparative Fractionation Concept (P. S. Eselem Bungu and H. Pasch, *Polym. Chem.*, 2017, 8, 4565–4575.),
2. Branching and Molar Mass Analysis of Low Density Polyethylene Using the Multiple Preparative Fractionation Concept (P. S. Eselem Bungu and H. Pasch, *Polym. Chem.*, 2018, 9, 1116–1131),
3. Combination of Preparative and Two-Dimensional Chromatographic Fractionation with Thermal Analysis for Branching Analysis of Polyethylene (P. S. Eselem Bungu, K. Pflug and H. Pasch, *Polym. Chem.*, 2018, 9, 3142–3157),
4. Comprehensive Analysis of Novel Grafted Polyethylenes Using Multidimensional Fractionation Methods (P. S. Eselem Bungu, K. Pflug, M. Busch and H. Pasch, *Polym. Chem.*, 2018, 9, 5051–5065)

submitted in this dissertation is based on actual and original work carried out by me. I further certify that these research papers have not been submitted and will not be submitted for obtaining any other qualification.

The author and co-authors listed in the manuscripts submitted in this dissertation made the following contributions:

Name	Email address	Nature of contribution	Contribution (%)
Candidate			
Paul Severin Eselem Bungu	paulbunu@sun.ac.za paul.bunu@gmail.com	Experimental work Data analysis Discussion of result Write-up the manuscripts Address reviewers comments	86
Co-author			
Kristina Pflug	kristina.pflug@pre.tu-darmstadt.de	Synthesis of the grafted polymers SEC-triple detection analysis	2
Markus Busch	markus.busch@pre.tu-darmstadt.de	Provided the grafted samples	2
Harald Pasch	hpasch@sun.ac.za	Supervision and mentoring Revision and correction of manuscript	10

Signature of Candidate:

Date:.....

Declaration by co-authors:

1. The declaration above accurately reflects the nature and extent of the contributions of the candidate and co-authors to the four manuscripts in this dissertation,
2. No other authors contributed to the four manuscripts in the dissertation besides those specified above, and
3. Potential conflicts of interest have been revealed to all interested parties and that the necessary arrangements have been made to use the materials in the four manuscripts in this dissertation.

Signature	Institutional Affiliation	Date
Declaration with signature in possession of candidate and supervisor	Technical University Darmstadt	
	Stellenbosch University	

Acknowledgments

I would like to express my heartfelt appreciation to the following people and institutions for their contribution towards the completion of this study:

- ❖ Firstly to **Prof. Harald Pasch**, my supervisor and mentor for providing me with the opportunity to study at this prestigious university. His continued guidance and mentorship have convincingly conveyed the spirit of adventure into research. I will remain indebted to him for the financial support and endless devotion to seeing that this project is realized.
- ❖ Special thanks go to my humble colleagues and friends **Dr. Anthony Ndiripo** and **Dr. Mohau Justice Phiri** for providing me with the training needed to operate the analytical instruments. Their willingness to be engaged in constructive discussions about data interpretations is highly appreciated.
- ❖ **Prof. Markus Busch** and **Dr. Kristina Pflug** for kindly supplying the grafted samples. Their invaluable contribution to the GPC-triple detection experiments and meaningful discussions will forever be remembered.
- ❖ The members of the **Pasch research group** for their input during group presentations and functions. Your contributions to the success of this project are highly appreciated.
- ❖ **Dr. Jaco Brand** and **Elsa Malherbe** of the NMR lab for their assistance in NMR data acquisition. Your input provided the basis of this research and I am thankful for that.
- ❖ The technical staff, **Mr Doen Koen**, **Mr Jim Motsweni** and **Mr Calvin Maart**, and the administrative staff **Mrs Erinda Cooper** and **Mrs Aneli Fourie**, for their hard work and support in ensuring the smooth running of this project.
- ❖ **Prof. Albert van Reenen** and the members of the **van Reenen research group** for accommodating me into their laboratory space, which has provided the platform to conduct meaningful research.
- ❖ **Dr. Divane Roberson** for training me on the SCALLS instruments and assisting me in designing the experimental procedure used for the SSA measurements, as well as translating the abstract. Your willingness in helping me is highly appreciated.
- ❖ My sincere gratitude goes to **Dr. Jonathan Molefi** for advising me into pursuing a career in Polymer Science, **Dr. Ruben Pfukwa** and **Prof. Brownhilder Neneh** for refereeing my bursary applications. Your inputs are highly appreciated.

ACKNOWLEDGMENTS

- ❖ My Family: my Parent; **Dr. Peter Ndula Bungu, Adieh Elomba Marguerite** and **Kuvin Florence Ntuchu**; My sibling; **Ikeh Tracy, Joyce Subin-Bih, Muluh Blessed-white**, and **Fanwi Jesse** for their continued love and support throughout this Journey.
- ❖ My daughter **Tyler Adieh-Kuvin** and her mother **Mmakopi Kgeogelo Phogole** for their love and support showed to me throughout these years.
- ❖ SASOL South Africa for providing the LDPE samples.
- ❖ I would also like to thank Sasol South Africa and the South Africa National Research Fund (NRF) for the financial support.
- ❖ All friends and family for the encouragement and motivation.
- ❖ I also like to acknowledge all those who have helped me directly or indirectly in the successful completion of this study. Your contributions are highly appreciated.
- ❖ Finally, I would like to thank **GOD** Almighty for the wisdom bestowed on me and the spiritual guidance provided throughout this life-learning journey.

C onference Proceedings

Aspects of this work were presented at the following conferences:

Conference Oral presentations:

- ❖ PS Eselem Bungu and Harald Pasch. Selectivity of Thermal Fractionation for the Analysis of Low Density Polyethylene: 7th International Conference For Polyolefins Characterization (ICPC) October 2018, Houston, Texas, USA.
- ❖ PS Eselem Bungu and Harald Pasch. Comprehensive Analysis of Branched Polyethylene: The Multiple Preparative Fractionation Concept. PISA Annual International Conferences and Golf Day, November 2017, Spier Wine Estate, Stellenbosch, South Africa.
- ❖ PS Eselem Bungu and Harald Pasch. Preparative Molar Mass Fractionation (MMF) Approach for the Analysis of Branched Polyethylene. 30th International Symposium on Polymer Characterization (ISPAC) June 2017, Johannes Kepler University, Linz, Austria.
- ❖ PS Eselem Bungu and Harald Pasch. Multidimensional Analytical Methods for Branched Polyethylene Homopolymer. Newton Fund International PhD Partnering Scheme Mini-Conference, September 2016, Stellenbosch University, Stellenbosch, South Africa

Conference Poster Presentations:

- ❖ PS Eselem Bungu and Harald Pasch. Preparative Fractionation Approach for Branched Polyethylene Analysis. 30th International Symposium on Polymer Characterization (ISPAC) June 2017, Johannes Kepler University, Linz Austria.
- ❖ PS Eselem Bungu and Harald Pasch. LDPE Microstructure Analysis Using Multidimensional Analytical Protocols. Sasol University Research Seminar, November 2017, SASOL Head Office, Johannesburg, South Africa.

A bstract

Low density polyethylene (LDPE) is a branched synthetic thermoplastic with a complex microstructure. In addition to the broad molar mass distribution (MMD), LDPE exhibits long chain branching (LCB) and short chain branching (SCB). Both LCB and SCB are statistically distributed across different polymer chains of varying molar masses, thus providing broad distributions in molar mass and branching. This interrelated MMD and branching distribution (BD) influences the end-use properties and, therefore, the applications. To be able to design new materials, comprehensive structure-property relationships must be established. To this aim, the microstructural parameters (MMD and BD) must be measured quantitatively and related to the thermophysical properties.

In the current study, the microstructure of different branched polyethylenes was investigated. The quantification and determination of MMD was achieved by multidetector size exclusion chromatography (SEC). The branch types and branching contents were quantitatively measured using carbon-13 nuclear magnetic resonance spectroscopy (^{13}C NMR). As an alternative and complementary method, SEC was coupled to an infrared detector to measure total branching and BD as a function of molar mass. LCB distributions were measured as a function of molar mass by SEC coupled to multiangle laser light scattering (MALLS).

Branching information as a function of crystallizability was obtained by crystallization analysis fractionation (CRYSTAF), solution crystallization analysis by laser light scattering (SCALLS) and differential scanning calorimetry (DSC). Chain branching was also measured by high-temperature solvent gradient interactive chromatography (HT-SGIC). The effects of BD and MMD on the thermophysical behaviour were investigated by observing the crystallization and melting behaviour using DSC. Thermal properties to a large extent determine the processing properties of a given material.

In the first part of this work, a multiple preparative fractionation concept was developed and used for the comprehensive characterization of LDPE. Narrowly dispersed molar mass and branching fractions were obtained using preparative molar mass fractionation (pMMF) and preparative temperature rising elution fractionation (pTREF) techniques, respectively. The molar mass and branching information were obtained by analysing the separated fractions using advanced analytical techniques. Cross-correlation of molar mass and branching was obtained by combining pTREF and pMMF results with SEC and CRYSTAF to construct 2D images of molar mass vs. branching.

ABSTRACT

In the second part of the work, the multiple fractionation concept was used to investigate the microstructural differences between different LDPE samples. With the help of pTREF and pMMF, fractions with narrow molar mass and branching were generated. The fractions were analysed for branching and molar mass and cross-fractionation plots highlighted the microstructural differences between the samples. From the preparative fractions having broad molar mass and branching ranges, libraries were obtained with samples (1) having similar molar masses but different degrees of branching and, alternatively, (2) having different molar masses but similar degrees of branching. These library samples were analysed by CRYSTAF, SGIC, and multidetector SEC to investigate the effects of branching and molar masses on thermal properties.

In the third part of this study, the multiple preparative fractionation concept was used to generate samples with similar molar mass/varying branching (pTREF) and similar branching/varying molar mass (pMMF). The library samples and bulk resins were analysed by DSC and thermal fractionation by successive self-nucleation and annealing (SSA) to provide information regarding crystal sizes and crystal size distributions. From the SSA results, methylene sequence length distribution (MSLD) plots were constructed providing information that was directly related to the branching and branching heterogeneity of these samples.

In the last part of this study, the molecular structure of novel grafted polymers HDPE-g-LDPE and their linear and branched PE references was investigated. Fractionations were conducted by pTREF to generate fractions with varying degrees of branching and/or grafting. The cross-correlation techniques (TREF-SEC and TREF-CRYSTAF) were used to compare the grafting products. In addition, 2D-LC experiments were conducted to correlate branching/grafting to molar mass.

Opsomming

Lae digtheid poliëtileen (LDPE) is 'n vertakte sintetiese termoplastiek met 'n komplekse mikrostruktuur. Benewens die breë molêre massa verspreiding (MMD), vertoon LDPE lang ketting vertakking (LCB) en kort ketting vertakking (SCB). Beide LCB en SCB word statisties versprei oor verskillende polimeerkettings van wisselende molêre massas, wat sodoende breë verspreidings in molêre massa en vertakking bied. Hierdie interafhanklike MMD en vertakkingsverspreiding (BD) beïnvloed die finale eienskappe en dus die toepassings. Om nuwe materiale te kan ontwerp, moet omvattende struktuur-eienskap verhoudings gevestig word. Vir hierdie doel moet die mikrostruktuur parameters (MMD en BD) kwantitatief gemeet word en verband hou met die termofisiese eienskappe. In die huidige studie was die mikrostruktuur van verskillende vertakte poliëtileen ondersoek. Die kwantifisering en bepaling van MMD is gedoen deur multidetektor grootte-uitsluitings chromatografie (SEC). Die vertakkingstipe en vertakkingsinhoud is kwantitatief gemeet met behulp van koolstof-13 kern magnetiese resonans spektroskopie (^{13}C NMR). As 'n alternatiewe en komplementêre metode was SEC gekoppel aan 'n infrarooi detektor om totale vertakking en BD as 'n funksie van molêre massa te meet. LCB verspreidings was gemeet as 'n funksie van molêre massa deur SEC te koppel aan multihoek laser lig verstrooiing (MALLS).

Vertakkingsinligting as 'n funksie van kristallisasie was verkry deur kristallisasie analise fraksionering (CRYSTAF), oplossing kristallisasie-analise deur laserligverstrooiing (SCALLS) en differensiële skanderingskalorimetrie (DSC). Kettingvertakking was ook gemeet deur hoë-temperatuur oplosmiddel-gradiënt interaktiewe chromatografie (HT-SGIC). Die effek van BD en MMD op die termofisiese gedrag was ondersoek deur die kristallisasie- en smeltgedrag met DSC waar te neem. Termiese eienskappe bepaal tot 'n groot mate die verwerkingseienskappe van 'n gegewe materiaal.

In die eerste deel van hierdie werk was 'n veelvoudige preparatiewe fraksionerings konsep ontwikkel en gebruik vir die omvattende karakterisering van LDPE. Smal verspreide molêre massa en vertakkingsfraksies was verkry deur onderskeidelik preparatiewe molêre massa fraksionering (pMMF) en preparatiewe temperatuurstyging elueringsfraksionering (pTREF) tegnieke. Die molêre massa en vertakkingsinligting was verkry deur die geskeide fraksies te analiseer met gebruik van gevorderde analitiese tegnieke. Kruiskorrelasie van molêre massa en vertakking was verkry deur pTREF en pMMF resultate te kombineer met SEC en CRYSTAF om 2D-beelde van molêre massa teen vertakking te konstrueer.

OPSOMMING

In die tweede deel van die werk was die veelvoudige fraksioneringskonsep gebruik om die mikrostruktuurverskille tussen verskillende LDPE monsters te ondersoek. Met behulp van pTREF en pMMF was fraksies met nou molêre massa en vertakking verkry. Die fraksies was geanaliseer vir vertakking en molêre massa en kruis-fraksioneringskurwes het die mikrostruktuurverskille tussen die monsters uitgewys. Uit die preparatiewe fraksies met breë molêre massa en vertakkingsreeks was biblioteke verkry van monsters (1) met soortgelyke molêre massas, maar verskillende grade van vertakking en alternatiewelik (2) met verskillende molêre massas, maar soortgelyke grade van vertakking. Hierdie biblioteekmonsters was met behulp van CRYSTAF, SGIC en multidetektor SEC ontleed om die effek van vertakking en molêre massas op termiese eienskappe te ondersoek.

In die derde deel van hierdie studie was die veelvoudige preparatiewe fraksioneringskonsep gebruik om monsters met soortgelyke molêre massa/wisselende vertakking (pTREF) en soortgelyke vertakking/wisselende molêre massa (pMMF) te verkry. Die biblioteekmonsters en grootskaalmonsters was geanaliseer deur DSC en termiese fraksionering deur opeenvolgende selfkernvorming en “annealing” (SSA) om inligting oor kristalgroottes en kristalgrootte verspreiding te verskaf. Metileen-reekslengte distribusiekurwes (MSLD) was opgestel vanuit die SSA resultate wat inligting verskaf het wat direk verband hou met die vertakking en vertakking heterogeniteit van hierdie monsters.

In die laaste gedeelte van hierdie studie was die molekulêre struktuur van nuwe “ent” polimere HDPE-g-LDPE en hul lineêre en vertakte PE verwysings ondersoek. Fraksionering was met pTREF uitgevoer om fraksies met verskillende grade van vertakking en/of “enting” te genereer. Die kruis-korrelasietegnieke (TREF-SEC en TREF-CRYSTAF) was gebruik om die “entings” produkte te vergelyk. Daarbenewens was 2D-LC eksperimente uitgevoer om die vertakking/“enting” met molêre massa te korreleer.

C contents

Declarations	i
Abstract.....	iii
Opsomming.....	v
Acknowledgements.....	vii
Conference Proceedings	ix
Content	x
List of Figures	xi
List of Symbols and Abbreviations	xii
1 Introduction and Aim of Study.....	1
1.1 Introduction	1
1.2 Research Question and Aim of Study	2
1.3 Research Objectives and Thesis Outline	3
1.4 References	4
2 Literature Review	7
2.1 Early Discovery of Polyethylene.....	7
2.2 Classes of Polyethylene.....	7
2.3 Free Radical Polymerization of Ethylene	9
2.4 The Microstructure of Branched Polyethylene	11
2.5 Advanced Characterization of Polyolefins	14
2.6 References	20
3 Comprehensive Analysis of Branched Polyethylene: The Multiple Preparative Fractionation Concept	23
4 Branching and Molar Mass Analysis of Low Density Polyethylene Using the Multiple Preparative Fractionation Concept.....	35
5 Combination of Preparative and Two-Dimensional Chromatography Fractionation with Thermal Analysis for Branching Analysis of Polyethylene	52
6 Comprehensive Analysis of Novel Grafted Polyethylene Using Multiple Fractionation Methods.....	71
7 Concluding Remarks.....	88

List of Figures

Figure 1: Schematic representation of HDPE (a), LLDPE (b) and LDPE (c).	8
Figure 2: Elementary reactions in the free radical homopolymerization of ethylene to low density polyethylene (modified from reference 14).	10
Figure 3: Morphology of a highly and sparsely branched LDPE molecule produced using (a) an autoclave reactor or higher temperature and (b) a tubular reactor or higher pressure.	11
Figure 4: Schematic morphological representation of the molecular structure and microstructural distribution of branched PE (LDPE).	13
Figure 5: Schematic presentation of the LEGO approach in the analysis of complex polyolefins (reproduced from ref 25)	15
Figure 6: Schematic representation of the TREF process, showing in (a) the crystallization step and (b) the elution step.	16
Figure 7: 3D plot obtained by combining TREF and SEC to obtain a bivariate distribution of polyolefin resins.	18
Figure 8: Diagram showing the variation in molar mass and branching of the (a) MMF and (b) TREF fractions	19
Figure 9: The multiple preparative fractionation: the concept versus the experiment.....	23
Figure 10: The multiple preparative fractionation concept provides sample libraries with different degrees of branching and different molar masses that are analysed regarding the LDPE microstructure	35
Figure 11: Multiple preparative fractionation of LDPE provides molar mass and branching fractions that were analysed regarding their thermal properties.	52
Figure 12: Chain heterogeneity in novel grafted polyethylene.	69

List of Symbols and Abbreviations

α	Mark-Houwink exponent
\bar{D}	Dispersity index
$[\eta]$	Intrinsic viscosity
dn/dc	Specific refractive index increment
^{13}C NMR	Carbon-13 nuclear magnetic resonance
BD	Branching distribution
BHT	2,6-d-tert-butyl-4-methylphenol
C1	Methyl branch
C2	Ethyl branch
C4	Butyl branch
C5	Amyl branched
C6	Hexyl branch
CCD	Chemical composition distribution
CEF	Crystallization elution fractionation
\bar{C}_n	Arithmetic mean methylene sequence length
CRYSTAF	Crystallization analysis fractionation
CSD	Crystal size distribution
CSTR	Continuously stirred tank reactor
CTA	Chain transfer agent
\bar{C}_w	Weighted mean methylene sequence length
$\bar{C}_w/\bar{C}_n, I_c$	Methylene sequence broadness index
DRI, RI	Differential refractive index
DEGMME	Diethylene glycol monomethyl ether
DSC	Differential scanning calorimetry
ELSD	Evaporation light scattering detector
FTIR	Fourier transform infrared
FRP	Free radical polymerization
g'	Branching index
K	Mark-Houwink parameter
ICI	Imperial Chemical Industries
IR	Infrared
LCB	Long chain branching
LCBD	Long chain branching distribution
LCBf, m	Long chain branching frequency
LDPE	Low density polyethylene
LLDPE	Linear low density polyethylene
\bar{L}_n	Arithmetic mean lamellar thickness
LS	Light scattering
\bar{L}_w	Weighted mean lamellar thickness
$\bar{L}_w/\bar{L}_n, I_l$	Lamellar thickness broadness index
HDPE	High density polyethylene
HDPE-g-LDPE	High density polyethylene grafted low density polyethylene
HPLC	High performance liquid chromatography
HT-2D-LC	High temperature two-dimensional liquid chromatography
HT-HPLC	High temperature high performance liquid chromatography
HT-SGIC	High temperature solvent gradient interactive chromatography
HT-SEC	High temperature size exclusion chromatography

LIST OF SYMBOLS AND ABBREVIATIONS

MALLS	Multiangle laser light scattering
MFI	Melt flow index
MMD	Molar mass distribution
MMF	Molar mass fractionation
M_n	Number-average molar mass
MSL	Methylene sequence length
MSLD	Methylene sequence length distribution
M_w	Weight-average molar mass
PE	Polyethylene
PP	Polypropylene
TREF	Temperature rising elution fractionation
pTREF	Preparative temperature rising elution fractionation
pMMF	Preparative molar mass fractionation
R_h	Hydrodynamic radius
R_g	Radius of gyration
SCALLS	Solution crystallization analysis by laser light scattering
SCB	Short chain branching
SCBD	Short chain branching distribution
SEC	Size exclusion chromatography
SC	Step crystallization
SGF	Solvent gradient fractionation
SHF	Super high frequency
SR	Solvent ratio
SSA	Successive self-nucleation and annealing
T	Temperature
TFA	Turbidity fractionation analysis
TCB	1,2,4-trichlorobenzene
TCE-d ₂	Deuterated 1,1,2,2-tetrachloroethane
T_c	Crystallization temperature
T_d	Dissolution temperature
T_m	Melting temperature
UHF	Ultra-high frequency
V_e	Elution volume
Visco, Vis	Viscometer
Wt %	Weight percent
X_c	Crystallinity

1 Introduction and Aim of Study

1.1 Introduction

The purpose of this research is to develop advanced analytical methods for the comprehensive characterization of branched polyethylene (PE) also known as low density polyethylene (LDPE). Despite being a homopolymer, branched PE exhibits a complex microstructure and is best known for its unique combination of long chain branching (LCB) and short chain branching (SCB) in addition to the broad molar mass distribution (MMD).¹⁻⁷ These molecular characteristics are responsible for the excellent processing and film forming properties. The molecular complexity of LDPE stems from the fact that branched macromolecules are produced by radical polymerization processes and different polymer resins are designed through different polymerization conditions such as different reactor types (autoclave or tubular), reactor shapes (square or narrow shape autoclave), by varying reactor temperature and pressure, as well as using different initiators.⁵⁻⁸

For polyolefins with broad chemical composition distributions (CCD), specific fractionation techniques have been developed that provide quantitative information on CCD. Temperature rising elution fractionation (TREF)⁹⁻¹⁶, crystallization analysis fractionation (CRYSTAF)^{9,14,17,18}, crystallization elution fractionation (CEF)^{17,19-21}, solution crystallization by laser light scattering (SCALLS)^{9,22-24} and differential scanning calorimetry (DSC)^{25,26} are different techniques designed to fractionate polyolefins according to crystallizability. Thermal fractionation protocols such as successive self-nucleation and annealing (SSA) and stepwise crystallization (SC) have been developed using DSC instruments to segregate polymer chains according to crystal size and tacticity.²⁷⁻³¹ Most recently, high temperature solvent gradient interactive chromatography (HT-SGIC), or in more general terms, high performance liquid chromatography (HT-HPLC), was introduced and is used to fractionate polyolefins according to linear ethylene sequences.^{17,32-36}

Carbon-13 nuclear magnetic resonance (¹³C NMR) spectroscopy is a technique with potential to specifically identify types of branches which are categorized into SCB (methyl, C1, to amyl, C5) and LCB (hexyl, C6, and longer).³⁷⁻⁴¹ This technique has been widely used to determine and quantify branching in polyethylene but is limited to providing average information on the number of branches in a bulk sample and not the branching distribution. As an alternative technique, Fourier transform infrared spectroscopy (FTIR) has been used for decades to study branching in polyethylene-1-olefin copolymers and branched PE.⁴²⁻⁴⁵

INTRODUCTION AND AIM OF STUDY

For the analysis of MMD of polyolefins, high temperature size exclusion chromatography (SEC) has been used to separate molecular species on the basis of their hydrodynamic volumes.⁴⁶⁻⁴⁹ When using an infrared (IR) or a differential refractive index (DRI) detector for concentration detection, with the help of a calibration function relative molar masses are obtained. Alternatively, molar mass sensitive detectors such as multiangle laser light scattering (MALLS) and online viscometer detectors are adapted after the SEC column for absolute molar mass measurements.^{46,49-51}

Even though these analytical techniques provide detailed microstructural information on complex polyolefins, they also face the following challenges: (1) smaller components may remain undetected due to low concentration and (2) individual techniques are unable to address the correlation effect between molar mass and branching. The first approach in addressing such challenges is to conduct fractionations in preparative scale, which provide fractions in mg to gram amounts that can be analyzed using other conventional and advanced analytical techniques.^{52,53} For this purpose, preparative TREF has been intensively used to fractionate polyolefin resins to obtain fractions with varying crystallizabilities, which are directly related to varying branching contents.^{11,29,54,55} Preparative solvent gradient fractionation (SGF)⁵² and preparative molar mass fractionation (MMF)⁵³ are preparative fractionation methods that provide fractions that vary in molar mass. Preparative TREF has been combined with SEC offline as in cross-fractionation to provide 2D images correlating branching and molar mass.⁵⁶ The second approach is through hyphenation, whereby a molar mass sensitive technique is inline with a detector that is sensitive towards branching or is combined online with another technique.^{17,57} SEC has been combined with FTIR or flash DSC through the LC transform interface to provide branching or crystallization distribution as a function of molar mass.^{11,58}

Hyphenated techniques have been developed through combining SEC with three different detectors including IR^{59,60} to provide methyl contents and MALLS/viscometer to provide LCB information, respectively, as a function of molar mass. Other hyphenated techniques include the combination of TREF/HPLC with SEC, which helps in addressing the interrelation between molar mass and branching.^{35,61,62}

1.2 Research question and aim of study

Polyolefin characterisation has been an intriguing research area for many years. This research area has led to the development of several analytical techniques capable of addressing the structure-property relationships of complex polyolefins. Currently, no suitable fractionation method is able to address branching distribution in LDPE without the interference of molar mass distribution, even though there is a strong need to understand the differences in the branching structure in branched PE

INTRODUCTION AND AIM OF STUDY

resins. The present research aims at developing such methods that are capable of addressing branching in LDPE irrespective of the molar mass effect, which is key to the understanding of the mechanical and processing properties of these complex molecules. In particular, a multiple preparative fractionation approach shall be developed that will be able to address the multiple molecular distributions in branched PE. Such fractionation protocol would initiate further broadly based research on the molecular structure of complex polyolefins.

1.3 Research Objectives and thesis outline

To conduct comprehensive analyses of branched polyethylenes, the molecular structure of a set of branched polyethylene resins provided by SASOL, South Africa, shall be investigated following the objectives as stated below:

- i. Use a representative LDPE resin and develop a multiple preparative fractionation concept. This concept is based on fractionating the resin into narrow dispersed molar mass and branching fractions that can be further analysed using advanced analytical methods.
- ii. Use the multiple preparative fractionation concept to address the microstructural differences between branched PE exhibiting similar bulk properties but differ in their melt flow index (MFI). The multiple preparative fractionation concept shall be used to obtain fraction/sample libraries with different molar masses and branching contents. These libraries will help to selectively address the effect of molar mass and branching on the behaviour of the branched polyethylene resins.
- iii. Use the multiple preparative fractionation concept in combination with thermal and chromatographic fractionation techniques to address branching in LDPE.
- iv. Evaluate the multiple preparative fractionation concept to obtain microstructural information and degree of grafting for novel grafted polyethylenes which are produced by grafting LDPE onto a high density polyethylene (HDPE) backbone to form HDPE-g-LDPE.

In **Chapter 1**, introductory information on the molecular structure of branched polyethylene is presented along with suitable techniques used for polyolefin characterization, in addition to the problem statement, the aim and the objectives of this research.

In **Chapter 2**, some historical background on polyethylene along with a brief summary introducing the different types of polyethylene is presented. Detailed literature on branched polyethylene in terms of its molecular complexity is covered here. This chapter provides in-depth knowledge of the various characterization techniques available for the analysis of polyolefins.

INTRODUCTION AND AIM OF STUDY

In **Chapter 3**, the multiple preparative fractionation concept for the analysis of branched polyethylene is developed.

In **Chapter 4**, three LDPE resins having different melt flow indexes are analysed for branching using the multiple preparative fractionation protocol established in Chapter 3. Fraction libraries constituting fractions with narrow molar mass and branching distributions are obtained and are used to evaluate the effect of branching and molar mass on the materials behaviour.

In **Chapter 5**, the multiple preparative fractionation technique is used in combination with thermal and chromatographic fractionation to address branching in a commercial branched polyethylene.

In **Chapter 6**, preparative TREF is combined with other analytical and hyphenated methods to analyse the degree of branching/grafting in novel grafted polyethylenes. The molecular structures of the grafted polymers are compared to reference materials that were produced under similar conditions as starting materials of the grafted product.

It should be noted that the work reported in **Chapters 3 to 6** is published

In **Chapter 7**, the outcome of the research and concluding remarks are summarized.

1.4 References

- 1 M. E. A. Cudby and A. Bunn, *Polymer*, 1976, **17**, 345–347.
- 2 D. E. Axelson, G. C. Levy and L. Mandelkern, *Macromolecules*, 1979, **12**, 41–52.
- 3 J. N. Hay, P. J. Mills and R. Ognjanovic, *Polymer*, 1986, **27**, 677–680.
- 4 D. E. Axelson and K. E. Russell, *Prog. Polym. Sci.*, 1985, **11**, 221–282.
- 5 G. Luft, R. Kämpf and H. Seidl, *Angew. Makromol. Chem.*, 1982, **108**, 203–217.
- 6 G. Luft, R. Kämpf and H. Seidl, *Angew. Makromol. Chem.*, 1983, **111**, 133–147.
- 7 G. Luft and M. Dorn, *Wiley Online Libr.*, 1990, **174**, 119–130.
- 8 R. O. Symcox and P. Ehrlich, *J. Am. Chem. Soc.*, 1962, **84**, 531–536.
- 9 C. L. P. Shan, W. A. deGroot, L. G. Hazlitt and D. Gillespie, *Polymer*, 2005, **46**, 11755–11767.
- 10 M. Zhang, D. T. Lynch and S. E. Wanke, *J. Appl. Polym. Sci.*, 2000, **75**, 960–967.
- 11 S. Cheruthazhekatt, T. F. J. Pijpers, G. W. Harding, V. B. F. Mathot and H. Pasch, *Macromolecules*, 2012, **45**, 2025–2034.
- 12 L. Wild and G. Glöckner, in *Separation Techniques - Thermodynamics - Liquid Crystal Polymers*, Springer, Berlin-Heidelberg, 1990, vol. 98, pp. 1–47.
- 13 B. Monrabal and P. del Hierro, *Anal. Bioanal. Chem.*, 2011, **399**, 1557–1561.
- 14 S. Anantawaraskul, J. B. P. Soares and P. M. Wood-Adams, in *Polymer Analysis - Polymer Theory*, Springer, Berlin-Heidelberg, 2005, vol. 182, pp. 1–54.
- 15 A. Ndiripo and H. Pasch, *Anal. Bioanal. Chem.*, 2015, **407**, 6493–6503.
- 16 F. M. Mirabella, *J. Liq. Chromatogr.*, 1994, **17**, 3201–3219.
- 17 H. Pasch and M. I. Malik, *Advanced Separation Techniques for Polyolefins*, Springer International Publishing, Cham, 2014.

INTRODUCTION AND AIM OF STUDY

- 18 H. Pasch, M. I. Malik and T. Macko, in *Polymer Composites – Polyolefin Fractionation – Polymeric Peptidomimetics – Collagens*, eds. A. Abe, H.-H. Kausch, M. Möller and H. Pasch, Springer, Berlin-Heidelberg, 2012, vol. 251, pp. 77–140.
- 19 B. Monrabal, N. Mayo and R. Cong, *Macromol. Symp.*, 2012, **312**, 115–129.
- 20 B. Monrabal, L. Romero, N. Mayo and J. Sancho-Tello, *Macromol. Symp.*, 2009, **282**, 14–24.
- 21 B. Monrabal, J. Sancho-Tello, N. Mayo and L. Romero, *Macromol. Symp.*, 2007, **257**, 71–79.
- 22 D. D. Robertson, R. Neppalli and A. J. van Reenen, *Polym. Test.*, 2014, **40**, 79–87.
- 23 S. Cheruthazhekatt, D. D. Robertson, M. Brand, A. van Reenen and H. Pasch, *Anal. Chem.*, 2013, **85**, 7019–7023.
- 24 I. Amer, A. van Reenen and M. Brand, *Polym. Int.*, 2015, **64**, 466–476.
- 25 R. Brüll, H. Pasch, H. G. Raubenheimer, R. Sanderson, A. J. van Reenen and U. M. Wahner, *Macromol. Chem. Phys.*, 2001, **202**, 1281–1288.
- 26 A. J. Van Reenen, R. Brull, U. M. Wahner, H. G. Raubenheimer, R. D. Sanderson and H. Pasch, *J. Polym. Sci. Polym. Chem.*, 2000, **38**, 4110–4118.
- 27 A. J. Müller and M. L. Arnal, *Prog. Polym. Sci.*, 2005, **30**, 559–603.
- 28 D. Cavallo, A. T. Lorenzo and A. J. Müller, *J. Polym. Sci. Part B Polym. Phys.*, 2016, **54**, 2200–2209.
- 29 Y. Xue, S. Bo and X. Ji, *Chin. J. Polym. Sci.*, 2015, **33**, 1000–1008.
- 30 C. Ding, G. Zhang, J. Gu, F. Cao and X. Zheng, *RSC Adv.*, 2017, **7**, 24870–24877.
- 31 J. Kang, F. Yang, T. Wu, H. Li, D. Liu, Y. Cao and M. Xiang, *J. Appl. Polym. Sci.*, 2012, **125**, 3076–3083.
- 32 H. Pasch, *Polym. Adv. Technol.*, 2015, **26**, 771–784.
- 33 T. Macko, R. Brüll, R. G. Alamo, F. J. Stadler and S. Losio, *Anal. Bioanal. Chem.*, 2011, **399**, 1547–1556.
- 34 A. Ndiripo, D. Joubert and H. Pasch, *J. Polym. Sci. Polym. Chem.*, 2016, **54**, 962–975.
- 35 R. Chitta, A. Ginzburg, G. van Doremaele, T. Macko and R. Brüll, *Polymer*, 2011, **52**, 5953–5960.
- 36 H. Pasch, L.-C. Heinz, T. Macko and W. Hiller, *Pure Appl. Chem.*, 2008, **80**, 1747–1762.
- 37 O. Sperber and W. Kaminsky, *Macromolecules*, 2003, **36**, 9014–9019.
- 38 E. F. McCord, W. H. Shaw and R. A. Hutchinson, *Macromolecules*, 1997, **30**, 246–256.
- 39 F. A. Bovey, F. C. Schilling, F. L. McCrackin and H. L. Wagner, *Macromolecules*, 1976, **9**, 76–80.
- 40 M. De Pooter, P. B. Smith, K. K. Dohrer, K. F. Bennett, M. D. Meadows, C. G. Smith, H. P. Schouwenaars and R. A. Geerards, *J. Appl. Polym. Sci.*, 1991, **42**, 399–408.
- 41 T. Usami and S. Takayama, *Macromolecules*, 1984, **17**, 1756–1761.
- 42 B. J. Crosby, M. Magnus, W. de Groot, R. Daniels and T. C. B. McLeish, *J. Rheol.*, 2002, **46**, 401.
- 43 T. Usami and S. Takayama, *Polym. J.*, 1984, **16**, 731–738.
- 44 Y. Xue, Y. Fan, S. Bo and X. Ji, *Chin. J. Polym. Sci.*, 2015, **33**, 508–522.
- 45 A. Malmberg, J. Liimatta, A. Lehtinen and B. Löfgren, *Macromolecules*, 1999, **32**, 6687–6696.
- 46 W. W. Yau and D. Gillespie, *Polymer*, 2001, **42**, 8947–8958.
- 47 T. Pathaweeisariyakul, K. Narkchamnan, B. Thitisak, W. Rungswang and W. W. Yau, *Polymer*, 2016, **107**, 122–129.
- 48 P. Tackx and J. Tacx, *Polymer*, 1998, **39**, 3109–3113.
- 49 W.-J. Wang, S. Kharchenko, K. Migler and S. Zhu, *Polymer*, 2004, **45**, 6495–6505.
- 50 S. Podzimek, *Light scattering, size exclusion chromatography, and asymmetric flow field flow fractionation: powerful tools for the characterization of polymers, proteins, and nanoparticles*, Wiley, Hoboken, NJ, 2011.
- 51 P. M. Wood-Adams, J. M. Dealy, A. W. deGroot and O. D. Redwine, *Macromolecules*, 2000, **33**, 7489–7499.
- 52 Y. Xue, S. Bo and X. Ji, *J. Polym. Res.*, 2016, **23**, DOI:10.1007/s10965-016-1026-1.
- 53 J. K. Jørgensen, Å. Larsen and I. Helland, *E-Polym.*, 2010, **10**, 1596–1612.

INTRODUCTION AND AIM OF STUDY

- 54 J. B. P. Soares and International Conference on Polyolefin Characterization, Eds., Polyolefin characterization: selected contributions from the conference: The First International Conference on Polyolefin Characterization (ICPC), Houston, TX (USA), October 16-18, 2006, Wiley-VCH, Weinheim, 2007.
- 55 A. Ndiripo, P. Eselem Bungu and H. Pasch, Polym. Int., 2018, DOI:10.1002/pi.5547.
- 56 M. J. Phiri, S. Cheruthazhekatt, A. Dimeska and H. Pasch, J. Polym. Sci. Polym. Chem., 2015, **53**, 863–874.
- 57 Y. Xue, S. Bo and X. Ji, J. Polym. Res., 2015, **22**, 1–10.
- 58 A. Krumme, M. Basiura, T. Pijpers, G. Vanden Poel, L. C. Heinz, R. Brüll and V. BF Mathot, Mater. Sci., 2011, **17**, 260–265.
- 59 W. W. Yau, A. Ortín and P. del Hierro, LC GC N. Am., 2011, 46–47.
- 60 B. Monrabal, J. Sancho-Tello, J. Montesinos, R. Tarín, A. Ortín and P. del Hierro, High Temperature Gel Permeation Chromatograph (GPC/SEC) with integrated IR5 MCT detector for Polyolefin Analysis: a breakthrough in sensitivity and automation., In: The application Book, LCGC Europe, Chester, 2012.
- 61 A. Ortin, B. Monrabal and J. Sancho-Tello, Macromol. Symp., 2007, **257**, 13–28.
- 62 A. Ginzburg, T. Macko, F. Malz, M. Schroers, I. Troetsch-Schaller, J. Strittmatter and R. Brüll, J. Chromatogr. A, 2013, **1285**, 40–47.

2 Literature Review

2.1 Early discovery of polyethylene

Ethylene, the principal feedstock for the production of polyethylene, was discovered over two hundred years ago and is made up of carbon and hydrogen only. Even though ethylene possesses many positive attributes, it was mainly used in the production of mustard gas (dichlorodiethyl sulphide), a poisonous weapon used during World War I. The high ethylene demand for warfare led to the construction of the first production plant. Towards the end of the war, it was not surprising that ethylene was available for a wide range of interesting applications including its use as an anaesthetic in the medical industry and in the production of ethylene dichloride, a valuable solvent for the production of oils and waxes.¹ Another emerging application was its use in the production of polyethylene (PE).

Polyethylene was accidentally discovered by four Dutch chemists as a white waxy material. A high pressure oxygen-initiated process was established by Imperial Chemical Industries (ICI).^{2,3} This discovery led to the genesis of the industrial production of low density polyethylene (LDPE). At that time, LDPE was used mainly as insulator material for ultra-high frequency (UHF) and super high frequency (SHF) coaxial cables for radar sets.⁴ Years later, another milestone discovery in the polyethylene industry emerged. Ethylene could be polymerized at a lower reactor pressure and temperature with the help of a catalyst to produce high density polyethylene (HDPE).^{2,5} Thereafter, copolymerization of ethylene with higher α -olefins using the catalytic procedure was introduced. This technique is used to produce the commonly known linear low density polyethylene (LLDPE). Today, polyethylene is the largest volume synthetic thermoplastic material available, with over 80 million metric tonnes global production reported in 2008 and a projected growth rate of over 5% per annum for the near future.^{2,6} In the following section, the characteristic differences between the HDPE, LLDPE and LDPE and their applications will be discussed.

2.2 Classes of polyethylene

Polyethylene (PE) consists of a large number of ethylene monomer units, having a general molecular formula of $(CH_2CH_2)_n$. PE exists in three widely used forms, which include high density polyethylene (HDPE), linear low density polyethylene (LLDPE) and low density polyethylene (LDPE).⁷ The molecular

LITERATURE REVIEW

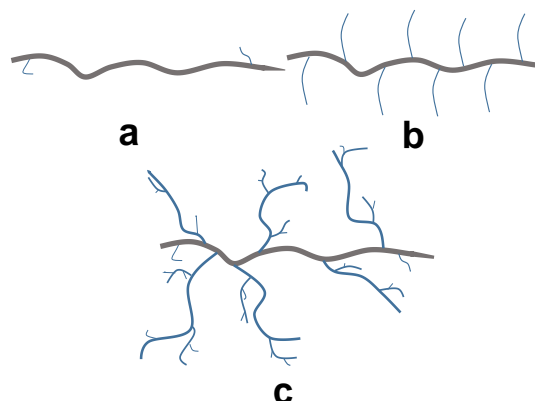


Figure 1: Schematic representation of HDPE (a), LLDPE (b) and LDPE (c).

structure of each polyethylene type is schematically presented in Fig. 1. HDPE is produced by catalytic polyaddition of ethylene at milder experimental temperatures (85 – 140 °C) and pressure (85 – 300 bars).^{2,8} This procedure leads to polymer chains with a linear polyethylene backbone as indicated in Fig. 1a. The absence or low concentration of branches along the PE backbone results in the close packing between adjacent molecules and, therefore, strong van der Waals interactions. This close packing results in materials with high tensile strength, toughness, high crystallinity and high density. Generally, HDPE resins exhibit densities ranging between 0.94 and 0.97 g/cm³.^{2,9}

LLDPEs is produced by catalytic copolymerization of ethylene with higher α -olefins as comonomers. The outcome of this combination generates polymer chains with branches that are similar to the one schematically presented in Fig. 1b. Branches in LLDPE exhibit defined lengths/sizes and are referred to as short chain branching (SCB). This technique is extremely beneficial to the industry in designing tailor-made PE resins with different properties by varying the comonomer contents and types. The branches on the polymer backbone cause the molecules to mix. Broad SCB distribution provides a wider melting/crystallization temperature range, which aids in enhancing sealability and stretching ability. In addition, the rigidity of the branches influences molecular packing, thereby affecting physical properties such as melting, crystallization, density etc. Depending on the comonomer content (SCB content), LLDPE resins may exhibit densities that vary from 0.91 to 0.93 g/cm³.^{9,10}

Commonly used catalysts include Ziegler-Natta and metallocene type catalysts. The Ziegler-Natta catalyst provides multiple reaction sites, which aid in generating PE chains with varying sizes and disordered branching distributions. This causes the final resins to exhibit broad molar mass and comonomer distributions. Alternatively, single-site metallocene catalysts are used to produce PE chains with homogeneous size distributions as well as evenly distributed short chain branches.^{2,7}

LITERATURE REVIEW

Lastly, LDPE is produced by free radical polymerization (FRP) processes at elevated temperatures (140 – 350 °C) and pressures (1000 – 3500 bars) that require an active initiator or catalyst to kick-start the reaction.^{11,12} Common initiators used include azo compounds, peroxides and oxygen. A schematic representation of a typical product with a complex architecture is shown in Fig. 1c. As is seen, LDPE molecules exhibit both long and short chain branches that are distributed in size and location. While a high level of LCB helps to increase impact strength and environmental resistance, a low LCB level improves optical properties, drawdown and tear strength. On the other hand, SCB controls the melting and crystallization behaviour of the resins. In addition, SCB also decreases the polymer density by altering the way the molecules pack. A typical density range of 0.91 to 0.94 g/cm³ is reported in the literature.² Summarized in Table 1 are typical characteristic properties of the different PE resins.^{2,13} In the next section, detailed literature focusing on the reaction mechanism and the molecular complexity of LDPE or branched PE is discussed.

Table 1: Summary of microstructural characteristics and applications of the different types of polyethylene resins.

PE	Comonomer	Production Process	Temperature and Pressure	Catalyst	Branch type	Properties	Application
HDPE	none	Homo-polymerization	85-140 °C 85-300 bars	-Ziegler-Natta -Metallocene	linear	-High density (0.94-0.97g/cm ³) -High strength -Toughness -Low stretching -Poor flow property	-Pipes -Thick films
LLDPE	α -olefins (n-butene and higher)	Co-polymerization	85-140 °C 85-300 bars	-Ziegler-Natta -Metallocene	SCB	-Low density (0.91-0.93 g/cm ³) -Good stretching -Toughness -Poor flow properties	-Stretch wraps -Thin films
LDPE	none	Homo-polymerization	140-350 °C 1000-3500 bars	-Peroxide -Oxygen -Azo compounds	LCB SCB	-Low density (0.91-0.94 g/cm ³) -Good processability -Poor toughness -Good clarity -Good ductility	Thin clarity films for: -Laminates -General packaging

2.3 Free radical polymerization of ethylene

As indicated earlier, LDPE is produced industrially by free radical polymerization (FRP) of ethylene either in an autoclave or in a tubular reactor under harsh reactor conditions (see Table 1 and Fig. 3). Typically, FRP occurs at reactor pressures between 1000 and 3500 bars. At such high pressures, ethylene exists as a liquid and the polymerization occurs in an excess of ethylene solution.² Kinetically, the reaction advances through the elementary steps indicated as 1 to 4 in Fig. 2¹⁴ and Scheme 1.¹⁵ In the initiation step, the initiator absorbs heat from the environment and undergoes homolytic cleavage to generate radicals that readily initiate the polymerization as indicated in (1).^{4,15-17} The radicals then attack the ethylene to generate initiator radicals (2), which is followed by repeated ethylene addition

LITERATURE REVIEW

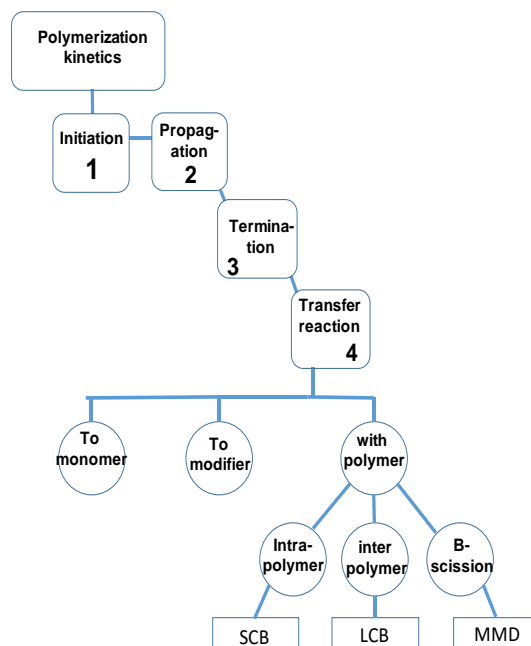


Figure 2: Elementary reactions in the free radical homopolymerization of ethylene to low density polyethylene (modified from reference 14).

to form macroradicals as indicated in (4). According to the findings of Tatsukami *et al.*¹⁸, no induction period exists with the oxygen-based polymerization process above 190 °C. At such high temperatures, the oxygen starts inhibiting the polymerization process, forming deactivated product and/or hydroperoxides as indicated in (3).

Initiation of oxygen:



Chain initiation reaction:



Retardation



Propagation:



Termination by combination:



Scheme 1: Representative reactions illustrating the initiation (1 and 2), retardation (3), propagation (4) and termination (5 and 6) steps of a radical polymerization process (modified from ref. 15).

LITERATURE REVIEW

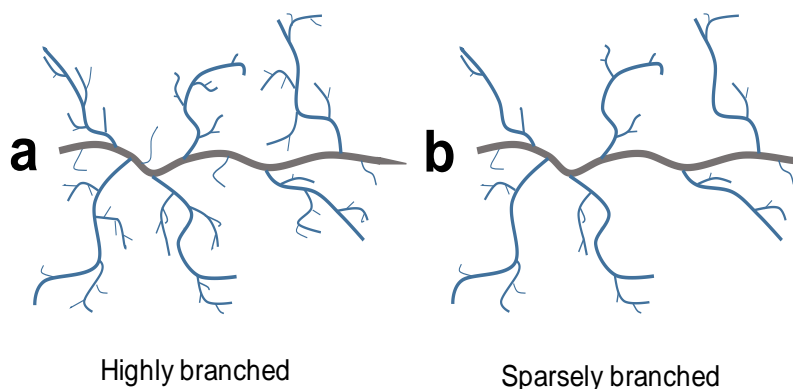


Figure 3: Morphology of a highly and sparsely branched LDPE molecule produced using (a) an autoclave reactor or higher temperature and (b) a tubular reactor or higher

Polymer molecules are formed by coupling two macroradicals into a larger size molecule (5), or by disproportionation reaction into two smaller size molecules (6). Chain transfer reactions proceed through multiple pathways (see Fig. 2) and are responsible for the formation of branches and other terminal groups. In the case where terminal functional groups are formed, the macroradicals abstract hydrogen from either a monomer or a modifier (e.g. solvent or chain transfer agent).

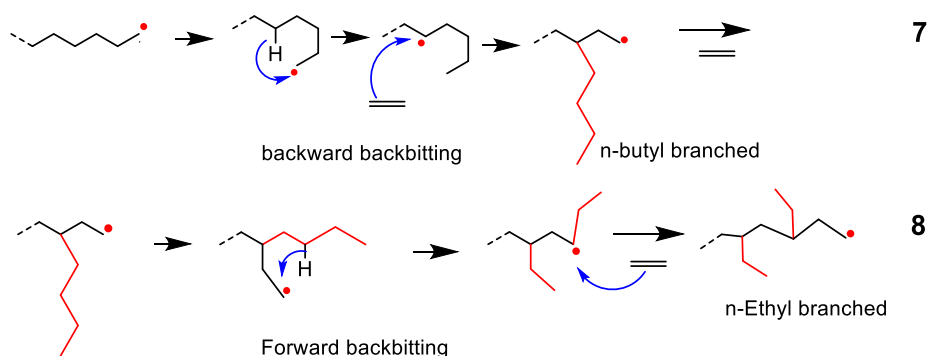
Branches are formed by radical transfer from a terminal carbon of a macroradical to an inner methylene carbon of the same or a different polymer molecule through hydrogen abstraction, followed by chain growth at the new radical site. The phenomenon by which radicals are transferred within the same macroradicals is called backbiting and leads to the formation of short chain branches. Alternatively, radical transfer to another molecule yields long chain branches.^{2,10,14,15,}

2.4 The microstructure of branched polyethylene

Polymer microstructure is defined by molecular parameters such as molar mass, branching, functional groups and comonomer content. These microstructural characteristics are capable of affecting polymer properties and applications. In the FRP reactor, the different reactions described in Fig. 2 occur simultaneously, thereby producing LDPE molecules with complex architectures as shown in Fig. 3. Branching and molar mass distributions are the principal molecular parameters influencing the melting and solution behaviours of LDPE resins.

While molar mass increases through chain growth reactions, i.e. continuous addition of ethylene onto the radical site, branches are formed by radical transfer reactions. Branching in LDPE is classified into long chain branching (LCB) and short chain branching (SCB). The later is formed by backbiting reactions, follow by chain growth reaction at the newly formed radical site as illustrated in 7 and 8

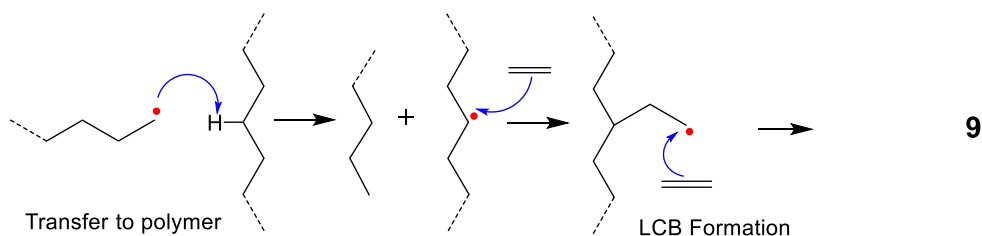
LITERATURE REVIEW



Scheme 2: Schematic representation for the formation of short chain branch (LCB) by backward backbiting (7) and forward backbiting (8) to form butyl and ethyl branches, respectively.

in Scheme 2.² The commonly known backward backbiting predominantly forms n-butyl branches.^{2,15,19,20} Depending on the applied conditions, secondary forward backbiting reactions may occur on the newly formed branched molecules to produce ethyl branches as indicated in (8). For a commercial high pressure process, n-butyl (C₄) branches are the principal short chain branches formed, which co-exist with smaller proportions of methyl (C₁), ethyl (C₂), amyl (C₅), and hexyl (C₆) branches, in a trifunctional branching system.

On the other hand, LCBs are formed via intermolecular chain transfer to macromolecules. This reaction occurs when a macroradical abstracts hydrogen from the backbone of a neighbouring polymer chain, followed by chain growth on the new radical site as indicated in (9). Even though the exact length of an LCB remains ill-defined, it constitutes tens or hundreds of repeated methylene units. From the rheological standpoint, LCB is defined as any branch capable of enhancing chain entanglement and induce side chain crystallization. From the point of view of ¹³C NMR, LCB branches are any chains longer than C₅ branches, since this technique is unable to distinguish side chains longer than C₆ branches.



Scheme 3: Schematic representation for the formation of long chain branch (LCB) by chain transfer to polymer.

Just like other synthetic polymers, LDPE is a statistically distributed material that exhibits a complex microstructure. The microstructural complexity stems from the fact that the polymer consists of molecules with different sizes and topologies as illustrated in Fig. 4. Microstructural heterogeneity is defined by the distributions in molecular size (molar mass distribution, MMD) and molecular topology

LITERATURE REVIEW

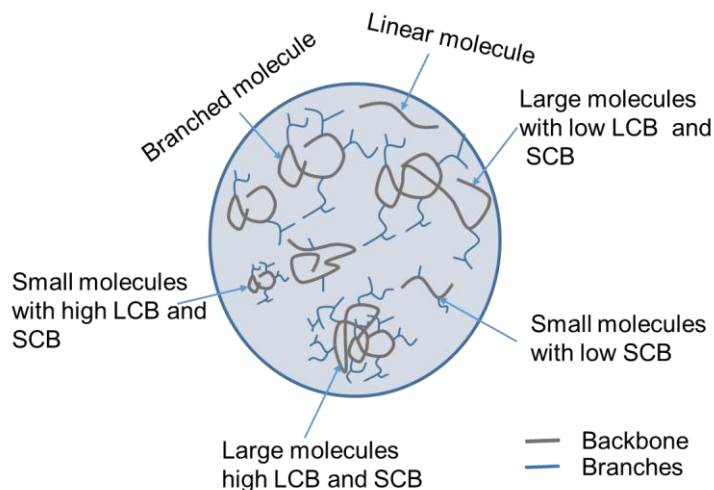


Figure 4: Schematic topological representation of the molecular structure and microstructural distribution of branched PE (LDPE).

(branching distribution, BD) of the polymer chains. In the field of polymer science, MMD is expressed in terms of the broadness index or dispersity (\mathfrak{D}), which is described by the ratio of the weight-average molar mass (M_w) and the number-average molar mass (M_n).

Earlier investigations have indicated that resins having similar average molar masses but different size or branching distributions may exhibit different rheological properties and, therefore, different mechanical properties and applications.²¹ One major challenge in the FRP process is to synthesize molecules with a well-defined molecular structure and narrow molar mass distribution. However, this challenge to a certain extent might be beneficial since broad MMDs provide LDPE resins with better elastic recovery and the ability of the melt to deviate from Newtonian behaviour, providing better processing ability. Polymer dispersity can be enhanced or reduced experimentally by altering the polymerization conditions (temperature and pressure). Depending on the desired product, increasing pressure or decreasing polymerization temperature foster chain growth reactions leading to a higher degree of polymerization and broad MMD. Other conditions that lead to broad MMDs include the use of active initiators such as oxygen and di-tertbutylperoxide and a square-shaped autoclave reactor. Reactors with shapes that ensure maximum mixing and alters residence time of each molecule will influence dispersity.²¹ Other investigations have demonstrated that polymers with broad MMDs can be obtained by using symmetrical difunctional peroxide initiators that readily dissociate.²²

On the other hand, resins with narrow MMDs are obtained by applying conditions that do not favour chain growth reactions but maintain uniform residence times for all molecules. This is achieved by increasing the polymerization temperature, using active initiators like dicyclohexyl peroxidecarbonate, and a narrow autoclave or a tubular reactor to produce polymer chains with a

LITERATURE REVIEW

higher degree of branching as indicated in Fig. 3a. In a situation whereby high pressure is applied, a small amount of chain transfer agent (CTA) may be used to control molar mass (chain growth). In LDPE resins, LCB often dictates the desired property since a higher level of LCB results in broad molar mass distributions. Experimentally, increasing polymerization temperatures result in an increased level of LCB and SCB. In this case, the length of the LCB is shorter since chain growth is hindered, leading to polymer chains with narrow MMDs. Alternatively, longer LCBs are formed at higher pressure and, therefore, broad MMDs are achieved.^{15,21,23} However, the degree of LCB can also be influenced by altering the feed gas temperature which is applied in situations whereby only an increase in LCB is desired without increasing the level of SCB. A high level of LCB or broad MMD improves impact strength, neck-in and environmental crack resistance. Although broad MMD resins improve impact strength, resins with narrow MMD but a higher degree of LCB provide better impact strength.²⁴

In industry, for example, a higher level of SCB controls the melting temperature, which improves the ability for polymer to seal at low temperature. When high sealability in combination with high polymer strength is desired, resins with low level of LCB but having broad SCBD is required. This is because LCB reduces the ability for molecules to mix. Low level of LCB also improves drawdown in coating grade resins. Therefore, LDPE properties vary significantly depending on the desired application.

In order to understand the characteristic behaviours of these resins and to assign them to specific applications, the development of structure-property relationships is essential and requires in-depth characterization of these complex resins. In the next section, the different characterization techniques and their uses will be highlighted.

2.5 Advanced characterization of polyolefins

In order to correlate polyolefin microstructure to the physical and mechanical properties, the microstructural parameters MMD and CCD, branching distribution (BD) and tacticity must be analyzed quantitatively. In a study by Ndiripo *et al.* the “LEGO” approach shown in Fig. 5 was proposed for the comprehensive microstructural analysis of complex polyolefin resins.²⁵ This approach incorporates the use of advanced chromatographic techniques such as; high temperature size exclusion (HT-SEC), high temperature solvent gradient interactive chromatography (HT-SGIC) and high temperature two-dimensional liquid chromatography (HT-2D-LC) in combination with crystallization-based techniques such as; temperature rising elution fractionation (TREF), crystallization analysis fractionation (CRYSTAF), crystallization elution fractionation (CEF), solution crystallization analysis by laser light scattering (SCALLS) and thermal analytical techniques such as; differential scanning calorimetry (DSC)

LITERATURE REVIEW

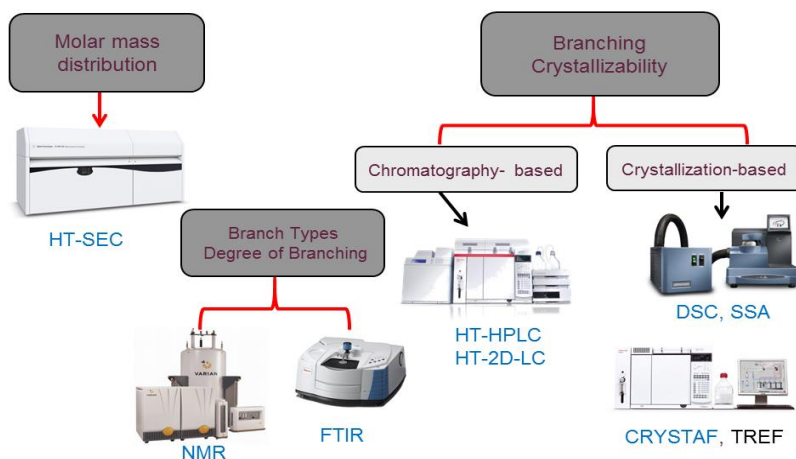


Figure 5: Schematic presentation of the “LEGO” approach in the analysis of complex polyolefins (reproduced from ref 25)

and successive self-nucleation and annealing (SSA) for the analysis of complex semicrystalline materials. In addition to this cluster of techniques, ^{13}C NMR and FTIR spectroscopy are also used to quantitatively measure the comonomer/branching contents as well as to determine the branch types, comonomer sequences and tacticities of these complex polymers.^{19,26-29}

Typically, SEC is used to fractionate polymer chains on the basis of hydrodynamic size and the size distribution is directly related to MMD. Conventionally, SEC is coupled either to concentration detectors such as the differential refractive index detector (DRI) or the infrared (IR) detector.³⁰ The concentration profile as a function of elution volume is converted to a MMD using a column calibration procedure. The calibration method assumes that (1) the molar mass is regularly defined over the calibration curve and (2) any molecule eluting late after the column must be smaller in size and thus in molar mass.^{31,32}

However, this is not true for complex polymers like LDPE since the molecular size of the eluting fractions does not depend on molar mass alone, but also on the molecular architecture and topology. This implies that high molar mass molecules with a higher level of branching will co-elute with low molar mass linear molecules due to a higher polymer coil density induced by the branches. In such complex systems, molar mass sensitive detectors such as light scattering or online viscometer are preferred. These detectors have the ability to measure the exact molecular size and branching by measuring the radius of gyration (R_g) or hydrodynamic radius (R_h) of the SEC fractions regardless of the elution volume.^{33,34} Accurate molar mass measurement by the LS detector also requires a concentration detector preferably an online RI to measure polymer concentration as well as the specific refractive index increment dn/dc in accordance with Eq. (1). where I is the intensity of the scattered light, M the molar mass and C , the polymer concentration.

LITERATURE REVIEW

$$I_{scattered} \propto M \times C \times \left(\frac{dn}{dc} \right)^2 \quad (1)$$

In recent years, triple detection SEC that integrates an online concentration detector (RI/IR) with multiangle laser light scattering and viscometer detectors (SEC-RI-MALLS-Vis) have been developed for the comprehensive microstructural characterisation of complex polymers. It is well known that polymer chains with similar hydrodynamic size will co-elute irrespective of their topology. On adapting special infrared detectors such as IR5 with SEC, chain branching can be measured as a function of MMD.^{30,35,36}

Chain crystallinity is an important physical characteristic, which varies with changes in the molecular structure and topology. These variations provide the fundamental link between compositional heterogeneity and physical properties of semi-crystalline polyolefins. To evaluate polyolefin microstructure based on chain structure, topology or architectural distributions, advanced techniques such as TREF³⁷⁻³⁹ and CRYSTAF^{35,40-40} were developed to fractionate polymer chains according to their crystallizability from dilute solution. Experimentally, CRYSTAF uses an infrared detector to measure changes in polymer concentration in dilute solution as crystallization occurs. On the other hand, fractionation by TREF proceeds through two experimental steps. Initially, the polymer undergoes static crystallization on a solid support (either sea sand or glass beads) by slowly cooling a mixture of polymer and support in a crystallization column (analytical TREF) or a glass reactor (preparative TREF). The polymer crystallizes on the support based on its crystallizability, while forming onion-like ring structures as indicated in Fig. 6a. Subsequently, a coherent solvent flow and successively rising column temperature elute the polymer fractions of the previously crystallized materials as indicated in Fig. 6b. In the case of analytical TREF, the polymer concentration is monitored using an infrared detector as the polymer elutes from the column.

Although good separation is achieved in TREF, the technique is time-consuming and requires excessive use of solvents. In recent times, Monrabal *et al.* have introduced crystallization elution fractionation

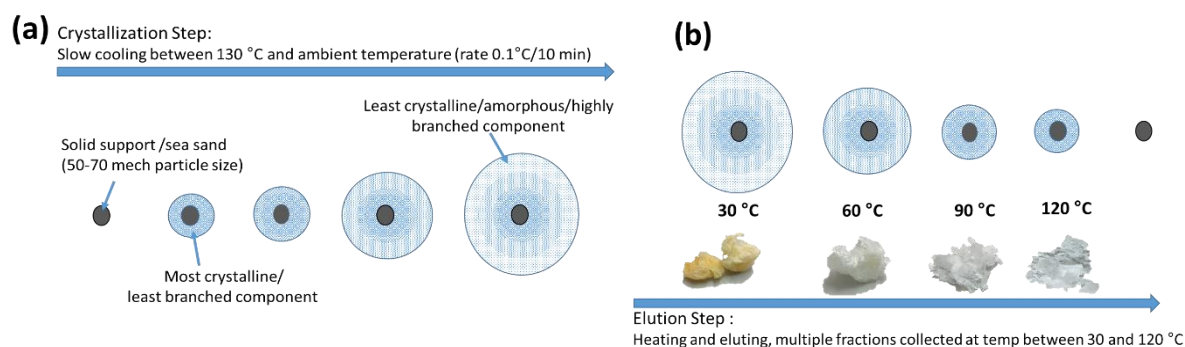


Figure 6: Schematic representation of the TREF process, showing in (a) the crystallization step and (b) the elution step.

LITERATURE REVIEW

(CEF)^{40,41-43}, which is a technique developed to minimize analysis time while ensuring improved separation. Different from TREF, CEF uses dynamic crystallization since a small solvent flow is allowed through the column as crystallization occurs. This process permits molecules with different molecular structure or crystallizability to crystallize at different locations in the column. This technique was reported previously to provide good separation for complex polyolefins and polymer blends at a reduced analysis time.

Most recently, Shan *et al.* introduced a new fractionation technique known as turbidity fractionation analysis (TFA), which is used to fractionate polyolefin resins based on solubility. This technique was used to evaluate comonomer composition distributions in linear low density polyethylene and compositional distributions in polyethylene blends.⁴⁴ The method was later modified by van Reenen and co-workers to a technique known as solution crystallization analysis by laser light scattering (SCALLS) and was used to study the crystallization kinetics of different types of polyolefins and polymer blends.⁴⁴⁻⁴⁷

While CRYSTAF profiles describe polymer behaviour as crystallization occurs, TREF and CEF provide the dissolution profiles as the polymer elutes from the column. SCALLS, on the other hand, combines both techniques by providing the crystallization and dissolution profiles in a single experimental run at the shortest possible time. Also, the procedure does not require sophisticated instrumentation as well as excessive use of solvent.

Unlike solution-based crystallization techniques, DSC⁴⁸⁻⁵¹ is a thermal analytical technique that characterizes polymer molecules in their solid state. This technique monitors the crystallization and melting behaviour as polymers are subjected to a controlled temperature program. The technique is commonly used by industry and academics as a quick analytical tool to qualitatively measure the chain composition of complex polymers while correlating the microstructural properties to the thermophysical behaviour.

In addition to conventional DSC experiments, DSC based fractionation techniques such as SSA and step crystallization (SC) have been developed.⁵²⁻⁵⁶ These techniques fractionate polyolefin resins thermally while providing in-depth structural information regarding SCB (PE), tacticity (PP) and chain heterogeneity. Fractionation by SSA occurs by segregation, whereby polymer chains with similar crystallizable methylene sequences (CMS) are segregated through continuous heating and cooling cycles while successively decreasing the self-seeding temperature (maximum heating temperature). This technique provides information regarding crystal size distribution (CSD), which is directly related to the chemical composition distribution in the chain structure.

LITERATURE REVIEW

It is often assumed that polymer chains exhibiting similar distributions in the crystallizable ethylene sequences (similar degree of branching) will co-crystallize irrespective of their molecular size.^{55,57} Therefore, by correlating the branching content to the crystallization temperature and crystal size, the polymer crystal size distribution is directly linked to the branching distribution.⁴⁹ All these different techniques are temperature-dependent and, therefore, suffer from the co-elution/co-crystallization effect. In addition, crystallization based techniques are limited to the crystallizable components of the polyolefin resin as amorphous fractions cannot be separated.

To overcome the challenges of crystallization-based techniques, high-temperature high performance liquid chromatography (HT-HPLC or HT-SGIC) was recently developed by Pasch and Macko as an alternative method for the analysis of complex polyolefin resins.^{37,40,58-63} This technique fractionates polyolefin chains according to van der Waals interactions with the stationary phase and not according to crystallizability.

The separation is governed by the adsorption/desorption capability of the Hypercarb (porous graphite particles) stationary phase on the polymer molecules. Unlike CRYSTAF and other temperature-dependent techniques, this method is capable of analysing both the amorphous and the crystalline polyethylene components since the fractionation is based on the interaction between the stationary phase and the linear ethylene backbone. Following the development of solvent gradient HPLC a 2D-LC technique capable of mapping branching/comonomer content distribution of complex polymers as a function of hydrodynamic volume (molar mass) was developed.^{40,64-46 65} This technique incorporates

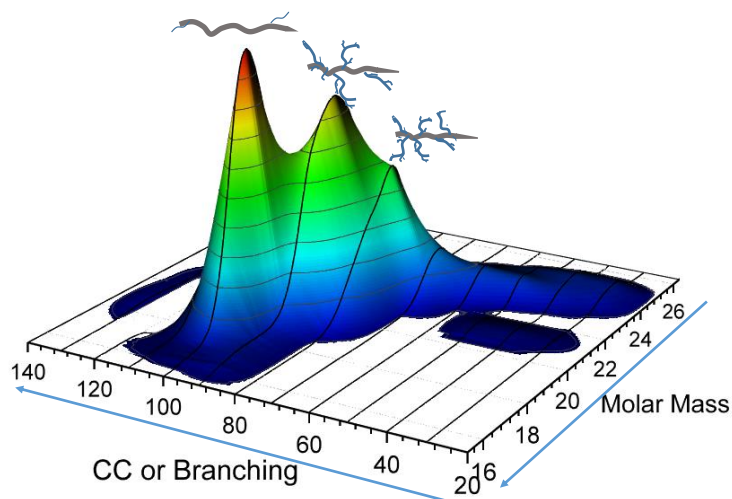


Figure 7: 3D plot obtained by combining TREF and SEC to obtain a bivariate distribution of polyolefin resins.

HPLC and SEC in one instrument such that fractions eluting from the HPLC column are subsequently being analysed by SEC providing bivariate distribution plots that correlate branching to molar mass or hydrodynamic volume similar to the one presented in Fig. 7. A similar technique whereby TREF is

LITERATURE REVIEW

coupled to SEC was also reported by Yau.^{49,67-69} These sophisticated but highly beneficial techniques have been used for the comprehensive microstructural characterization of complex polyolefins such as impact polypropylene, ethylene co- and terpolymers.

Typically, ^{13}C NMR spectroscopy is used to elucidate the molecular structure of complex polymers. This technique is suitable for quantitative measurements of branching (LDPE), comonomer content (LLDPE), tacticity and comonomer sequence units of complex polyolefin resins.⁷⁰ Although, ^{13}C NMR is a more precise analytical technique used to characterize branching, it is limited to providing average information and not the distribution. Branching distribution information, on the other hand, has been obtained by coupling FTIR with fractionation techniques. For example, chemical composition distribution of complex polymer resins has been obtained offline by coupling SEC or HPLC to FTIR. In this case, the eluting SEC⁶⁵ or HPLC⁶⁷ fractions are collected on a germanium disc via the LC-transform interface and analysed offline using FTIR.

Despite the wide variety of techniques reported for the characterization of complex polymers, a more comprehensive approach in establishing suitable structure-property relationships for highly heterogeneous systems is to perform fractionation on a preparative scale. Commonly used preparative techniques include preparative TREF (pTREF),^{71,72} having been used to obtain molecular species with varying branching but narrow branching distributions. On the other hand, preparative molar mass fractionation (pMMF) provides fractions with given molar masses and narrow molar mass dispersities. The fractionation process is governed by phase separation induced by a continuous decrease of the dissolution power of a solvent system either by adding a non-solvent to the polymer

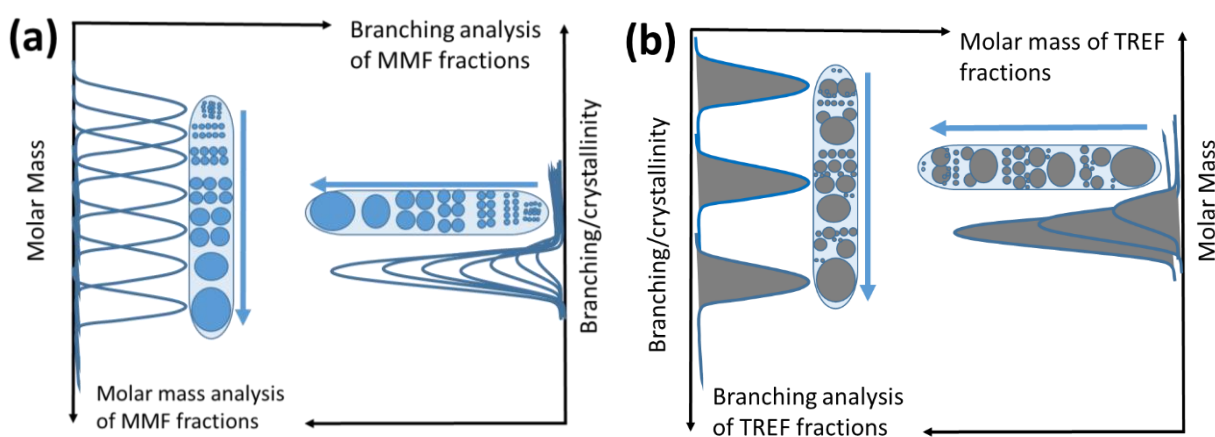


Figure 8: Diagram showing the variation in molar mass and branching of the (a) MMF and (b) TREF fractions. solution or by preferential evaporation of the solvent in a solvent/non-solvent mixture.^{73,74}

Alternatively, molar mass fractions can be obtained by solvent gradient fractionation (SGF). With this method, fractions are obtained by dissolving/eluting the samples with varying ratios of solvents and

LITERATURE REVIEW

non-solvents in binary mixtures.^{74,75} These fractionation methods provide fractions in milligrams to gram amounts that can be analysed further using other advanced techniques like SEC, NMR, DSC, etc.

While pTREF fractionation provides fraction libraries with varying branching or crystallizabilities, pMMF and SGF are more selective towards molar mass and, thereby, produce fractions with varying molar masses irrespective of composition/branching as presented in Fig. 8. As clearly illustrated in Fig. 8a, the MMF fractions demonstrate high selectivity towards molar mass, while showing no major changes in branching content. On the other hand, analysis of the TREF fractions in Fig 8b, display varying branching content, while molar mass remains almost unchanged. These techniques have been extensively used to study the chain composition in complex polymer systems. As an alternative method to the conventional 2D liquid chromatography using HPLC/TREF-SEC, cross-fractionation techniques have also been established for the analysis of polyolefins. These techniques combine data from the preparative fractionation methods such as pTREF and analytical data from SEC to establish 2D plots similar to the one presented in Fig. 7.

3 References

- 1 F. B. Arentz, *J. Chem. Edu.*, 1925, **2**, 459.
- 2 D. B. Malpass, *Introduction to Industrial Polyethylene: Properties, Catalysts, and Processes*, John Wiley & Sons, Inc., Hoboken, NJ, USA, 2010.
- 3 E. Bamberger and F. Tschirner, *Ber. Dtsch. Chem. Ges.*, 1900, **33**, 955–959.
- 4 A. Bertucco and G. Vetter, Eds., *High pressure process technology: fundamentals and applications*, Elsevier, Amsterdam, 1. ed., 2001.
- 5 S. D. Ittel, L. K. Johnson and M. Brookhart, *Chem. Rev.*, 2000, **100**, 1169–1204.
- 6 O. G. Piringer and A. L. Baner, Eds., *Plastic Packaging*, Wiley-VCH Verlag GmbH & Co. KGaA, Weinheim, Germany, 2008.
- 7 T. C. Mun, *Production of Polyethylene Using Gas Fluidized Bed Reactor*, Hydrogen Processing, 2003.
- 8 C. Gabriel, *Einfluss der molekularen Struktur auf das viskoelastische Verhalten von Polyethylenschmelzen*, Shaker, Aachen, 2001.
- 9 A. J. Peacock, *Handbook of Polyethylene: Structures, Properties, and applications*, Dekker, New York, 2000.
- 10 C. Vasile, Ed., *Handbook of polyolefins*, Marcel Dekker, New York, NY, 2. ed., rev. and expanded., 2000.
- 11 M. H. C. M. van Boxtel and M. Busch, *Macromol. Theory Simul.*, 2001, **10**, 25–37.
- 12 S. W. Ewart, T. W. Karjala and M. Demirors, *J. Polym. Sci. A: Polym. Chem.*, 2017, **55**, 861–866.
- 13 J. B. P. Soares and T. F. L. McKenna, in *Polyolefin Reaction Engineering*, Wiley-VCH Verlag GmbH & Co. KGaA, Weinheim, Germany, 2012, pp. 1–13.
- 14 M. Busch, *Macromol. Theory Simul.*, 2001, **10**, 408–429.
- 15 C. Kiparissides, G. Verros and J. F. Macgregor, *J. Macromol. Sci., Part C: Polym. Rev.*, 1993, **33**, 437–527.
- 16 V. A. Bhanu and K. Kishore, *Chem. Rev.*, 1991, **91**, 99–117.
- 17 R. O. Symcox and P. Ehrlich, *J. Chem. Soc.*, 1962, **84**, 531–536.
- 18 Y. Tatsukami, T. Takahashi and H. Yoshioka, *Makromol. Chem.*, 1980, **181**, 1107–1114.

LITERATURE REVIEW

- 19 E. F. McCord, W. H. Shaw and R. A. Hutchinson, *Macromolecules*, 1997, **30**, 246–256.
- 20 W. Rungswang, K. Narkchamnan, N. Petcharat, B. Thitisak and T. Pathaweeisariyakul, *Polym. Bull.*, 2017, **74**, 3229–3242.
- 21 G. Luft, R. Kämpf and H. Seidl, *Angew. Makromol. Chem.*, 1983, **111**, 133–147.
- 22 G. Luft and M. Dorn, *Angew. Makromol. Chem.*, 1990, **174**, 119–130.
- 23 G. Luft, R. Kämpf and H. Seidl, *Angew. Makromol. Chem.*, 1982, **108**, 203–217.
- 24 D. Lignell, *Possibilities of autoclave LDPE process*, Theses and Publications, Arcada University of Applied Sciences, Helsinki, Finland, 2015.
- 25 A. Ndiripo, *Comparative Study on the Molecular Structure of Ethylene/1-octane, Ethylene/1-heptene and Ethylene/1-pentene Copolymer Using Advanced Analytical Methods*, Masters thesis, Stellenbosch University, Stellenbosch, 2015.
- 26 D. E. Axelson, G. C. Levy and L. Mandelkern, *Macromolecules*, 1979, **12**, 41–52.
- 27 Q. Zhang, P. Chen, X. Xie and X. Cao, *J. Appl. Polym. Sci.*, 2009, **113**, 3027–3032.
- 28 D. E. Axelson and K. E. Russell, *Prog. Polym. Sci.*, 1985, **11**, 221–282.
- 29 M. De Pooter, P. B. Smith, K. K. Dohrer, K. F. Bennett, M. D. Meadows, C. G. Smith, H. P. Schouwenaars and R. A. Geerards, *J. Appl. Polym. Sci.*, 1991, **42**, 399–408.
- 30 A. Ortín, B. Monrabal, J. Montesinos and P. del Hierro, *Macromol. Symp.*, 2009, **282**, 65–70.
- 31 A. Krumme, M. Basiura, T. Pijpers, G. Vanden Poel, L. C. Heinz, R. Bruell and V. B. F. Mathot, *Mater. Sci.*, 2011, **17**, 260–265.
- 32 W. W. Yau, *Polymer*, 2007, **48**, 2362–2370.
- 33 M. Wagner, K. Reiche, A. Blume and P. Garidel, *Pharm. Devl. Technol.*, 2013, **18**, 963–970.
- 34 S. Podzimek, *Light Scattering, Size Exclusion Chromatography, and Asymmetric Flow Field Flow Fractionation: Powerful Tools for the Characterization of Polymers, Proteins, and Nanoparticles*, Wiley, Hoboken, NJ, 2011.
- 35 W. W. Yau, A. Ortín and P. del Hierro, *LC GC North America*, 2011, 46–47.
- 36 B. Monrabal, J. Sancho-Tello, J. Montesinos, R. Tarín, A. Ortín and P. del Hierro, *High Temperature Gel Permeation Chromatograph (GPC/SEC) with integrated IR5 MCT detector for Polyolefin Analysis: a breakthrough in sensitivity and automation.*, In : The application Book, LCGC Europe, Chester, 2012.
- 37 M. J. Phiri, S. Cheruthazhekatt, A. Dimeska and H. Pasch, *J. Polym. Sci. A: Polym. Chem.*, 2015, **53**, 863–874.
- 38 F. M. Mirabella, *J. Liq. Chromatogr.*, 1994, **17**, 3201–3219.
- 39 L. Wild and G. Glöckner, in *Separation Techniques Thermodynamics Liquid Crystal Polymers*, Springer Berlin Heidelberg, Berlin, Heidelberg, 1990, vol. 98, pp. 1–47.
- 40 H. Pasch and M. I. Malik, *Advanced Separation Techniques for Polyolefins*, Springer International Publishing, Cham, 2014.
- 41 B. Monrabal, L. Romero, N. Mayo and J. Sancho-Tello, *Macromol. Symp.*, 2009, **282**, 14–24.
- 42 B. Monrabal, J. Sancho-Tello, N. Mayo and L. Romero, *Macromol. Symp.*, 2007, **257**, 71–79.
- 43 B. Monrabal, N. Mayo and R. Cong, *Macromol. Symp.*, 2012, **312**, 115–129.
- 44 C. L. P. Shan, W. A. deGroot, L. G. Hazlitt and D. Gillespie, *Polymer*, 2005, **46**, 11755–11767.
- 45 I. Amer, A. van Reenen and M. Brand, *Polym. Int.*, 2015, **64**, 466–476.
- 46 S. Cheruthazhekatt, D. D. Robertson, M. Brand, A. van Reenen and H. Pasch, *Anal. Chem.*, 2013, **85**, 7019–7023.
- 47 D. D. Robertson, R. Neppalli and A. J. van Reenen, *Polym. Test.*, 2014, **40**, 79–87.
- 48 A. J. Van Reenen, R. Brull, U. M. Wahner, H. G. Raubenheimer, R. D. Sanderson and H. Pasch, *J. Polym. Sci. A: Polym. Chem.*, 2000, **38**, 4110–4118.
- 49 R. Brüll, N. Luruli, H. Pasch, H. G. Raubenheimer, E. R. Sadiku, R. Sanderson, A. J. van Reenen and U. M. Wahner, *e-Polymers*, 2003, **3**, 785–793.
- 50 A. Prasad, *Polym. Eng. Sci.*, 1998, **38**, 1716–1728.
- 51 R. Brüll, H. Pasch, H. G. Raubenheimer, R. Sanderson, A. J. van Reenen and U. M. Wahner, *Macromol. Chem. Phys.*, 2001, **202**, 1281–1288.

LITERATURE REVIEW

- 52 M. Keating, I.-H. Lee and C. S. Wong, *Thermochim. Acta*, 1996, **284**, 47–56.
- 53 F. Zhang, J. Liu, Q. Fu, H. Huang, Z. Hu, S. Yao, X. Cai and T. He, *J. Polym. Sci. B: Polym. Phys.*, 2002, **40**, 813–821.
- 54 D. Cavallo, A. T. Lorenzo and A. J. Müller, *J. Polym. Sci. B: Polym. Phys.*, 2016, **54**, 2200–2209.
- 55 A. J. Müller and M. L. Arnal, *Prog. Polym. Sci.*, 2005, **30**, 559–603.
- 56 Y. Xue, S. Bo and X. Ji, *J. Polym. Res.*, 2015, **22**, doi.org/10.1007/s10965-015-0809-0.
- 57 M. Zhang and S. E. Wanke, *Polym. Eng. Sci.*, 2003, **43**, 1878–1888.
- 58 H. Pasch, *Polym. Adv. Technol.*, 2015, **26**, 771–784.
- 59 H. Pasch, M. I. Malik and T. Macko, in *Polymer Composites – Polyolefin Fractionation – Polymeric Peptidomimetics – Collagens*, eds. A. Abe, H.-H. Kausch, M. Möller and H. Pasch, Springer Berlin Heidelberg, Berlin, Heidelberg, 2012, vol. 251, pp. 77–140.
- 60 T. Macko, R. Brüll, R. G. Alamo, F. J. Stadler and S. Losio, *Anal. Bioanal. Chem.*, 2011, **399**, 1547–1556.
- 61 H. Pasch, L.-C. Heinz, T. Macko and W. Hiller, *Pure Appl. Chem.*, 2008, **80**, 1747–1762.
- 62 A. Ginzburg, T. Macko, F. Malz, M. Schroers, I. Troetsch-Schaller, J. Strittmatter and R. Brüll, *J. Chromatogr. A*, 2013, **1285**, 40–47.
- 63 R. Chitta, A. Ginzburg, G. van Doremaele, T. Macko and R. Brüll, *Polymer*, 2011, **52**, 5953–5960.
- 64 A. Ginzburg, T. Macko, V. Dolle and R. Brüll, *J. Chromatogr. A*, 2010, **1217**, 6867–6874.
- 65 S. Cheruthazhekatt, T. F. J. Pijpers, G. W. Harding, V. B. F. Mathot and H. Pasch, *Macromolecules*, 2012, **45**, 2025–2034.
- 66 A. Ortin, B. Monrabal and J. Sancho-Tello, *Macromol. Symp.*, 2007, **257**, 13–28.
- 67 J. B. P. Soares and International Conference on Polyolefin Characterization, Eds., *Polyolefin characterization: selected contributions from the conference: The First International Conference on Polyolefin Characterization (ICPC), Houston, TX (USA), October 16-18, 2006*, Wiley-VCH, Weinheim, 2007.
- 68 M. Zhang, D. T. Lynch and S. E. Wanke, *J. Appl. Polym. Sci.*, 2000, **75**, 960–967.
- 69 W. W. Yau, *Macromol. Symp.*, 2007, **257**, 29–45.
- 70 E. T. Hsieh and J. C. Randall, *Macromolecules*, 1982, **15**, 1402–1406.
- 71 Y. Xue, S. Bo and X. Ji, *Chin. J. Polym. Sci.*, 2015, **33**, 1000–1008.
- 72 S. Anantawaraskul, J. B. P. Soares and P. M. Wood-Adams, in *Polymer Analysis Polymer Theory*, Springer Berlin Heidelberg, Berlin, Heidelberg, 2005, vol. 182, pp. 1–54.
- 73 J. K. Jørgensen, Å. Larsen and I. Helland, *e-Polymers*, 2010, **10**, 1596–1612.
- 74 F. Francuskiewicz, *Polymer Fractionation*, Springer Berlin Heidelberg, Berlin, Heidelberg, 1994.
- 75 Y. Xue, S. Bo and X. Ji, *J. Polym. Res.*, 2016, **23**, DOI: 10.1007/s10965-016-1026-1.

3 Comprehensive Analysis of Branched Polyethylene: The Multiple Preparative Fractionation Concept

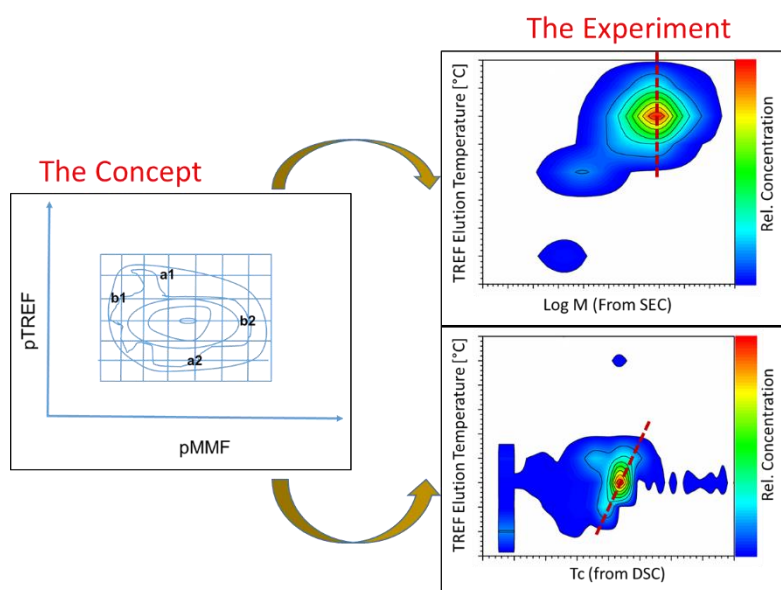


Figure 9: The multiple preparative fractionation: the concept versus the experiment.

In the first part of this study, the multiple preparative fractionation concept for the characterization of branched polyethylene was established. The concept entails the use of preparative temperature rising elution fractionation (pTREF) and preparative molar mass fractionation (pMMF) to fractionate branched polyethylene into narrow fractions with varying degrees of branching and different molar mass distributions, respectively. These fractions were further analysed by SEC, CRYSTAF and ^{13}C NMR to obtain molar mass and branching information.

Cross-correlation methods were established by combining pTREF/pMMF data with SEC and CRYSTAF data, which enabled the construction of two-dimensional contour diagrams, relating branching to molar mass. In addition, the selectivity of the different fractionation methods was evaluated. It was observed that pMMF provides narrowly dispersed molar mass fractions that exhibit broad branching distributions. Alternatively, pTREF provided fractions with narrow branching distributions but broad molar mass distributions.

A detailed discussion of this work has been published (**P. S. Eselem Bungu and H. Pasch, Polym. Chem., 2017, 8, 4565–4575.**) and is presented in this chapter.



Cite this: *Polym. Chem.*, 2017, **8**, 4565

Comprehensive analysis of branched polyethylene: the multiple preparative fractionation concept

P. S. Eselem Bungu  and H. Pasch  *

The branching distributions in low density polyethylene (LDPE) which originate from the radical polymerization processes can be expressed as short chain branching (SCB) and long chain branching (LCB). Since both molecular size and branching influence the physical properties of LDPE, structure–property correlations can be established only if these parameters are determined quantitatively. For the comprehensive analysis of branched polyethylene, we propose a multiple preparative fractionation approach. Using a representative low density polyethylene, we demonstrate how selective preparative fractionation provides fractions with different molar masses and branching architectures for offline analyses. More specifically, we show that preparative molar mass fractionation (pMMF) provides fractions with different molar masses but similar branching while preparative temperature rising elution fractionation (pTREF) can produce fractions with similar molar masses but different branching. These fractions (in mg quantities) can be analyzed consecutively by nuclear magnetic resonance, thermal analysis or micromechanics to yield selective and quantitative correlations between molecular size (molar mass), short chain and long chain branching.

Received 29th May 2017,
Accepted 2nd July 2017
DOI: 10.1039/c7py00893g
rsc.li/polymers

Introduction

Low-density polyethylene (LDPE) is a group of thermoplastic materials that is manufactured industrially from cheap ethylene feedstock *via* radical polymerization processes. These radical processes produce polymer chains with different branching architectures. The randomness in length and number of the branches often leads to the formation of multiple phase materials (amorphous, semi-crystalline and crystalline) with complex microstructures.

Typically, LDPE is a homopolymer that exhibits a molar mass distribution (MMD) and a branching (or molecular topology) distribution (BD). As a result of the radical polymerization process long chain branches (LCB) and short chain branches (SCB) are formed that are statistically distributed producing long and short chain branching distributions, LCBD and SCBD, respectively. The physical properties of LDPE (melting, crystallization, flow, toughness *etc.*) are determined by the correlation of MMD, LCBD and SCBD and, therefore, the quantitative analysis of these molecular parameters is of high relevance.

Typically, the MMD of polyolefins is analyzed by high-temperature size exclusion chromatography (HT-SEC).^{1–3} SEC fractionates polymers according to their hydrodynamic size in solution and for linear homopolymers, there is a direct corre-

lation between hydrodynamic size and molar mass. For linear copolymers, the hydrodynamic size is a function of molar mass and chemical composition while for branched homopolymers the hydrodynamic size depends on molar mass as well as the number and the length of the branches. For LDPE this means that true molar masses can be obtained from HT-SEC only if the branching structure is known. Depending on the desired information, different types of detectors are used in HT-SEC. Refractive index and infrared detectors are used as concentration detectors while more advanced detectors such as online viscometers (Visco) or light scattering (LS) detectors provide information on molecular size/molar mass.^{4–10} The chain branching as a function of hydrodynamic size can be analyzed by the coupling of HT-SEC and Fourier transform infrared spectroscopy (FTIR). This can be done using a flow cell that is placed in the FTIR spectrometer or using the LC Transform approach. With the LC Transform interface, SEC fractions are collected on a germanium disc which is later analyzed by FTIR using offline techniques.^{3,11–13} In SEC of LDPE, the major problem is that macromolecules with similar hydrodynamic sizes may have different molar masses depending on the BD. Branching increases the polymer coil density in solution leading to the situation in which low molar mass linear macromolecules have the same hydrodynamic size as high molar mass branched macromolecules. Those macromolecules cannot be fractionated by SEC and will instead, co-elute. Co-elution of linear and branched macromolecules is not limited to the low molar mass part of the molar mass distribution, however, it is most visible from the upcurving of the molar

Department of Chemistry and Polymer Science, University of Stellenbosch,
PO Box X1, 7602 Matieland, South Africa. E-mail: hpasch@sun.ac.za

CHAPTER 3

Paper

View Article Online
Polymer Chemistry

mass and size reading of the MALLS detector at the low molar mass part of the MMD.

For the analysis of branching in LDPE, several authors^{14–19} have highlighted the use of nuclear magnetic resonance (NMR) and FTIR as quick analytical tools. ¹³C NMR studies have shown that LDPE constitutes both short chain branches and long chain branches. The predominant types of short branches are *n*-butyl groups co-existing with smaller amounts *n*-ethyl and *n*-amyl groups. These short branches are presumably formed by intramolecular “backbiting” reactions of the growing chains. Branches longer than *n*-amyl, *i.e.* *n*-hexyl and longer by (¹³C NMR) definition are called long chain branches and may consist of tens or hundreds of ethylene repeating units. The resolution in ¹³C NMR is not sufficient to differentiate between LCBs of different lengths and the carbon signal at around 32.1 ppm is assigned to CH₂ groups of branches with six carbons and longer. Therefore, NMR is a very feasible method for SCB analysis but less powerful for the analysis of LCB.

One of the fundamental problems in polyolefin analysis is that the exact nature of LCB is still ill-defined. Considering Flory's theory, the thermodynamic properties and the elements governing phase structure of a copolymer (or a branched homopolymer) depend on the comonomer (branch) content incorporated and not the nature or size of the comonomer (branch) assuming that the comonomer (branch) is non-crystallizable (excluded from the crystal lattice). This was highlighted in a communication by van Reenen *et al.*^{20–22} whereby the melting point depression of propylene/higher α -olefin copolymers proved to be independent of the comonomer type but rather on the comonomer content incorporated. However, as soon as the branches are sufficiently long to crystallize (side chain crystallization), the physical properties will be influenced not only by the number but also by the length of branches. Therefore, SCB may influence the morphological and solid state properties of the polymer, but LCB impacts the rheological and processing properties most pronouncedly.^{3,21}

For the comprehensive analysis of the molecular heterogeneity of LDPE and the establishment of structure–property correlations, it is essential to determine the BD as a function of MMD. Both BD and MMD influence crystallinity, rheology and processing conditions of LDPE.

As has been demonstrated extensively, bulk LDPE can be fractionated regarding branching and molar mass by crystallizability-based and solubility-based methods, respectively. Typical crystallization-based fractionation techniques include temperature rising elution fractionation (TREF),^{3,23–25} crystallization analysis fractionation (CRYSTAF),^{1,25,26} crystallization elution fractionation (CEF)^{1,27,28} and solution crystallization by laser light scattering (SCALLS).^{26,29} Unfortunately, all these techniques suffer from co-crystallization effects and cannot be used for non-crystallizing (amorphous) components. More recently, Pasch *et al.*^{1,12,30,31} introduced high-temperature solvent gradient interactive chromatography (HT-SGIC), also known as high-temperature high-performance liquid chromatography (HT-HPLC). This technique is able to fractionate polyolefins according to their chemical composition or

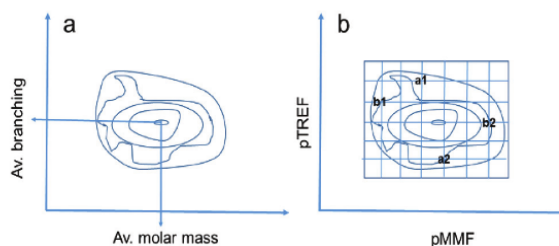


Fig. 1 Bulk sample analysis by NMR (average branching) and SEC (molar mass) (a) and multiple fractionations by pTREF (branching distribution) and pMMF (molar mass distribution) (b), a1, a2, b1, b2 present fractions with distinct BD and MMD.

branching irrespective of their crystallizability. Accordingly, this technique is a selective fractionation technique for both crystalline and non-crystalline materials.

A more comprehensive approach to evaluating molecular heterogeneity in terms of BD and/or MMD in heterogeneous systems is to perform fractionations on a preparative scale as in preparative TREF (pTREF),^{11,23,24,32} solvent gradient fractionation³³ and preparative molar mass fractionation (pMMF).³⁴ These techniques produce fractions in mg or g quantities that differ in branching (pTREF) and molar mass (pMMF) which can then be subjected to further analysis by NMR, FTIR or thermal analysis to provide in-depth information on branching and molar mass. Although all these techniques have their limitations, combining them in multiple fractionations and hyphenated techniques is the key to providing comprehensive microstructural information on LDPE.

The present study aims at presenting the feasibility of the multiple preparative fractionation concept. For one selected LDPE, multiple fractionations and analyses shall be conducted to show what specific molecular information can be obtained from each method. This approach shall be contrasted to the bulk analysis of the sample. The focus is on using pTREF and pMMF in combination with other advanced techniques like HT-HPLC, CRYSTAF, HT-SEC, and ¹³C NMR to map the distribution of both LCB and SCB, as well as to determine the branching content as a function of MMD. The multiple fractionation approach is schematically presented in Fig. 1. Different from the bulk analysis providing average branching and molar mass information irrespective of their distributions (Fig. 1a), the multiple fractionation approach produces fractions that are distinctively different in branching and molar mass, see fractions a1, a2, b1 and b2 in Fig. 1b. These are part of the bulk sample distributions but highlight certain parts of the samples more specifically.

Experimental section

Materials

Sasol Technology Ltd and PCD Linz (Austria) provided the branched and linear polyethylene (PE), respectively, used in

CHAPTER 3

View Article Online

Polymer Chemistry

Paper

this study. 1,2,4-Trichlorobenzene (TCB), 1-decanol, diethylene glycol monoethyl ether (DEGME), xylene and sea sand used in the analyses (except stated otherwise) were obtained from Sigma-Aldrich and were used as received. Table 1 summarizes the physical properties of the branched and the linear PE. For better comparison, samples with rather similar molar masses were selected. The molar masses (polystyrene equivalents) were determined by HT-SEC, the thermal properties were determined by DSC, the elution volumes (V_e) are from HT-HPLC.

High-temperature size exclusion chromatography (HT-SEC)

The samples were analysed using a PL 220 high-temperature chromatograph (Church Stretton, UK) equipped with a differential refractive index (RI) detector, three PLgel Olexis columns (300 mm \times 7.5 mm i.d.) and a PLgel Olexis guard column (50 \times 7.5 mm i.d.) (Agilent Technologies, UK) operating at 150 °C. The eluent 1,2,4-trichlorobenzene (TCB) stabilized with 2,6-*d*-tert-butyl-4-methylphenol (BHT, 0.0125%) was used at a flow rate of 1 mL min⁻¹. All samples (~2 mg) were dissolved in TCB (2 mL) for 1–2 hours and 0.2 mL of the solutions was injected. Linear polystyrene standards (Agilent Technologies, UK) with narrow MMD were used for calibration. The molar mass values reported for LDPE and the linear PE (PE 260 K hereafter) in Table 1 are polystyrene equivalents. All measurements were performed in triplicate.

GPC-IR-LS-VIS (GPC triple detector or GPC-3D) system

The long chain branching analysis was obtained using a high temperature PolymerChar GPC-IR system (Polymer Char Laboratories Ltd) equipped with a Wyatt Dawn Heleos II as LS detector, three Shodex UT 806 M columns, one Shodex UT 807 column and a Shodex UT-G guard column. The average particle sizes of all columns were 30 μ m. The experimental conditions were the same as stated for HT-SEC. The MALLS data were processed with the Astra software version 6.1.6.5 (Wyatt Technology). The data were processed via a Zimm plot of 1st order and a dn/dc value of $-0.1040 \text{ mL g}^{-1}$ was used for all the samples.

Crystallization analysis fractionation (CRYSTAF)

Crystallization from solution was monitored using a 200 Polymer Char S.A (Valencia, Spain) CRYSTAF instrument. Each analyte (~20 mg) was simultaneously dissolved in TCB (35 mL) in 5 stainless steel reactors with stirring at 160 °C. After the samples were completely dissolved (~150 min), the tempera-

ture of the reactor was reduced to 100 °C and stabilized for 60 min. The crystallization step was conducted by slowly reducing the solution temperature to 30 °C at a linear cooling rate of $0.1 \text{ }^\circ\text{C min}^{-1}$ to minimize the effect of co-crystallization. During the cooling stage, the solution concentration was measured as a function of temperature and the results were recorded using an infrared detector.

Differential scanning calorimetry

The thermal properties of the samples were determined using a TA Instruments Q100 DSC system, calibrated with indium metal standard. Calibration was done according to standard procedures and the melting and crystallization temperatures were measured under the same experimental conditions of heating and cooling at a scanning rate of $10 \text{ }^\circ\text{C min}^{-1}$ and a temperature ranging between 10–200 °C. The samples were subjected to three temperature cycles, with the first cycle (first heating) being used to erase the sample thermal history. The crystallization and melting temperatures reported in Table 1 were recorded during the first cooling and second heating cycles. After each cycle, the temperature was kept isothermal for 2 min. The measurements were conducted in a nitrogen atmosphere at a purge gas flow rate of 50 mL min^{-1} . All measurements were conducted in triplicate.

High temperature high performance liquid chromatography (HT-HPLC)

HT-HPLC chromatograms were obtained using a solvent gradient interactive chromatographic system (SGIC) constructed by Polymer Char (Valencia, Spain). The instrument is composed of an autosampler (which is a separate unit connected to the injector with a heated transfer line), two separate ovens, switching valves and two pumps which are equipped with vacuum degassers (Agilent, Waldbronn, Germany). For solvent gradient elution in HPLC, a high-pressure binary gradient pump was used. An evaporating light scattering detector (ELSD, model PL-ELS 1000, Polymer Laboratories, Church Stretton, England) was used with the following parameters: a gas flow rate of 1.5 SLM, 160 °C nebulizer temperature and an evaporation temperature of 270 °C. All samples were fractionated using a $100 \times 4.6 \text{ mm i.d.}$ Hypercarb column (Hypercarb®, Thermo Scientific, Dreieich, Germany) packed with porous graphite particles (particle diameter: 5 μ m; pore size: 250 Å and surface area: $120 \text{ m}^2 \text{ g}^{-1}$). The column temperature was maintained at 160 °C in the column oven. The mobile phase flow rate during analysis was 0.5 mL min^{-1} . To achieve separation, a linear gradient was applied from 100% 1-decanol to 100% TCB within 10 min after sample injection. The conditions were held for 20 min before re-establishing 1-decanol to 100 vol%. Samples were injected at a concentration of 1–1.2 mg mL⁻¹, using 20 μ L of each sample during analysis.

Carbon 13 nuclear magnetic resonance spectroscopy (NMR)

The ¹³C NMR analyses of the samples and fractions were carried out using a 600 MHz Varian Unity Inova NMR spectrometer at a resonance frequency of 150 MHz. All samples

Table 1 Physical properties of branched PE and linear PE

Sample	M_w^a (kg mol^{-1})	\bar{D}	T_c (°C)	T_m (°C)	X_c^b (%)
Branched PE ^c	338.9 ± 12	9.1	63.0 ± 0.2	111.2 ± 0.3	42.2
Linear PE ^d	402.9 ± 15	2.5	111.9 ± 0.1	134.6 ± 0.2	77.5

^a As determined by HT-SEC. ^b $X_c = (\Delta H_m / \Delta H_m^{\text{PE}} \times 100)$, 294 J g^{-1} .
^c LDPE. ^d HDPE.

CHAPTER 3

[View Article Online](#)

Paper

Polymer Chemistry

(~60 mg) were dissolved in deuterated 1,1,2,2-tetrachloroethane-d₂ (TCE-d₂) (95.5+ atom% D, Sigma-Aldrich). The TCE-d₂ was also used as an internal reference (74.3 ppm), and the analyses were performed at 120 °C.

Preparative temperature rising elution fractionation (pTREF)

Preparative TREF was carried out using an instrument build in-house. A dilute solution (~1 wt%) was made by dissolving the LDPE (3.0 g) in xylene (300 cm³) in a glass reactor at 130 °C. Irganox 1010 (2% w/w) (Ciba Speciality Chemicals, Switzerland) was added as a stabilizer to prevent thermo-oxidative degradation of the LDPE during the fractionation. The reactor was quickly immersed into a temperature-controlled oil bath and filled with a crystallization support (sea sand). The oil bath, the support, and the reactor were preheated and maintained at 130 °C to prevent the uncontrolled recrystallization of the LDPE. To ensure a controlled crystallization of the LDPE under the TREF conditions, the oil bath was cooled to ambient temperature (~25 °C) at a rate of 1 °C h⁻¹. The polymer-coated sand was transferred into a stainless steel column which was placed in a modified GC oven for elution. A continuous flow of preheated xylene was used to elute the polymer fractions as the oven temperature was raised at predetermined intervals. The eluted solutions (~500 cm³) were dried by evaporating the eluent using a rotor vap at a vacuum pressure of 30–40 mbar and then precipitating the fractions with acetone. The fractions were then dried under vacuum to a constant weight. The fractionation process was conducted in triplicate.

Preparative molar mass fractionation (pMMF)

The molar mass fractions were obtained by dissolving LDPE (3.0 g) in xylene solvent (300 mL) in a glass reactor for 1–2 h at 130 °C. The solution temperature was slowly reduced and maintained at the fractionation temperature of 115 °C. The non-solvent diethyleneglycol monoethylether, (DEGMEE) was slowly added to the polymer solution under stirring until a first stable cloud point was observed. The solution was left for 12 h to settle. The precipitate (first fraction) formed was slowly removed using a suction device, washed in acetone, filtered and dried to a constant weight under vacuum. The second fraction was obtained by adding DEGMEE (10 mL) to the polymer solution and the remainder of the fractions were obtained by increasing the volume of DEGMEE by 5 mL *i.e.* 10, 15, 20, 25, 30 mL for fractions 2 to 6, respectively, until no further precipitation was observed. Fraction 7 was obtained by precipitating the solubles by adding a substantial amount of acetone to the remaining solution at room temperature. The complete pMMF analysis, took about 4 day. The fractionation process was conducted in triplicate.

Results and discussion

Analysis of the bulk resin

Branching in polyethylene is typically analyzed by a variety of methods including fractionation and thermal analysis.

Measuring crystallizability by CRYSTAF and TREF or the melting and crystallization temperatures by DSC provides information on the decrease in crystallinity as compared to linear polyethylene as well as on the length of crystallizable segments in a given branched structure. HT-SEC coupled to multiangle laser light scattering (MALLS) measures the radius of gyration (R_g) as a function of molar mass. The deviation of the behaviour of a branched sample from the behaviour of a linear standard provides a branching index. The branching index, however, is typically valid only for higher molar masses. At the low end of the MMD, co-elution of linear and branched molecules occurs and a true branching index cannot be measured.

The results of the bulk sample analyses are presented in Fig. 2. In all cases, the behaviour of the branched PE is compared to a linear reference. The CRYSTAF curves for both the linear and branched PE shown in Fig. 2a display typical rather monomodal crystallization curves. The crystallization of PE from a dilute TCB solution is recorded at temperatures ranging between 30 and 100 °C. In this case, molecules that crystallize between 80 and 90 °C are considered to be highly crystalline and linear in nature. This behaviour is seen for the linear PE reference although small amounts of material crystallize at lower temperatures indicating some branching. On the other hand, the crystallization of the branched PE is observed at temperatures between 30 to 80 °C. The crystallization temperature depends on the degree of branching and to some extent on the molar mass. Components that mainly consist of extremely highly branched and/or very low molar mass species do not crystallize at temperatures above 30 °C and are presented as a rectangular box defined as the 'soluble part'.^{1,26,30,35} As shown in Fig. 2a, the linear PE exhibits a narrow crystallization profile around 85 °C and contains a relatively low amount of the soluble components. This is an indication for a highly linear PE. In contrast, the branched PE exhibits a broadband crystallization profile with a peak crystallization temperature of 63 °C.

A significant amount of non-crystallizing species was observed, indicating a high topological heterogeneity of the sample. Quantitative information on BD can be obtained only after fractionating the sample and analyzing the fractions by NMR since the CRYSTAF profile is influenced by both branching and molar mass.

Fig. 2b illustrates the DSC melting behaviour of the linear and branched PEs. The narrow and highly intense melting peak observed around 134 °C is typical of linear PE having a high crystallinity. In contrast, the branched counterpart exhibits a melting peak with lower intensity at around 111 °C indicating a material with low crystallinity. The difference in the melting temperatures is solely due to the presence of short and long chain branches, resulting in a shorter ethylene sequence backbone.^{3,14,35–37} From the melt enthalpies the percentage crystallinity (X_c) can be calculated which is 77.5% for linear PE and 42.2% for the branched sample, see Table 1.

HT-HPLC has been proven to provide quantitative information on the CCD of ethylene copolymers. The elution

CHAPTER 3

View Article Online

Polymer Chemistry

Paper

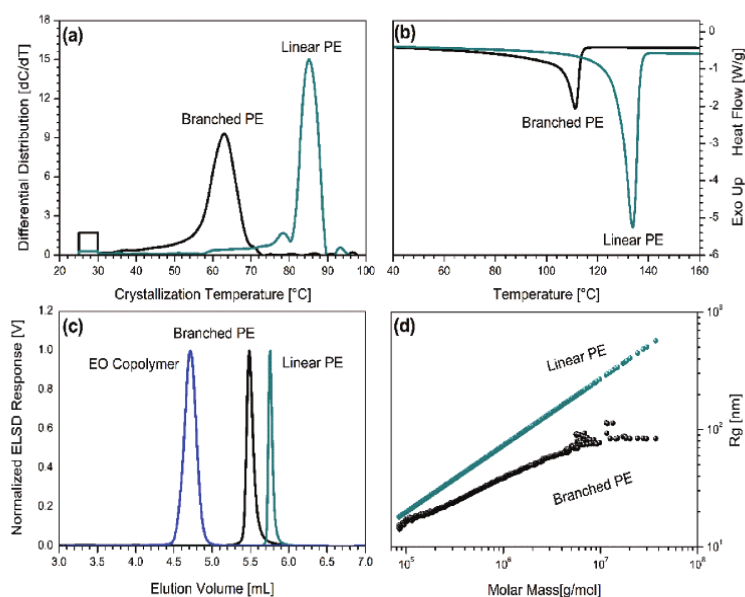


Fig. 2 Plots comparing the compositional differences of a branched LDPE (338.9 kg mol⁻¹) shown in black and a linear PE reference (402.9 K mol⁻¹) shown in green. (a) CRYSTAF analyses were performed in TCB at a cooling rate of 2 °C min⁻¹, (b) DSC melting endotherms were recorded at a heating rate of 10 °C min⁻¹, (c) HPLC elugrams were obtained using gradient elution from 100% 1-decanol to 100% TCB in 10 min at a flow rate of 0.5 mL min⁻¹ and a column temperature of 160 °C; the ethylene/1-octene copolymer (13.9 mol% octene) was used to show the typical behaviour of a short chain branched material; (d) SEC-IR-MALLS-Vis obtained in TCB, at a flow rate of 1 mL min⁻¹ and a column temperature of 150 °C.

volume can be directly related to the comonomer content in LLDPE. Not much is known so far about the behaviour of LDPE in HT-HPLC. The chromatograms displayed in Fig. 2c were used to investigate the structural and compositional differences between a linear and a randomly branched PE, and an ethylene/1-octene copolymer (13.9 mol% comonomer content). The separation is governed by the adsorption/desorption capabilities of the Hypercarb® (porous graphite particles) stationary phase at 160 °C and not the sample crystallizability. In the first step of the separation, the analyte is introduced into the column in the presence of a poor solvent. The polymer chains with longer uninterrupted ethylene sequences are strongly adsorbed by the porous graphite particles. The branched molecules with shorter ethylene sequences are adsorbed to a lesser extent. By introducing TCB (good solvent), the adsorbed chains are desorbed from the stationary phase and the molecules are eluted according to increasing ethylene sequence length. In the case reported in Fig. 2c, linear PE exhibits a narrow elution peak at 5.63 mL, indicating highly linear species of high homogeneity. On the other hand, the branched PE elutes earlier at 5.48 mL, with a slightly broader elution profile indicating some degree of heterogeneity in the sample. Lastly, the ethylene/1-octene copolymer interacts to the least extent with the stationary phase and exhibits a broader elugram at 4.72 mL. This is due to a high amount of comonomer incorporation (13.9 mol%) resulting in a high degree of SCB. The broadness of the elugrams indicate molecular heterogeneity. The HPLC observations correlate well with the

CRYSTAF and DSC findings reported in Fig. 2a and b, respectively, as well as with literature data.^{1,30,38} Similar to CRYSTAF, the elution behaviour in HT-HPLC is influenced not only by the molecular topology but also by molar mass. It is, therefore, essential to have molar mass information in addition to chemical composition information.

The molar mass analysis of the samples is conducted by HT-SEC coupled to a MALLS detector, see Fig. 2d. R_g for each SEC fraction was measured as a function of molar mass and was then compared to the linear reference sample of the same molar mass. The conformation plots relate R_g of the polymer molecules in solution to the molar mass (M) using eqn (1).

$$R_g = KM^\alpha \quad (\text{where } K \text{ and } \alpha \text{ are constants}) \quad (1)$$

For the linear reference material, typical values of the intercept (K) and the slope (α) of 0.029 and 0.57, respectively, were determined. An α value of 0.57 is typical of a random coil conformation of a linear PE. For the branched PE, in the low molar mass region the R_g reading is parallel to the linear reference but at lower K values indicating the presence of SCB. At molar masses above 10⁵ g mol⁻¹, the conformation plot for the branched PE deviates significantly from the linear reference as the molar mass increases, giving an α value of 0.36. Such α values correspond to randomly branched polymers. The large drift in the α value is mainly due to LCB. In the higher molar mass region above 10⁶ g mol⁻¹, the α value decreases further

CHAPTER 3

View Article Online

Paper

Polymer Chemistry

and may be explained by an increase in the degree of LCB as well as the size of the branches. One has to bear in mind that the SEC behaviour of branched polymers is complex and typically co-elution of linear and branched macromolecules takes place. Therefore, molar masses from SEC are rather apparent and not absolute molar masses. A more detailed investigation of the SEC behaviour of these samples will be the subject of a separate study. For a more detailed analysis of the branching structure, ^{13}C NMR spectroscopy was also used to determine and quantify the branch types and branching content of the branched sample as shown in Fig. 3 and Table 2.

The ^{13}C spectral peaks were assigned based on literature.^{2,3,14,37,39}

An isolated ethyl branch can be identified by the methyl carbon (CH_3) assigned as '2' resonating at 11.05 ppm. The assigned methylene carbons (CH_2) '4' and '5' resonating at 23.32 ppm and 32.64 ppm are used to identify the butyl and amyl branches, respectively.

The ethyl, butyl and amyl branches are referred to as SCBs. Branches with six carbon atoms and longer are referred to as LCB. This is because, the resolution in ^{13}C NMR is insufficient to differentiate branches longer than five carbon and are identified in the spectrum by the CH_2 carbon atom assigned as 6 resonating at 32.16 ppm. The content of each branch type calculated per thousand carbons (branch/1000C) was measured in accordance with Usami and others,⁴⁰ and the results are given in Table 2 show that the butyl branches constitute the highest amount (5.9/1000C), while the amyl branches were the lowest (0.1/1000C).

In conclusion, the analysis of the bulk sample with a variety of advanced analytical methods proved that single methods providing isolated information on molar mass and branching do not give a comprehensive picture on the molecular hetero-

Table 2 Branching information of Branched PE as obtained by ^{13}C NMR

Branch type	Ethyl (2)	Butyl (4)	Amyl (5)	LCB (6)	SCB	Total branches
Branching content (/1000C)	0.89	5.91	0.1	1.75	6.9	8.65
$\delta_{\text{(exp)}}$ (ppm)	11.05	23.32	32.64	32.16	—	—
$\delta_{\text{(lit)}}$ (ppm) ^{3,23}	11.25	23.61	32.94	32.42	—	—

$\delta_{\text{(exp)}}$ = experimental chemical shift; $\delta_{\text{(lit)}}$ = chemical shift reported in literature.

geneity of branched PE. Most essential information such as the correlation of MMD and BD can only be obtained *via* multiple (preparative) fractionation protocols. Preferably, fractionation according to molar mass, *e.g.* pMMF, should be combined with fractionation according to branching (crystallizability), *e.g.* pTREF, to provide fractions (A) with similar molar masses but different degrees of branching and (B) with similar degrees of branching but different molar masses for further studies

Preparative fractionation of branched PE

As is schematically shown in Fig. 1, branched PE consists of a huge variety of molecular species with distinct molar mass and branching distributions. Molecules with similar molar masses may be heterogeneous regarding branching just as molecules with similar branching may differ in molar mass. As can be seen in Fig. 1b, fractions a1 and a2 described molecular species within the bulk sample having distinct branching architecture but having similar molar mass. On the contrary, fraction b1 and b2 constitutes species with very close branch-

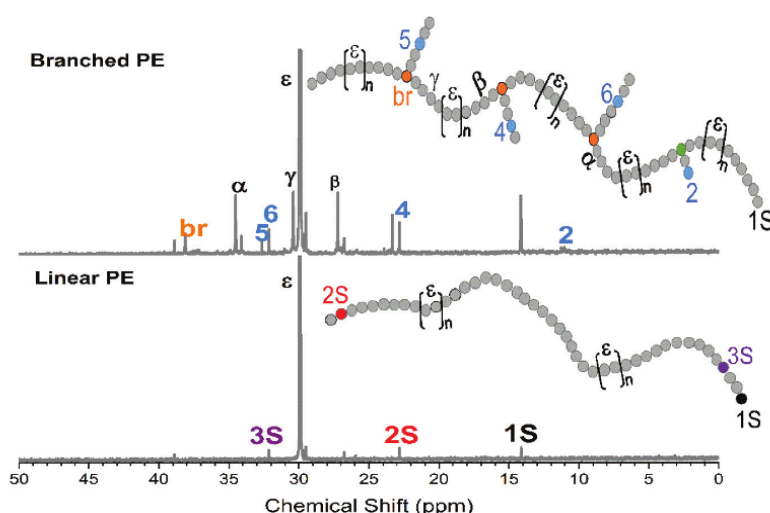


Fig. 3 High resolution ^{13}C NMR of linear and branched PE recorded in TCE-d_2 at 120°C . The chemical shift correction was achieved using TCE-d_2 peak as the internal Standard.

CHAPTER 3

View Article Online

Polymer Chemistry

Paper

ing, but differ significantly in the molecular sizes. Bulk sample analysis does not address these differences and very frequently the overall properties of the bulk resin only reflect the properties of the main components. The contributions of smaller components are often neglected.

In order to comprehensively elucidate the molecular heterogeneity of the branched PE, it was fractionated preparatively by TREF and MMF as indicated schematically in Fig. 1b. TREF permits the isolation of fractions which are different in the microstructure, while fractions with different molar masses irrespective of their microstructure are acquired *via* the MMF approach.

In the current study, pTREF fractions were collected at 30, 60, 70, 80, 90, and 130 °C. The weight percent (wt%) amount of each fraction is expressed as a function of the TREF elution temperature as shown in Fig. 4a. Here it can be seen that the 80 °C fraction is the major component and constitutes about 54.7 wt% of the bulk resin. The 30 °C and 130 °C fractions, which form the soluble and presumably the highly crystalline components, respectively, contribute about 2.4 and 1.6 wt% of the bulk and are, therefore, the minor components. The TREF distribution profile is comparable to the CRYSTAF profile shown in Fig. 2a which is in line with literature reports.^{27,32}

As for the pMMF experiments, fractions were obtained by titrating increasing amounts of a non-solvent to the polymer solution, to obtain fractions of different molar masses as described in the experimental part. The weight percent amount of each fraction is expressed as a function of the pMMF fraction number as shown in Fig. 4b. As can be seen, the relative amount of the fractions decreases with increasing pMMF fraction number which assumingly corresponds to decreasing molar masses of the fractions. It was noted that approximately 80 wt% of the resin were obtained from the first three precipitates (fractions 1–3) while the remaining 20 wt% constitutes fractions 4–7.

The pTREF and pMMF fractions were analysed by HT-SEC using standard conditions with a concentration detector (RI).

Accordingly, the presented MMDs are not true molar masses but polystyrene equivalents. Nonetheless, the molar mass trends are valid and provide important information on the molar mass differences of the fractions, see results in Fig. 5 and Table 3, respectively. With the exception of the 30 °C fractions which exhibit bimodal MMD, the pTREF fractions display monomodal MMDs. The 70 °C fraction exhibits a shoulder in the low molar mass region. It also forms the transition between the low-molar-mass low-crystallinity components (30 and 60 °C) and the high-molar-mass high-crystallinity components (80 and 90 °C).

Fig. 5b displays the individual MMDs for the pMMF fractions. As can be seen, the molar masses of the fractions decrease as the pMMF fraction number increases. A decrease in molar masses from 579.9 to 20.1 kg mol⁻¹ and dispersities from 4.4 to 2.7 were observed for pMMF fractions 1 to 7.

The relevance of the multiple fractionation approach can be seen clearly when the pTREF and pMMF fractions are analyzed by CRYSTAF. As is shown in Fig. 2 and 6, the CRYSTAF profile of the bulk sample is rather uniform indicating that the sample contains some non-crystallizable material along with components that crystallize between 40 and 70 °C.

The CRYSTAF curves for all individual pTREF and pMMF fractions are presented in Fig. 6. Comparing these curves with the crystallization curve of the bulk sample it is obvious that the fractions reveal more structural details. As can be seen in Fig. 6a, the 30 °C pTREF fraction consists mainly of soluble components as indicated by the rectangular peak around 30 °C. The 60 °C fraction shows a crystallization profile between 30 and 55 °C indicating a significant heterogeneity in branching while the 70 and 80 °C fractions exhibit rather narrow unimodal crystallization profiles. The 90 and 130 °C fractions on the other hand exhibit bimodal crystallization profiles that might indicate co-crystallizing species. As is clearly shown, the soluble (non-crystallizable) components within the fractions decrease with increasing TREF elution temperatures indicating a decrease in the amount of highly branched com-

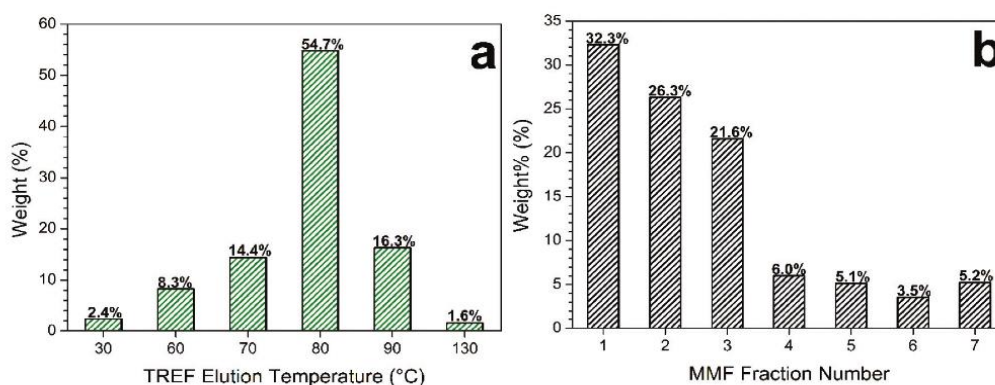


Fig. 4 Preparative fractionation of branched PE. (a) pTREF fractions were obtained by eluting the crystallized sample using xylene at a temperature between 30 to 130 °C. (b) pMMF fractions were precipitated from solution by stepwise increasing the amount of non-solvent at a solution temperature of 115 °C.

CHAPTER 3

View Article Online

Paper

Polymer Chemistry

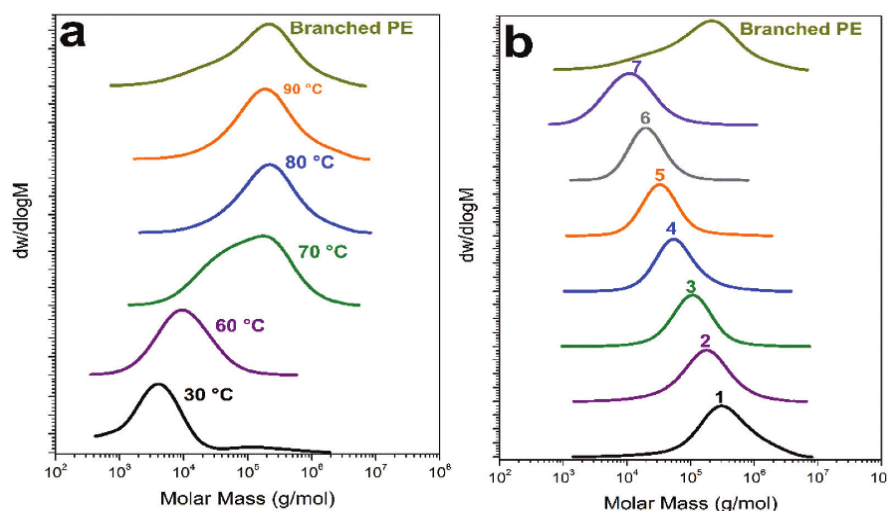


Fig. 5 MMDs obtained by HT-SEC of (a) the pTREF fractions and (b) the pMMF fractions. SEC data for the 130 °C fractions was omitted because the fraction was in limited amount at the time of the analyses.

Table 3 Data obtained from the analyses of the pTREF and pMMF fractions by HT-SEC-RI, DSC, CRYSTAF and HT-HPLC

Parameters	TREF elution temperature (°C)						LDPE (bulk)
	30	60	70	80	90	130	
M_w^a (kg mol ⁻¹)	25.4 ± 1.1	17.5 ± 1.1	235.7 ± 6.5	388.7 ± 9.6	385.5 ± 9.2	—	338.9 ± 8.6
M_n^a (kg mol ⁻¹)	2.4 ± 0.1	6.2 ± 0.2	42.7 ± 1.1	89.9 ± 3.1	78.4 ± 3.1	—	37.2 ± 1.1
\bar{D}	10.4	2.8	5.5	4.3	4.9	—	9.1
T_m (DSC) (°C)	84.3 ± 0.3	100.1 ± 0.3	108.6 ± 0.2	111.7 ± 0.1	113.7 ± 0.2	111.1 ± 0.2	111.2 ± 0.2
T_c (DSC) (°C)	76.1 ± 0.2	90.5 ± 0.2	95.5 ± 0.2	98.8 ± 0.1	101.8 ± 0.3	99.5 ± 0.3	98.6 ± 0.1
T_c (CRYSTAF) (°C)	—	49.6 ± 0.5	59.3 ± 0.5	63.7 ± 0.6	65.0 ± 0.6	63.5 ± 0.7	63.0 ± 0.6
X_c (DSC)	0.12	0.37	0.42	0.47	0.48	—	0.42
V_e^c (mL)	3.87	5.26	5.39	5.43	5.45	5.46	5.48

Parameters	MMF fraction number						
	1	2	3	4	5	6	7
M_w^a (kg mol ⁻¹)	579.9 ± 15.1	278.8 ± 8.2	165.5 ± 5.5	103.8 ± 4.1	55.7 ± 2.2	29.8 ± 0.6	20.1 ± 0.3
M_n^a (kg mol ⁻¹)	130.5 ± 4.1	77.2 ± 3.1	60.1 ± 2.2	41.0 ± 1.8	25.2 ± 1.1	16.4 ± 0.3	7.3 ± 0.1
\bar{D}	4.4	3.6	2.8	2.5	2.2	1.8	2.7
T_m (DSC) (°C)	109.2 ± 0.1	111.5 ± 0.1	112.3 ± 0.2	114.4 ± 0.2	114.6 ± 0.1	114.0 ± 0.2	109.2 ± 0.3
T_c (DSC) (°C)	96.8 ± 0.2	97.1 ± 0.1	98.1 ± 0.2	100.3 ± 0.2	102.6 ± 0.3	102.8 ± 0.2	101.6 ± 0.2
T_c (CRYSTAF) (°C)	63.8 ± 0.5	63.9 ± 0.6	65.0 ± 0.6	66.1 ± 0.7	65.7 ± 0.4	59.6 ± 0.5	49.6 ± 0.7
X_c	0.41	0.42	0.42	0.42	0.40	0.41	0.41
V_e^c (mL)	5.67	5.61	5.59	5.57	5.34	5.15	4.75

^a All molar data are polystyrene equivalents. ^b $X_c = (\Delta H_m / \Delta H_m^{PE} \times 100)$, 294 J g⁻¹. ^c V_e HPLC elution volume as detected by the evaporative light scattering detector (ELSD).

ponents in the same order. In general, the crystallization temperature increases with increasing TREF elution temperature and can be attributed to decreasing SCB. This result is in agreement with literature.^{32,41} A different picture is obtained for the pMMF fractions, as seen in Fig. 6b. The peak crystallization temperature of pMMF fractions 1–5 is almost the same. However, a broadening in the crystallization profiles and an increase in the non-crystallizing fraction is observed as the

pMMF fraction number increases. This correlates with the decrease in molar masses from fraction 1 to fraction 7.

In a next step, the data obtained by the preparative fractionations were combined with the HT-SEC (log M) and CRYSTAF (crystallization temperature) information in two-dimensional (2D) contour plots. The 2D contour plots were constructed by cross-combining (a) pTREF-SEC, (b) pTREF-CRYSTAF, (c) pMMF-SEC and (d) pMMF-CRYSTAF, see Fig. 7. A confirmation

CHAPTER 3

View Article Online

Polymer Chemistry

Paper

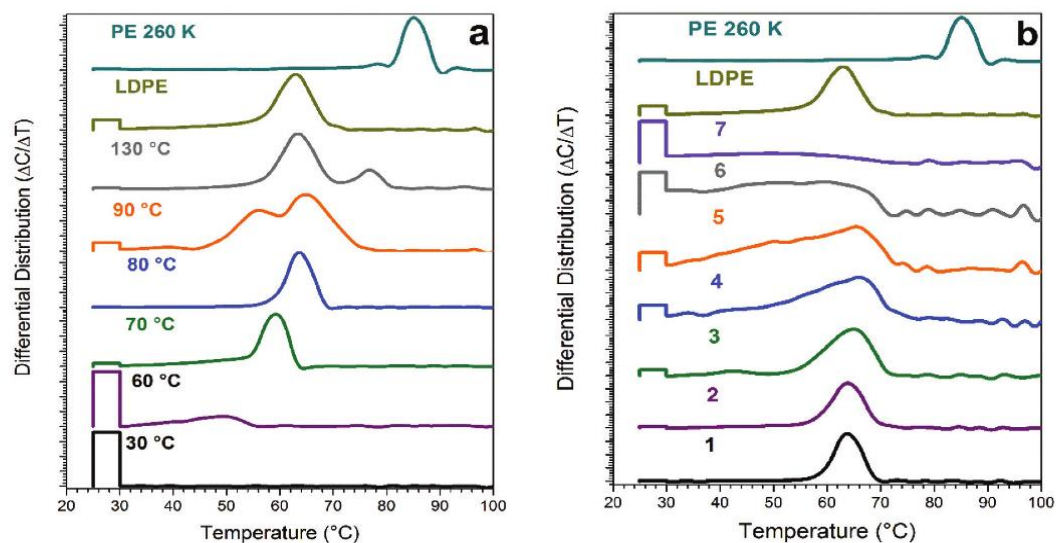


Fig. 6 CRYSTAF crystallization profiles as obtained in TCB between 100 and 30 $^{\circ}\text{C}$ at a cooling rate of 2 $^{\circ}\text{C min}^{-1}$. (a) pTREF fractions and (b) pMMF fractions.

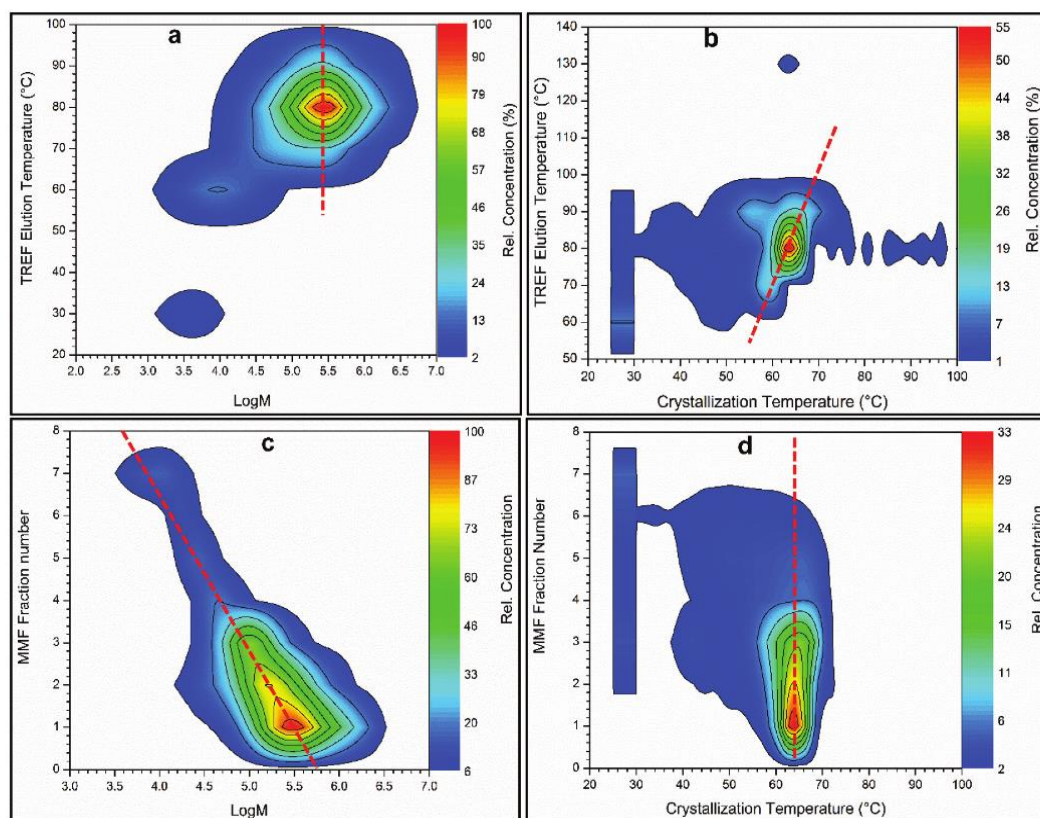


Fig. 7 Two-dimensional contour plots of branched PE showing (a) pTREF-SEC, (b) pTREF-CRYSTAF, (c) pMMF-SEC and (d) pMMF-CRYSTAF cross-fractionation.

CHAPTER 3

View Article Online

Paper

Polymer Chemistry

of the assumption that pMMF fractionates mainly with regard to molar mass is presented in Fig. 7c where a linear dependence is obtained between the MMF fraction number and $\log M$. This indicates that pMMF using the present experimental conditions is rather insensitive to branching. Accordingly, it can be assumed that from different bulk samples fractions can be obtained that have the same molar mass but different branching distributions. With this approach, the branching can be analyzed more selectively by ^{13}C NMR.

The fact that the different molar mass fractions have rather similar branching distributions can be seen in Fig. 7d, where for the highest molar mass fractions (pMMF fractions 1–5) similar peak maximum crystallization temperatures are obtained. For lower molar masses this is not the case since a significant broadening of the crystallization temperature range and an increase in the concentration of soluble (non-crystallizing) material is seen. The molar mass dependence of pTREF is seen in Fig. 7a. This plot indicates that the fractions eluting at low TREF temperatures have different and significantly lower molar masses than the fractions eluting at higher TREF temperatures. For these fractions, it can be assumed that TREF fractionation is influenced by both molar mass and branching distribution. For the fractions eluting at higher TREF temperatures, this is not the case indicating that at these conditions fractionation is mainly due to differences in the branching distribution. As can be seen in Fig. 7b, the TREF fractions show differences in the branching distribution. An increase in the peak maximum crystallization temperature is observed as the TREF elution temperature increases. The 60 °C fraction shows a high amount of non-crystallizable components. As the TREF elution temperature increases, the amount of the non-crystallizable components decreases and the fractions exhibit broader crystallization patterns indicating broad BD. A typical bimodal BD is observed for the 90 °C TREF fraction.

Conclusion

Low density polyethylene exhibits a complex branching structure in addition to the molar mass distribution. The branching structure is characterized by a statistical distribution of short chain (up to C_5) and long chain branches (C_6 and higher). The analysis of bulk samples by advanced methods including HT-SEC, HT-HPLC, CRYSTAF, DSC and ^{13}C NMR provides information on the molar mass distribution, branching and crystallizability/crystallinity but a correlation between these parameters using single method measurements is not possible.

To be able to correlate different molecular parameters, a multiple preparative fractionation approach is proposed. pTREF fractionates according to crystallizability and it is demonstrated that high molar mass fractions are obtained that are different in branching but similar in molar mass. Complementary, pMMF can be used to fractionate LDPE with regard to molar mass into fractions that are different in molar

mass but similar in branching. From both pTREF and pMMF fractions are obtained in mg quantities that can be subjected to further analyses, e.g. ^{13}C NMR, HT-HPLC and comprehensive HT-2D-LC. The aim of this work was to demonstrate the concept of multiple preparative fractionations. It is expected that the analysis of fractions (from different samples) that have similar molar masses but different branching or *vice versa* will provide significantly more detailed information on the branching structure and the correlation between molar mass and SCBD/LCBD. Such investigations will be the subject of a forthcoming study.

Acknowledgements

The authors would like to acknowledge the following people: Kristina Pflug and Professor Markus Busch for the GPC-3D analyses, Sasol Technology Ltd and PCD LINZ (Austria) for providing the branched and linear samples used in this project and the South Africa National Research Fund (NRF) for funding the project. Special thanks also go to Elsa Malherbe and Jaco Brand, Central Analytical Facilities (CAF) at Stellenbosch University for the NMR analyses.

Notes and references

- 1 H. Pasch, *Polym. Adv. Technol.*, 2015, **26**, 771–784.
- 2 Z. Dobkowski, *Fluid Phase Equilib.*, 1998, **152**, 327–336.
- 3 Y. Xue, Y. Fan, S. Bo and X. Ji, *Chin. J. Polym. Sci.*, 2015, **33**, 508–522.
- 4 P. Tackx and J. C. J. F. Tacx, *Polymer*, 1998, **39**, 3109–3113.
- 5 W. W. Yau, *Polymer*, 2007, **48**, 2362–2370.
- 6 H. Benoit and P. Doty, *J. Phys. Chem.*, 1953, **57**, 958–963.
- 7 C. Gabriel, *Influence of molecular structure on the viscoelastic behavior of polyethylene melts*, Shaker, Aachen, 2001.
- 8 S.-H. Yoo and J. Jane, *Carbohydr. Polym.*, 2002, **49**, 307–314.
- 9 P. M. Wood-Adams and J. M. Dealy, *Macromolecules*, 2000, **33**, 7481–7488.
- 10 J. D. Ferry, *Viscoelastic properties of polymers*, Wiley, New York, 3rd edn, 1980.
- 11 A. Krumme, M. Basiura, T. Pijpers, G. Vanden Poel, L. C. Heinz, R. Bruell and V. B. F. Mathot, *Mater. Sci.*, 2011, **17**, 260–265.
- 12 S. Cheruthazhekatt, G. W. Harding and H. Pasch, *J. Chromatogr., A*, 2013, **1286**, 69–82.
- 13 S. Cheruthazhekatt, T. F. J. Pijpers, G. W. Harding, V. B. F. Mathot and H. Pasch, *Macromolecules*, 2012, **45**, 2025–2034.
- 14 Q. Zhang, P. Chen, X. Xie and X. Cao, *J. Appl. Polym. Sci.*, 2009, **113**, 3027–3032.
- 15 D. E. Axelson, G. C. Levy and L. Mandelkern, *Macromolecules*, 1979, **12**, 41–52.
- 16 D. C. Bugada and A. Rudin, *Eur. Polym. J.*, 1987, **23**, 809–818.
- 17 M. E. A. Cudby and A. Bunn, *Polymer*, 1976, **17**, 345–347.

CHAPTER 3

[View Article Online](#)

Polymer Chemistry

Paper

- 18 H. N. Cheng, *Polym. Bull.*, 1986, **16**, 445–452.
- 19 M. De Pooter, P. B. Smith, K. K. Dohrer, K. F. Bennett, M. D. Meadows, C. G. Smith, H. P. Schouwenaars and R. A. Geerards, *J. Appl. Polym. Sci.*, 1991, **42**, 399–408.
- 20 A. J. Van Reenen, R. Brüll, U. M. Wahner, H. G. Raubenheimer, R. D. Sanderson and H. Pasch, *J. Polym. Sci., Part A: Polym. Chem.*, 2000, **38**, 4110–4118.
- 21 R. Brüll, H. Pasch, H. G. Raubenheimer, R. Sanderson, A. J. van Reenen and U. M. Wahner, *Macromol. Chem. Phys.*, 2001, **202**, 1281–1288.
- 22 R. Brüll, N. Luruli, H. Pasch, H. G. Raubenheimer, E. R. Sadiku, R. Sanderson, A. J. van Reenen and U. M. Wahner, *e-Polym.*, 2003, **3**, 785–793.
- 23 Y. Xue, S. Bo and X. Ji, *J. Polym. Res.*, 2015, **22**, 1–10.
- 24 M. J. Phiri, S. Cheruthazhekatt, A. Dimeska and H. Pasch, *J. Polym. Sci., Part A: Polym. Chem.*, 2015, **53**, 863–874.
- 25 B. Monrabal and P. del Hierro, *Anal. Bioanal. Chem.*, 2011, **399**, 1557–1561.
- 26 C. L. P. Shan, W. A. deGroot, L. G. Hazlitt and D. Gillespie, *Polymer*, 2005, **46**, 11755–11767.
- 27 B. Monrabal, L. Romero, N. Mayo and J. Sancho-Tello, *Macromol. Symp.*, 2009, **282**, 14–24.
- 28 B. Monrabal, J. Sancho-Tello, N. Mayo and L. Romero, *Macromol. Symp.*, 2007, **257**, 71–79.
- 29 S. Cheruthazhekatt, D. D. Robertson, M. Brand, A. van Reenen and H. Pasch, *Anal. Chem.*, 2013, **85**, 7019–7023.
- 30 A. Ndiripo, D. Joubert and H. Pasch, *J. Polym. Sci., Part A: Polym. Chem.*, 2016, **54**, 962–975.
- 31 R. Cong, A. W. deGroot, A. Parrott, W. Yau, L. Hazlitt, R. Brown, M. Cheatham, M. D. Miller and Z. Zhou, *Macromol. Symp.*, 2012, **312**, 108–114.
- 32 Y. Xue, S. Bo and X. Ji, *Chin. J. Polym. Sci.*, 2015, **33**, 1000–1008.
- 33 Y. Xue, S. Bo and X. Ji, *J. Polym. Res.*, 2016, **23**, 1–8.
- 34 J. K. er Jørgensen, A. Larsen and I. Helland, *e-Polym.*, 2010, **10**, 1596–1612.
- 35 A. Ndiripi, *Comparative Study on the molecular structure of ethylene/1-octene, ethylene/1-heptene and ethylene/1-pentene copolymers using advance analytical methods*, University of Stellenbosch, 2015.
- 36 H. Pasch and M. I. Malik, *Advanced Separation Techniques for Polyolefins*, Springer International Publishing, Cham, 2014.
- 37 A. Prasad, *Polym. Eng. Sci.*, 1998, **38**, 1716–1728.
- 38 T. Macko, R. Brüll, R. G. Alamo, F. J. Stadler and S. Losio, *Anal. Bioanal. Chem.*, 2011, **399**, 1547–1556.
- 39 J. N. Hay, P. J. Mills and R. Ognjanovic, *Polymer*, 1986, **27**, 677–680.
- 40 T. Usami and S. Takayama, *Macromolecules*, 1984, **17**, 1756–1761.
- 41 A. Ndiripo and H. Pasch, *Anal. Bioanal. Chem.*, 2015, **407**, 6493–6503.

4 Branching and Molar Mass Analysis of Low Density Polyethylene Using the Multiple Preparative Fractionation Concept

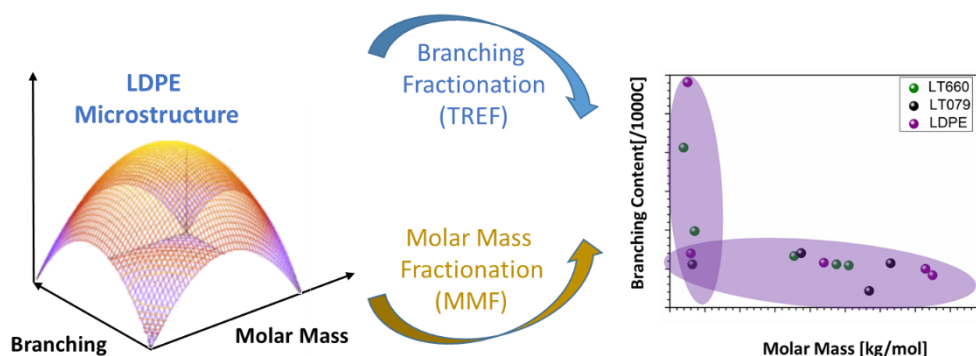


Figure 10: The multiple preparative fractionation concept provides sample libraries with different degrees of branching and different molar masses that are analysed regarding the LDPE microstructure

In the second part of this study, the multiple preparative fractionation concept was used to evaluate branching in low density polyethylenes (LDPE) having comparable average molar masses and branching, but exhibiting differences in crystallinity and melt flow indexes (MFI).

Bulk analysis of the samples using different advanced analytical methods was not able to explain the differences in crystallinity and MFI. Therefore, the resins were fractionated by pTREF and pMMF to obtain fractions with narrow branching and molar mass distributions, respectively. The fractions were then analysed using a set of analytical techniques, including SEC, CRYSTAF and ^{13}C NMR to obtain molar mass and branching information. Two-dimensional correlation diagrams constructed by combining pTREF/pMMF data with SEC and CRYSTAF revealed distinct microstructural differences between the different LDPEs.

As a result of the multiple fractionation approach, libraries were obtained with (A) samples having similar branching but different molar masses and (B) samples having similar molar masses but different branching. Correlation between molar mass and branching was obtained by plotting the molar mass data obtained by SEC against branching data obtained by ^{13}C NMR. Using CRYSTAF, DSC, HPLC and SEC-MALLS, library samples were compared that were similar in one property (e.g. molar mass) but distributed in another property (e.g. branching). This enabled to observe the effect of one property on polymer behaviour without the influence of the other property. This approach significantly enhanced the selectivity of the analytical investigations.

The details of this work have been published (P. S. Eselem Bungu and H. Pasch, *Polymer Chemistry*, **2018**, *9*, 1116–1131) and are presented in this chapter.



Cite this: *Polym. Chem.*, 2018, **9**, 1116

Branching and molar mass analysis of low density polyethylene using the multiple preparative fractionation concept

P. S. Eselem Bungu  and H. Pasch  *

Despite being a homopolymer, low density polyethylene (LDPE) exhibits a complex molecular structure that is determined by multiple molar mass and branching distributions. For a comprehensive microstructural analysis, preparative fractionation methods are combined with multiple advanced analysis techniques. Preparative temperature rising elution fractionation (pTREF) and preparative molar mass fractionation (pMMF) are used to fractionate three LDPE resins with different melt flow indexes into fractions with narrower branching and molar mass distributions, respectively. The chain structures of the bulk resins and their corresponding pTREF and pMMF fractions are further analyzed using size exclusion chromatography, crystallization analysis fractionation, differential scanning calorimetry, high-temperature solvent gradient interactive chromatography and SEC coupled to molar mass sensitive detectors to provide detailed information particularly on long chain branching and its correlation to molar mass. It is shown that the multiple fractionation concept is a powerful approach to generate LDPE sample libraries that may constitute fractions (samples) of comparable molar masses and different branching structures or alternatively have comparable branching but different molar masses. Cross-fractionation of these library samples with advanced analytical techniques provides in-depth information on the molecular heterogeneity of these samples as compared to bulk sample analysis.

Received 14th December 2017,
Accepted 7th February 2018

DOI: 10.1039/c7py02076g

rsc.li/polymers

Introduction

The advanced characterization of complex polyolefins has steadily gained impetus due to the increasing need to establish structure–property relationships for the design and manufacturing of novel or improved materials.^{1–5} Unlike natural polymers which frequently exhibit well-defined structural characteristics, the molar mass, chemical composition and molecular topology of *e.g.* polyolefins are distributed. In the case of ethylene polymerization, the processes (catalyzed or radical), the catalysts (Ziegler-Natta or single-site) and the reactor types (autoclave or tubular) all influence the obtained molar mass dispersities, chemical composition and topological complexity of the final product.^{6–11} Several experimental protocols which include the homopolymerization of ethylene, the copolymerization of ethylene with higher α -olefins, polymer grafting and polymer blending have been developed to generate polymer chains with different molecular properties as schematically shown in Fig. 1. These different approaches are essential to produce polyolefins that are designed for specific applications. Polymer architecture (branching and comonomer content) and

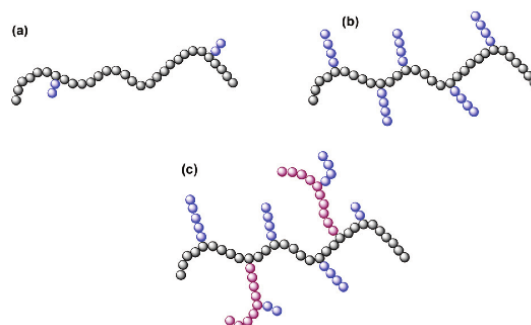


Fig. 1 Schematic representation of the molecular structure of (a) high density polyethylene, HDPE, and (b) linear low density polyethylene, LLDPE, produced *via* ethylene homopolymerization and copolymerization of ethylene and 1-hexene, respectively. Alternatively, low density polyethylene, LDPE (c), is produced by high-pressure radical polymerization of ethylene.

molar mass are the two main molecular parameters that determine the materials' properties. For a comprehensive molecular characterization of complex polyolefins, several analytical protocols have been developed to provide an in-depth picture of these complex molecules.^{6–9} Size exclusion chromatography

Department of Chemistry and Polymer Science, University of Stellenbosch, PO Box X1, 7602 Stellenbosch, South Africa. E-mail: hpasch@sun.ac.za

(SEC) fractionates polyolefins based on hydrodynamic volume. Using different detector setups (concentration- and molar mass sensitive detectors) molar mass distributions are determined *via* standard calibration^{1,2} or the direct measurement of weight (or viscosity) average molar masses by using multiple detector combinations such as triple detection (SEC-IR-MALLS-Vis).^{1,2,12,13} Here, SEC integrates a concentration detector (RI/IR), a multiangle light scattering detector (MALLS) and a viscometer (Vis) detector to measure absolute molar masses ($M_{w(ab)}$), radii of gyration (R_g) and intrinsic viscosities ($[\eta]$) for the eluting fractions. These parameters are processed further to evaluate long chain branching (LCB) as a function of molar mass. For short chain branching (SCB) and/or other functional group characterization, highly sensitive composition detectors such as Fourier transform infrared spectroscopy (FTIR) can be used.

Chain crystallinity is an important physical characteristic of polyolefins that is linked to polymer architecture (branching and comonomer content, tacticity, *etc.*) and molar mass. Advanced techniques such as crystallization analysis fractionation (CRYSTAF),^{1,2,14} crystallization elution fractionation (CEF),^{2,3,15} temperature rising elution fractionation (TREF),^{1,2,14,16,17} solution crystallization by laser light scattering (SCALLS)^{3,18,19} and differential scanning calorimetry (DSC)^{5,20} are extensively used to correlate the crystallization/melting behavior of a sample with its molecular properties. Unfortunately, most techniques suffer from co-crystallization/co-elution effects. On the other hand, only crystallizable components can be analyzed while amorphous material does only provide bulk information. High-temperature solvent gradient interaction chromatography (HT-SGIC) has been designed more recently to fractionate polymer chains according to linear ethylene sequence lengths irrespective of crystallinity or crystallizability.^{1,2,21–23} This analytical technique does not suffer from co-crystallization and is capable of analyzing both the amorphous and crystalline components of complex polymers.

The concept of multiple preparative fractionations combining *e.g.* temperature rising elution fractionation (pTREF) and molar mass fractionation (pMMF) was introduced in previously published works.^{1,24} Although both pTREF and pMMF do not provide monodisperse fractions, they do provide fractions that have significantly reduced heterogeneities in chemical composition/branching and molar mass, respectively. The techniques produce 'libraries' of fractions in mg to g amounts that can be analyzed further to obtain in-depth knowledge regarding the polymer microstructure. The interplay between the chemical composition/branching and molar mass contributes immensely towards the physical properties of the materials, however, it is very challenging to evaluate the effects of these parameters independently.

The current study aims at demonstrating the high relevance of the multiple preparative fractionation approach as compared to bulk sample analysis for the comprehensive analysis of low density polyethylene (LDPE). Using pMMF, 'homogenous' molar mass fractions shall be obtained that still

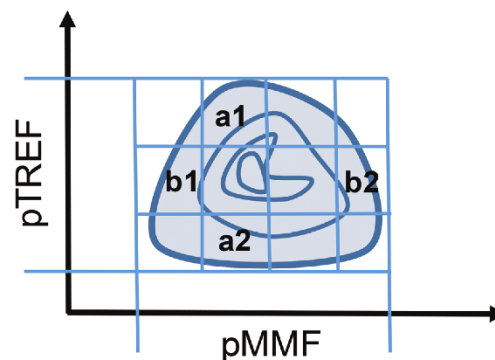


Fig. 2 Theoretical contour plot describing preparative fractions obtained by TREF with different branching but similar molar masses (*e.g.* a1 and a2) and MMF with different molar masses but similar branching (*e.g.* b1 and b2).

have a broad distribution of degrees of branching. Alternatively, pTREF will provide 'homogenously' branched fractions that might exhibit broad molar mass distributions as schematically shown in Fig. 2. The fractions a₁ and a₂ represent components with very similar molar masses but different branching, while b₁ and b₂ are fractions with similar branching frequencies but different molar masses. The multiple distributions of such fractions will be addressed using a range of advanced analytical methods.

Experimental

Materials and methods

Sasol Technology Ltd provided a set of LDPE resins (LT660, LT079 and LDPE) with different melt flow indexes (MFI), while PCD Linz (Austria) provided the polyethylene used as a linear reference. Except stated otherwise, the xylene, 1,2,4-trichlorobenzene (TCB), 1-decanol, diethylene glycol monomethyl ether (DEGME) and sea sand (50–70 MESH) used throughout this study were purchased from Sigma Aldrich and were used as received. The physical properties of the LDPEs are summarized in Table 1. The densities, MFIs, the reactors used as well as sample applications were obtained from the samples' data sheets. The molar masses (weight averages M_w), DSC melting and CRYSTAF crystallization temperatures were measured using HT-SEC, DSC and CRYSTAF, respectively. Information on the linear reference standard was reported in previously published work.¹

High-temperature size exclusion chromatography (HT-SEC)

The samples were analysed using a PL 220 high-temperature chromatograph (Church Stretton, UK) equipped with a differential refractive index (RI) detector, three PLgel Olexis columns (300 mm × 7.5 mm i.d.) and a PLgel Olexis guard column (50 × 7.5 mm i.d.) (Church Stretton, UK) operating at 150 °C. The eluent 1,2,4-trichlorobenzene (TCB) stabilized with 2,6-d-tert-

CHAPETR 4

View Article Online

Paper

Polymer Chemistry

Table 1 Summary of the physical properties of three LDPE resins

LDPE resins	LT660	LT079	LDPE
Density (g cm ⁻³) at 20 °C ^a	0.922	0.922	0.91–0.94
$M_{w(RI)}$ (kg mol ⁻¹) ^b	227.5	269.1	338.9
D^b	4.0	5.2	6.6
$M_{w(LS)}$ (kg mol ⁻¹) ^c	183.9	217.1	264.9
D^c	6.2	7.5	10.5
$T_c(\text{CRYSTAF})$ (°C)	60.1	61.3	63.0
$T_m(\text{DSC})$ (°C)	110.0	110.9	111.2
X_c^d	36.6	47.1	42.3
MFI (g per 10 min) ^a	2.0	0.75	—
Reactor ^a	Tubular	Tubular	—
Application ^a	General packaging (20 to 50 µm), clarity and thin film	General packaging (50 to 80 µm) and lamination film	—

^a Obtained from Sasol's product data sheet. ^b Determined by HT-SEC-RI, polystyrene equivalents. ^c Determined by GPC-LS. ^d $X_c = (\Delta H_m / \Delta H_m^{\text{PE}} \times 100)$, $\Delta H_m^{\text{PE}} = 293 \text{ J g}^{-1}$.

butyl-4-methyl phenol (BHT, 0.0125%) was used at a flow rate of 1 mL min⁻¹. All samples (~2 mg) were dissolved in TCB (2 mL) for 1–2 hours and 0.2 mL of the solutions were injected. Eleven linear polystyrene standards (Polymer Laboratories, Church Stretton, UK) with molar masses ranging from 0.58 to 6035 kg mol⁻¹ and narrow molar mass dispersities between 1 and 1.35 were used for calibration. The molar mass values reported for the branched polymers in Table 1 (as specified) and the fractions in Table 3 are polystyrene equivalents. All measurements were performed in triplicate.

SEC-triple detector system

Long chain branching analyses were obtained using a high-temperature PolymerChar GPC-IR system (Polymer Char Laboratories Ltd) equipped with an IR5 detector in hyphenation with a Wyatt Dawn Heleos II LS detector and an online Visco H502 viscometer detector, three Shodex UT 806 M columns, one Shodex UT 807 column and a Shodex UT-G guard column. The average particle sizes of all columns were 30 µm. The experimental conditions were the same as stated for HT-SEC. The MALLS data were processed with the Astra software version 6.1.6.5 (Wyatt Technology) and a dn/dc value of $-0.1040 \text{ mL g}^{-1}$ was used for all the samples.

Crystallization analysis fractionation (CRYSTAF)

Crystallization from solution was monitored using a Polymer Char (Valencia, Spain) CRYSTAF 200 instrument. Each analyte (~20 mg) was simultaneously dissolved in TCB (35 mL) in five stainless steel reactors with stirring at 160 °C. After the samples were completely dissolved (~150 min), the temperature of the reactor was reduced to 100 °C and stabilized for 60 min. The crystallization step was conducted by slowly reducing the reactor temperature to 30 °C at a linear cooling rate of

0.1 °C min⁻¹ to minimize the effect of co-crystallization. During the cooling stage, the solution concentration was measured using an infrared detector as a function of temperature and the results were recorded.

Differential scanning calorimetry (DSC)

The thermal properties of the samples were determined using a TA Instruments Q100 DSC system, calibrated with indium metal standard. Calibration was done according to standard procedures and the melting and crystallization temperatures were measured under the same experimental conditions of heating and cooling at a scanning rate of 10 °C min⁻¹ in a temperature ranging between 10–200 °C. The samples were subjected to three temperature cycles, with the first cycle (first heating) being used to erase the sample thermal history. The crystallization and melting temperatures reported in Table 1 were recorded during the first cooling and second heating cycles. After each cycle, the temperature was kept isothermal for 2 min. The measurements were conducted in a nitrogen atmosphere at a purge gas flow rate of 50 mL min⁻¹. All measurements were conducted in triplicate.

Carbon-13 nuclear magnetic resonance spectroscopy (¹³C NMR)

The ¹³C NMR analyses of the samples and fractions were carried out using a 600 MHz Varian Unity Inova NMR spectrometer at a resonance frequency of 150 MHz. All samples (~60 mg) were dissolved in 0.3 mL deuterated 1,1,2,2-tetrachloroethane-d₂ (TCE-d₂) (95.5+ atom% D, Sigma-Aldrich), making a sample concentration of ~200 mg mL⁻¹. TCE-d₂ was also used as an internal reference (74.3 ppm). The samples were pre-dissolved in the NMR tube to obtain a homogenous solution at 130 °C and were analysed overnight at 120 °C. The relaxation delay time (15 s), acquisition time (0.87 s), number of scans (3539) were used. The nomenclature and peak assignments used were in conformity with Xue and others.^{25–27}

High-temperature high-performance liquid chromatography (HT-HPLC)

HT-HPLC chromatograms were obtained using a solvent gradient interactive chromatographic system (SGIC) constructed by Polymer Char (Valencia, Spain). The instrument is composed of an autosampler (which is a separate unit connected to the injector with a heated transfer line), two separate ovens, switching valves and two pumps which are equipped with vacuum degassers (Agilent, Waldbronn, Germany). For solvent gradient elution in HPLC, a high-pressure binary gradient pump was used. An evaporative light scattering detector (ELSD, model PL-ELS 1000, Polymer Laboratories, Church Stretton, England) was used with the following parameters: a gas flow rate of 1.5 SLM, 160 °C nebulizer temperature and an evaporation temperature of 270 °C. All samples were fractionated using a 100 × 4.6 mm i.d. Hypercarb column (Hypercarb®, Thermo Scientific, Dreieich, Germany) packed with porous graphite particles (particle diameter: 5 µm; pore size: 250 Å and surface area: 120 m² g⁻¹). The column tempera-

CHAPETR 4

View Article Online

Polymer Chemistry

Paper

ture was maintained at 160 °C in the column oven. The mobile phase flow rate during analysis was 0.5 mL min⁻¹. To achieve separation, a linear gradient was applied from 100% 1-decanol to 100% TCB within 10 min after sample injection. The conditions were held for 20 min before re-establishing 1-decanol to 100 vol%. Samples were injected at a concentration of 1–1.2 mg mL⁻¹, using 20 µL of each sample during analysis.

Preparative temperature rising elution fractionation (pTREF)

Preparative TREF was carried out using an instrument built in-house. A dilute solution (~1 wt%) was made by dissolving the LDPE (3.0 g) in xylene (300 mL) in a glass reactor at 130 °C. Irganox 1010 (2% w/w) (Ciba Speciality Chemicals, Switzerland) was added as a stabilizer to prevent thermo-oxidative degradation of the LDPE during the fractionation. The reactor was quickly immersed in a temperature-controlled oil bath while adding sea sand (crystallization support). The oil bath, the support, and the reactor were preheated and maintained at 130 °C to prevent uncontrolled recrystallization of the molecules. To ensure controlled crystallization under the TREF conditions, the oil bath was cooled to ambient temperature (~25 °C) at a rate of 1 °C h⁻¹. The polymer-coated sand was transferred into a stainless steel column, which was placed in a modified GC oven prior to elution. A continuous flow of preheated xylene was used to elute the polymer fractions as the oven temperature was raised at predetermined intervals. The eluted solutions (~500 mL) were dried by evaporating the eluent using a rotary evaporator at a vacuum pressure of 30–40 mbar and then precipitating the fractions with acetone. The fractions were then dried under vacuum to a constant weight.

Preparative molar mass fractionation (pMMF)

The molar mass fractions were obtained by dissolving LDPE (3.0 g) in xylene solvent (300 mL) in a glass reactor for 1–2 h at 130 °C. The solution temperature was slowly reduced and maintained at the fractionation temperature of 115 °C. The non-solvent diethylene glycol methyl ether, (DEGME) was slowly added to the polymer solution under stirring until a first stable cloud point was observed. The solution was left for 12 h to settle. The precipitate (first fraction) formed was slowly removed using a suction device, washed in acetone, filtered and dried to a constant weight under vacuum. The second fraction was obtained by adding DEGME (10 mL) to the polymer solution and the remainder of the fractions were obtained by increasing the volume of DEGME by 5 mL *i.e.* 10, 15, 20, 25, 30 mL for fractions 2 to 6, respectively, until no further precipitation was observed. Fraction 7 was obtained by precipitating the solubles by adding excess acetone to the remaining solution at room temperature.

Results and discussion

Bulk sample analysis

Chain crystallinity is an important physical characteristic of polyolefins that is influenced most prominently by molar mass

and branching (short chain branching, SCB, or long chain branching, LCB). Previous studies highlighted that highly crystalline polyolefins exhibit long uninterrupted ethylene sequence backbones.^{1,3,28,29} Branches along linear polymer chains disrupt the chain linearity and therefore, crystallinity decreases. The decrease in crystallinity is dependent on the number and to an extent, the length of branches incorporated.^{8,20,30} In the current study, the branching of selected LDPE resins with similar molar masses but different MFIs will be studied using crystallization-based methods such as CRYSTAF and DSC. These techniques monitor the crystallization and melting behaviors of polymer chains as a function of temperature. Alternatively, HPLC will be used to separate PE chains regarding long linear ethylene sequences.^{1,2} To complement these techniques, NMR will be used to quantify the degree of branching of these samples. On the other hand, SEC will be used for molar mass determination. In a first step, all these techniques are used to analyze the bulk samples which is followed by preparative fractionations and subsequent analyses of the fractions.

The bulk samples analyses of the three LDPE samples are summarized in Fig. 3. Fig. 3a displays the molar mass distribution (MMD) curves that indicate that all samples have unimodal broad MMDs with a small shoulder at lower molar mass for sample LDPE. Samples LT660 and LT079 have similar molar masses while the molar mass of sample LDPE is slightly higher. The fact that LT660 and LT079 have similar molar masses but distinctively different MFIs indicates that they must have different branching structures.

The crystallization behavior of the bulk resins as measured by CRYSTAF is presented in Fig. 3b. A detailed description of the CRYSTAF crystallization procedure is reported in previously published work.¹ All three samples display unimodal crystallization profiles, with decreasing amounts of soluble (non-crystallizing) components from LDPE to LT660. For reference, a linear PE was also investigated exhibiting a narrow crystallization profile with a peak crystallization temperature at around 85 °C. This behavior is typical for a highly crystalline polyethylene structure constituting longer linear uninterrupted ethylene polymer sequences. In contrast, the LDPEs display rather broad crystallization profiles with peak crystallization temperatures ranging between 60 and 63 °C that can be ascribed to highly branched PE topologies.

DSC was also used to measure the melting behavior of the samples and similar behaviors were found. The melting endotherms in Fig. 3c were taken from the second heating cycle. The melting peak at 133 °C is typical of highly crystalline linear PE while the rather unimodal melting endotherms with peak melting temperatures between 110 and 111 °C are characteristic for branched PE homopolymers. The samples were analyzed further by HT-SGIC using a solvent gradient of 1-decanol/TCB. The principles governing the HPLC separation were described in previously published work.¹ The individual elugrams of the three branched resins along with a linear PE and a highly branched ethylene-1-octene copolymer (LLDPE, 13.9 mol% octene) are presented in Fig. 3d. The narrow peak

CHAPETR 4

Paper

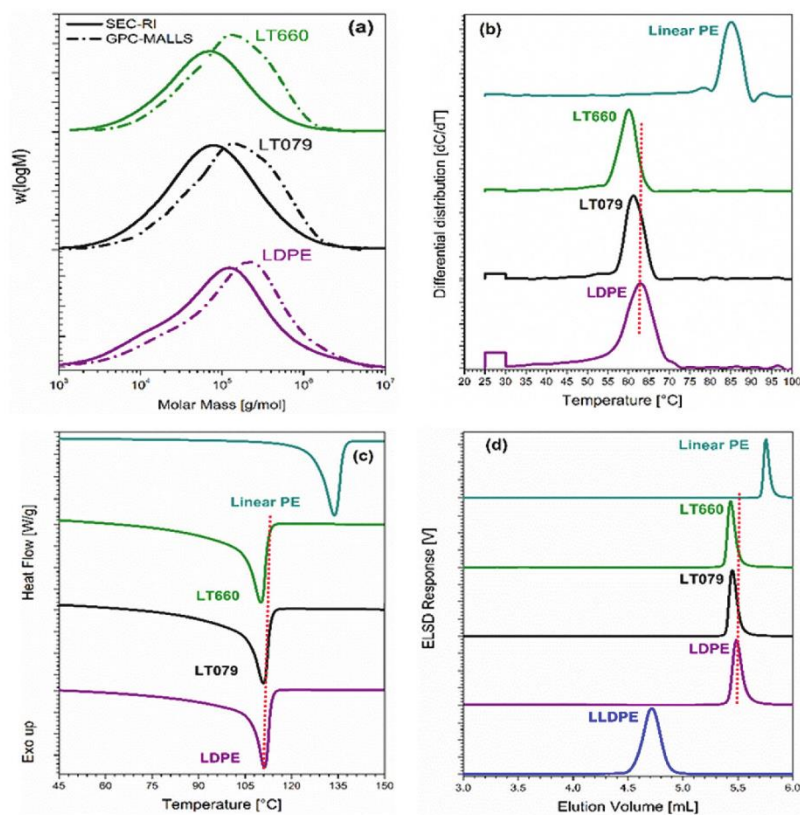
View Article Online
Polymer Chemistry

Fig. 3 Plots displaying characteristic behaviours of three branched PEs in comparison with the linear counterpart. (a) Molar mass distributions as obtained by HT-SEC and GPC-MALLS, (b) CRYSTAF crystallization profiles obtained in TCB, (c) DSC melting endotherms, (d) HPLC elugrams using solvent gradient HPLC.

observed around 5.76 mL is due to PE with a long linear backbone, while the broader elugram with a peak maximum at 4.71 mL is due to PE chains with a high degree of SCB (LLDPE). LT660, LT079 and LDPE, on the other hand, display broad elugrams at 5.44, 5.45 and 5.48 mL, respectively, which are a result of the complex branched structure of these samples. It is important to note that all these analytical results did not show any significant difference between samples LT660 and LT079 that could explain their different MFIs.

To understand the differences in the molecular structure of these branched resins, ^{13}C NMR experiments were conducted to obtain more quantitative branching information as presented in the spectra in Fig. 4. Based on previous reports and references therein,^{1,25,26,31–33} the peaks were assigned. The peaks labelled α , α_a , β , γ , ϵ , and br constitute the backbone carbons. The assigned peaks “a” and “b” are attributed to methyl (C_1) and ethyl (C_2) branches, while the peaks assigned as “c” and “e” are due to butyl (C_4) and amyl (C_5) branches, respectively. Branches longer than an amyl branch (*i.e.*, C_6 branch and longer) are referred to as LCB and are assigned as “d”. This particular signal may also constitute end-group carbons of the main chains. The peak assignments and

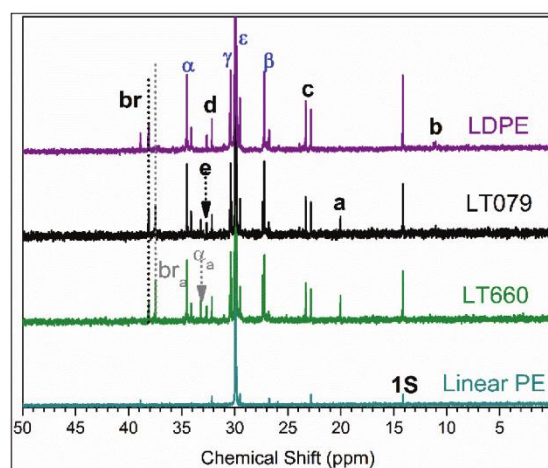


Fig. 4 ^{13}C NMR spectra of LDPE, LT079 and LT660 and a reference linear PE recorded in TCE-d_2 at 120 °C.

CHAPETR 4

View Article Online

Polymer Chemistry

Paper

Table 2 Branching information of LT660, LT079 and LDPE as determined by ^{13}C NMR spectroscopy, expressed as branches/1000C

Sample name	Branched type						Total branches
	Methyl	Ethyl	Butyl	Amyl	LCB	SCB	
LT660	1.78	—	3.98	0.42	2.83	6.18	9.0
LT079	2.2	—	4.81	0.31	2.23	7.32	9.65
LDPE	—	0.89	5.91	0.1	1.75	7.0	8.65
δ_{exp}	20.03	11.05	23.32	32.64	32.16	—	—
δ_{lit}	20.30	11.25	23.61	32.94	32.42	—	—

 δ_{exp} = experimental chemical shift, δ_{lit} = chemical shift reported in literature.^{25–27,31}

the respective chemical shifts are given in Table 2. Due to the given resolution and sensitivity of ^{13}C NMR spectroscopy, this technique is suitable for the analysis of SCB. It is less feasible, however, for LCB analysis since it cannot distinguish between different branches that are C_6 or longer.^{1,25}

Still, the technique is able to see differences between LT660 and LT079. LT660 having a higher MFI has a higher LCB/SCB ratio than sample LT079 with a lower MFI.

SEC with triple detection combining a concentration detector (RI) with two molar mass sensitive detectors (MALLS and Vis) is the most promising technique for LCB branching characterization of the bulk samples.^{1,13,34–36} This technique provides more detailed qualitative and quantitative information as it presents LCB as a function of molar mass. For more literature on this technique, consult previously published work.^{1,13,35,37,38}

For a linear polymer, there exists a linear relationship between the molecular size (or intrinsic viscosity) and molar mass as described by eqn (1) and (2).³⁴

$$R_g = 0.029 M^{0.57} \quad (1)$$

(where intercept $K = 0.029$ and the slope $a = 0.57$)

$$[\eta] = 5.3 \times 10^{-2} M^{0.703} \quad (2)$$

(where intercept $K = 5.3 \times 10^{-2}$ and the slope $\alpha = 0.703$).

In the case of a branched polymer, the molecular size is influenced not only by molar mass but also by the degree of LCB. For linear and branched polymers of the same molar mass, the presence of LCB is identified by the deviation of the conformation plot of branched molecules from their linear counterpart, most noticeable in the higher molar mass region. The conformation plots R_g vs. molar mass comparing the branched PE resins to an ideal linear PE of the same molar mass are presented in Fig. 5. For linear molecules in a thermodynamically good solvent typical intercept (K) and gradient (a) values of 0.57 and 0.029, respectively, were used.^{1,34} The conformation plots for LT660, LT079 and LDPE are divided into three molar mass segments as described by the rectangular boxes labelled 1–3, corresponding to the low (1), medium (2) and high (3) molar mass regions. At the low molar mass end of segment 1, LDPE and LT079 lie on the linear plot but are continuously deviating away from the linear plot as the molar mass increases. In contrast, the lower molar mass end of LT660 deviates from the linear plot and converges with the plots of the other branched samples towards the high molar mass end. This indicates that LT660 has a higher number of branches in the low molar mass region as compared to samples LDPE and LT079. Such branches might have a plasticizing effect, which would explain the higher MFI of this sample compared to LT079.

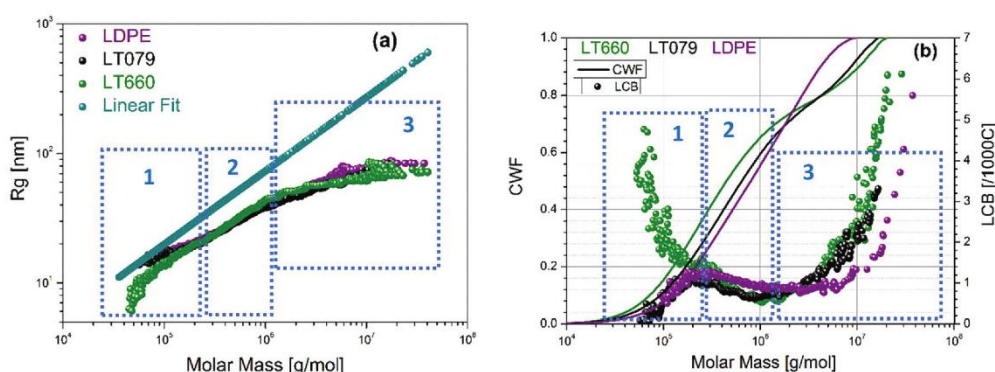


Fig. 5 Long chain branching information as determined by SEC-triple detection: (a) conformation plots and (b) LCB distribution plots. CWF is the cumulative weight fraction per molar mass that is obtained by integrating the individual molar mass distribution plots of the bulk resins presented in Fig. 3a.

CHAPETR 4

View Article Online

Paper

Polymer Chemistry

From the conformation plots, information on the number of long chain branches and the LCB frequency (LCBf) can be extracted. The calculations are based on eqn (3)–(5)^{11,13,34,35} that link the radii of gyration of the branched and linear macromolecules to the number of long chain branches (m) or LCBf.

$$g = \left[\frac{\langle Rg^2 \rangle_{Br}}{\langle Rg^2 \rangle_{Li}} \right]_M \quad (3)$$

$$g = \left[\left(1 + \frac{m}{7} \right)^{1/2} + \frac{4m}{9\pi} \right]^{-1/2} \quad (4)$$

$$\frac{LCB}{1000C} = \lambda = Rm \times \frac{1000}{M} \quad (5)$$

where, m = LCBf, long chain branching per molecule, $R = 14$, the factor of repeated molar mass units.

Again, the most remarkable difference between the samples is seen in the low molar mass region (segment 1) where the number of long chain branches for LT660 is significantly higher compared to LT079 and LDPE, see Fig. 5b. The amount of molecules within this molar mass segment correspond to ~18, 24 and 33 wt% of LDPE, LT079 and LT660, respectively. The high amount of highly branched low molar mass molecules in LT660 as found by triple detector SEC confirms the previous statement on MFI differences between LT660 and LT079.

Preparative fractionations

Although bulk analysis provides some qualitative branching and molar mass information, comprehensive information on all molecular parameters cannot be obtained. This is due to the fact that both molar mass and branching influence melting and crystallization (DSC, CRYSTAF) and cannot be separated from each other. On the other hand Fig. 5 shows that for the present samples LCBf is very complex and cannot be just described by triple detector SEC. Moreover, the contribution of smaller constituents within the bulk resins might be neglected when only bulk analyses are done. To be able to

compare fractions with similar branching and varying molar masses or similar molar masses but different branching, preparative fractionations to obtain fraction libraries are the most feasible approach. Therefore, further work follows a multiple preparative fractionation protocol. The bulk resins were fractionated preparatively by TREF to obtain fractions in mg to g amounts with narrow branching distributions, but broad molar mass dispersities. These fractions were obtained as described in Fig. 6a. Alternatively, fractions with narrow molar mass distribution but presumable broad branching dispersities were obtained preparatively through pMMF as schematically described in Fig. 6b. Fig. 7 presents the weight percentage distributions of the fractions as a function of elution temperature (pTREF) and fraction number (pMMF). For the TREF analysis, six fractions were collected between 30 and 130 °C. Comparable amounts of fractions for the different samples were obtained at 30, 60, 80 and 130 °C TREF elution temperature. The major differences were observed in the 70 °C and 90 °C fractions whereby fraction amounts of 35, 27 and 15 wt% (70 °C fraction) and 3, 6 and 17 wt% (90 °C fraction) were obtained for LT660, LT079 and LDPE, respectively, see Fig. 7a. Amounts of 52, 56 and 59 wt% for LT660, LDPE and LT079, respectively, were obtained for the 80 °C fractions forming the majority component of the bulk resins. As can be seen from the molar mass readings, the highly branched (low TREF temperature) fractions have low molar masses while the fractions of 70 to 130 °C which have lower degrees of branching have quite similar high molar masses. Alternatively, pMMF provided seven molar mass fractions obtained at solvent ratios between 0.38 and 0.95 v/v (see full details in Table 3). As can be seen clearly, for all samples a trend to lower molar masses with increasing fraction number is observed. This proves the high selectivity of pMMF regarding molar mass fractionation. The main difference in the pMMF fractions of the different samples is observed in fractions 3, which constitute about 12, 17 and 22 wt% of LT660, LT079 and LDPE, respectively. Fractions 1 to 3 form the majority components with combined weight percentages of 76, 80 and 82 wt% for LT660, LDPE and LT079, respectively.

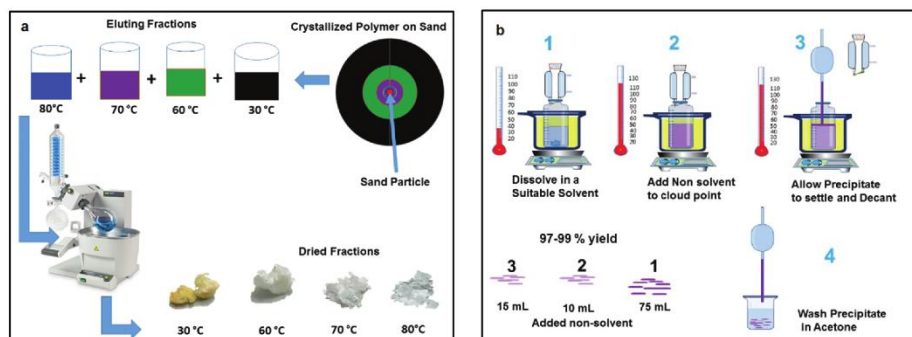


Fig. 6 Schematic representation of the preparative fractionation processes corresponding to (a) pTREF and (b) pMMF. Experimental details are given in the experimental section.

CHAPETR 4

View Article Online

Polymer Chemistry

Paper

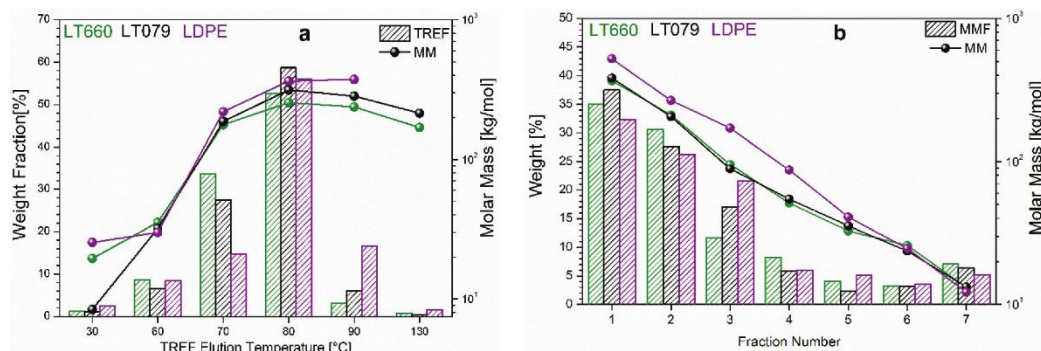


Fig. 7 Results of pTREF (a) and pMMF fractionations (b). Weight percentages and corresponding molar masses of fractions of LDPE, LT660 and LT079 as a function of (a) TREF elution temperature and (b) MMF fraction number.

Analysis of preparative fractions

SEC-RI was used for the molar mass analysis of the preparative fractions. The molar mass distribution curves for the TREF fractions are presented in Fig. 8a–c. As clearly seen, three main molar mass fractions could be identified corresponding to the 30, 60 and 70–130 °C TREF elution temperatures, respectively. Correlating their molar masses to that of the bulk sample, it is evident that the molar mass of the bulk resin corresponds well to the molar masses of the fractions eluting between 70 and 130 °C TREF temperatures which are the majority fractions. Evidently, the three resins display rather similar molar mass distribution patterns. The MMDs for the MMF fractions are presented in Fig. 9a–c. The molar masses of the MMF fractions decrease with an increase in the non-solvent ratio, *i.e.* an increase in the MMF fraction number from 1 to 7. With increasing non-solvent ratio, the molar masses shift to lower values. Noticeably, all samples display similar molar mass patterns, a clear indication that MMF is highly selective towards molar mass and not branching. The molecular parameters of the TREF and MMF fractions are summarized in Table 3. From these data, bivariate distribution plots can be constructed that give a more detailed idea on the differences between different samples. More importantly, they provide useful information on the selectivity of different methods to exhibit these differences. The bivariate plots were constructed by combining SEC and MMF data (Fig. 10a and b) or SEC and TREF data (Fig. 10c and d) for LT660 and LT079, respectively. Similar plots for LDPE were reported in previously published work.¹ The comparison of the different plots provides a number of interesting observations regarding differences between the two samples. The TREF-SEC plots look rather identical and do not reveal any differences between the samples. It is important to note that the higher TREF fractions (70 °C and higher) all exhibit similar molar mass distributions. This indicates that those fractions are fractionated primarily according to branching and the molar mass (as long as it is sufficiently high) does not play a dominating role. Only for the lower

(highly branched) TREF fractions, the molar mass influence can be seen clearly. The MMF-SEC plots also exhibit a high degree of similarity. However, for sample LT660 a bimodality is seen at high molar masses (Fig. 10a) while for sample LT079 a rather continuous decrease in molar mass with increasing fraction number is observed (Fig. 10b). This difference shall be explored further at a later stage.

To further study the structural differences between the prep fractions, the crystallization behaviour of the fractions was monitored using CRYSTAF. The 2D contour plots presented in Fig. 11a–d represent bivariate distributions of LT660 and LT079 that were constructed by cross combining CRYSTAF and MMF data as shown in Fig. 11a and b as well as CRYSTAF and TREF data as given Fig. 11c and d, respectively. Compared to the bivariate distribution plots in Fig. 10, the plots presented in Fig. 11 show very clear differences between the samples. The most obvious difference between samples LT660 and LT079 as seen in the CRYSTAF-MMF plots is the bimodality in crystallization for MMF fraction 2 of sample LT660. This distinct difference could not be observed when analysing the bulk resins. The components crystallizing at 50 °C assumingly have a higher degree of branching as compared to the bulk of the fraction crystallizing at 62 °C. It is important to note that all MMF fractions exhibit the same peak max crystallization temperature although their molar masses are distinctively different. This observation confirms a previous statement that MMF is fractionating predominantly according to molar mass and is rather insensitive to branching. In a similar way, the CRYSTAF-TREF plots reveal distinct differences between the samples. Apart from the differences in the amounts of soluble material (rectangular band at 30 °C that does not crystallize) the slopes in the TREF-CRYSTAF plots are different, see Fig. 11c and d.

This is a clear indication that the TREF fractionation behavior of the two samples is different. This is in agreement with previous findings that the chemical composition/branching of the bulk sample influences TREF fractionation. As a consequence, at similar TREF elution temperatures fractions of

CHAPETR 4

View Article Online

Paper

Polymer Chemistry

Table 3 Molecular parameters of the MMF and TREF fractions and comparison to the bulk resins

MMF fractions								
Fraction number	SR ^a (v/v)	Sample name	M _w ^b (kg mol ^{−1})	Đ	Branching ^c (/1000C)	T _m ^d (°C)	T _c ^e (°C)	X _c (%)
Bulk	—	LT660	223.5	4.0	9.0	110.0	60.1	36.5
		LT079	260.1	5.2	9.6	110.9	61.3	47.0
		LDPE	313.9	6.6	8.7	111.2	63.0	42.2
1	0.38	LT660	367.6	2.7	19.7	107.8	61.0	40.5
		LT079	384	2.2	9.2	109.3	62.5	39.2
		LDPE	523.2	2.6	10.2	109.2	63.8	41.3
2	0.43	LT660	211.5	2.0	8.1	109.4	61.8	39.2
		LT079	206.3	1.8	10.7	109.9	62.0	40.4
		LDPE	267.1	3.2	9.8	111.5	63.9	42.0
3	0.50	LT660	95.5	1.9	12.7	110.0	61.4	39.5
		LT079	89.2	1.6	11.1	111.2	61.0	45.0
		LDPE	171.7	2.2	8.9	112.3	65.0	42.0
4	0.60	LT660	51.1	1.7	11.1	112.1	60.9	45.7
		LT079	54.5	1.4	10.4	113.2	62.6	42.2
		LDPE	87.3	1.6	22.9	114.4	66.1	42.0
5	0.75	LT660	32.7	1.3	13.0	113.2	60.9	47.0
		LT079	35.4	1.3	11.1	114.3	61.9	45.4
		LDPE	40.8	1.4	18.1	114.6	65.7	40.0
6	0.95	LT660	25.9	1.3	14.7	113.2	62.2	49.0
		LT079	23.7	1.2	11.4	114.6	63.8	47.6
		LDPE	24.7	1.4	15.6	114.0	59.6	41.0
7	Excess acetone	LT660	13.2	1.7	15.0	111.3	59.8	49.2
		LT079	13.3	1.6	14.1	112.2	57.9	44.2
		LDPE	12.2	1.8	16.8	109.2	49.6	41.0

TREF fractions							
Elution temp. (°C)	Sample name	M _w kg mol ^{−1}	Đ	Branching (/1000 C)	T _m (DSC) (°C)	T _c (CRYSTAF) (°C)	X _c (%)
30	LT660	19.5	6.5	41.3	69.7	—	16.8
	LT079	8.4	3.0	—	73.1	—	26.8
	LDPE	25.4	10.4	58.1	84.3	—	12.3
60	LT660	35.3	2.5	19.7	101.5	52.7	44.9
	LT079	32.0	2.5	11.15	100.9	52.6	46.7
	LDPE	30.0	2.6	14.0	100.1	49.6	37.3
70	LT660	177.3	3.0	13.3	107.7	58.3	44.2
	LT079	187.3	4.6	14.0	107.9	60.1	46.9
	LDPE	219.7	5.2	11.6	108.6	59.3	42.3
80	LT660	255.2	3.2	10.9	109.8	61.6	44.5
	LT079	315.0	3.5	11.4	109.9	62.4	41.0
	LDPE	364.6	3.8	10.1	111.7	63.7	46.5
90	LT660	237.6	2.8	11.2	110.4	61.2	40.4
	LT079	284.3	3.3	4.3	110.9	62.0	40.7
	LDPE	374.7	3.6	8.3	113.7	65.0	47.8
130	LT660	169.3	36.8	—	100.7	—	—
	LT079	214.6	3.6	—	108.4	—	—
	LDPE	—	—	—	111.1	63.5	-

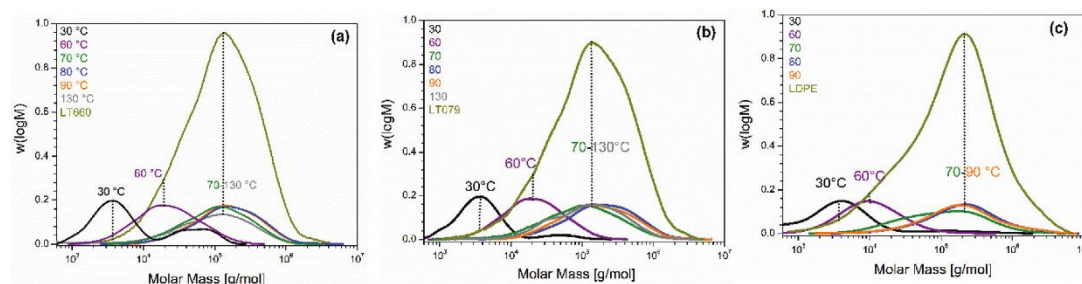
^a Non-solvent to solvent ratio. ^b From SEC. ^c From ¹³C NMR. ^d From DSC. ^e From CRYSTAF.

Fig. 8 MMD curves comparing the TREF fractions to the bulk resins, (a) LT660, (b) LT079 and (c) LDPE.

CHAPETR 4

View Article Online

Polymer Chemistry

Paper

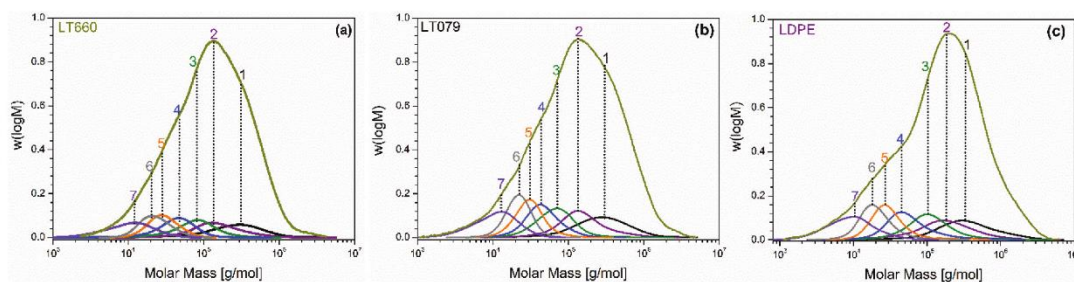


Fig. 9 MMD curves comparing MMF fractions to the bulk resins, (a) LT660, (b) LT079 and (c) LDPE.

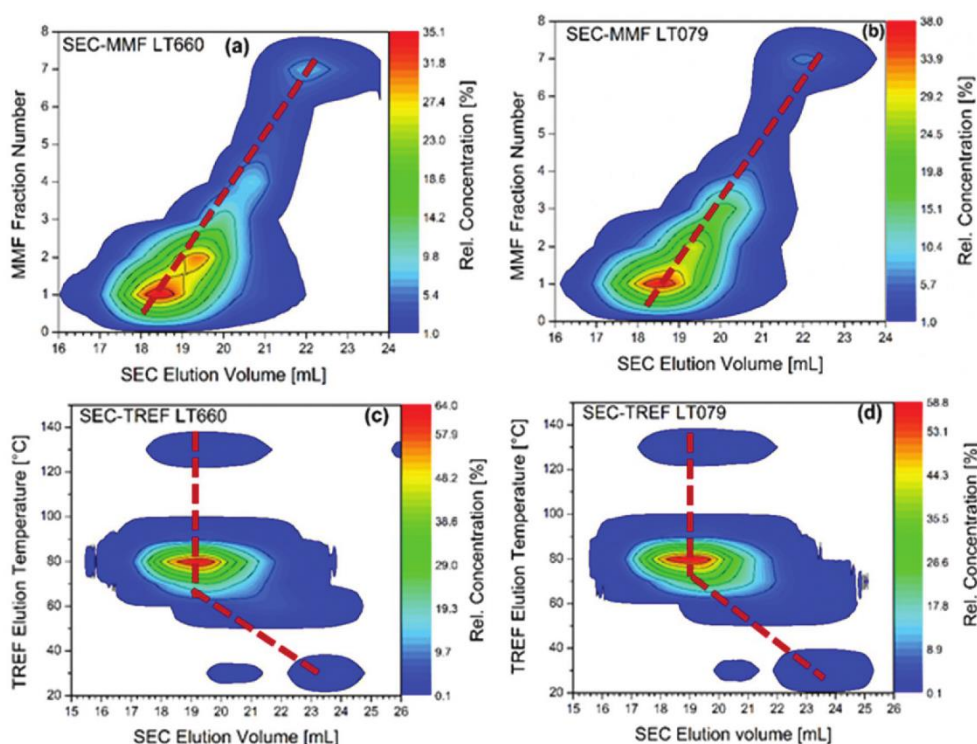


Fig. 10 Bivariate distribution plots of LT660 and LT079 obtained by combining SEC-MMF (a, b) or SEC-TREF data (c, d). Samples LT660 (a, c) and LT079 (b, d).

different compositions are obtained. This is most obviously seen in the 80 °C TREF fractions. In the case of LT660, a bimodal CRYSTAF profile between 53 and 60 °C is obtained while for the same fraction of LT079 a monomodal CRYSTAF profile at 62 °C is seen. In addition, these fractions contain a small amount of material crystallizing at 35 °C. The CRYSTAF data for the 30 and 130 °C fractions were omitted due to insufficient amounts of materials. Generally, it is seen that for LT660 the crystallization temperature range spreads from 35 to 80 °C while for LT079 the spread is much lower from 50 to 75 °C. As has been stated earlier in this study, sample LT660

seems to have a significantly broader and more complex branching distribution.

The individual prep fractions were analysed regarding branching by ^{13}C NMR spectroscopy and the branching frequencies (number of branches per 1000C) were calculated from the NMR spectra in accordance with the procedure described in previously published works and references therein.^{1,32,33,39,40} These results are summarized in Table 3. Based on the NMR and the SEC results of the MMF and TREF fractions, fraction libraries are compiled and presented as library plots degree of branching vs. molar mass, see

CHAPETR 4

Paper

View Article Online

Polymer Chemistry

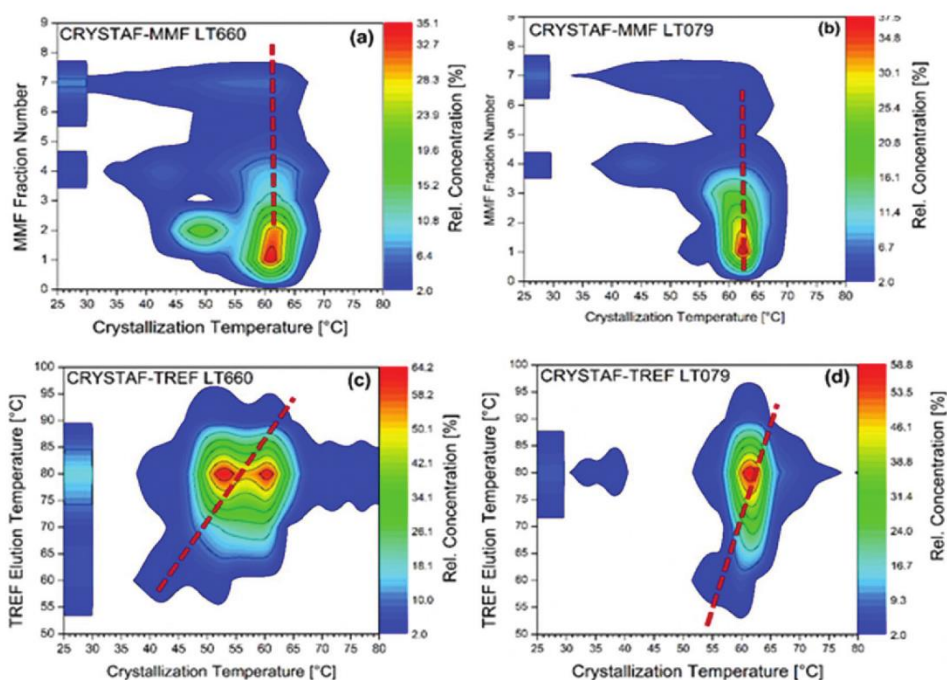


Fig. 11 Bivariate distribution plots of LT660 and LT079 obtained by combining CRYSTAF–MMF (a, b) and CRYSTAF–TREF data (c, d). Samples LT660 (a, c) and LT079 (b, d).

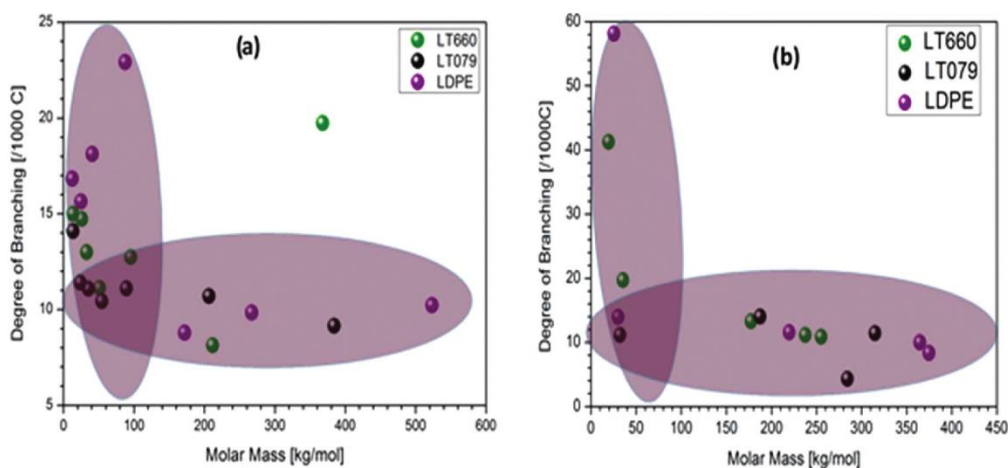


Fig. 12 Experimental fraction libraries constituting fractions of LT660, LT079 and LDPE with similar branching but different molar masses as well as similar molar masses but different branching obtained from pMMF (a) and pTREF (b).

Fig. 12. In these libraries, fractions with similar molar masses but different branching frequencies, as well as fractions with similar branching frequencies but different molar masses, are marked by coloured areas. The interesting feature of this approach is that sets of samples (fractions) are

produced that have one similar property, *e.g.* molar mass, and one varying property, *e.g.* branching. The way these samples are produced (pMMF or pTREF) becomes largely irrelevant. A comparison of the analytical behaviour of different samples can now be based on only one parameter

CHAPETR 4

View Article Online

Polymer Chemistry

Paper

(molar mass or branching) which is fundamentally not possible with the bulk samples that exhibit complex MMDs and SCBDs/LCBDs.

Comparison of samples obtained from the experimental fraction libraries

The first idea on the feasibility of the sample library approach is presented in Fig. 13. Branching analysis as a function of molar mass is obtained by SEC-IR. In Fig. 13a two samples (LDPE 5 and LT079 4) having similar MMDs but different total branching (18.1/1000C vs. 10.4/1000C) are compared. Clearly, the branching contents (expressed as CH₃/1000C) of the two samples show different trends. As expected the branching content of sample LDPE 5 is higher at all molar masses. However, the branching content of LT079 4 is constant for all molar masses while for LDPE 5 the branching content drastically increases at high molar masses.

A more subtle comparison between samples LDPE 5 and LT079 4 is presented in Fig. 14. This comparison is based on CRYSTAF crystallization, DSC melting, HPLC elution and the Mark-Houwink plots. Similar to the conformation plots (R_g vs. molar mass), the Mark-Houwink plots ($[\eta]$ vs. molar mass) provide information on branching by comparing a linear standard to the branched sample. The CRYSTAF plots in Fig. 14a present very broad crystallization profiles for LDPE 5 and LT079 4 with distinct shapes. The less branched LT079 4 exhibits two main peaks with peak crystallization temperatures at 44 and 62 °C. In contrast, the highly branched LDPE 5 displays a rather monomodal but very broad crystallization profile with a slightly higher peak crystallization temperature of ~65 °C. Both samples contain comparable amounts of soluble components, which are assigned to highly branched species. From these results alone no conclusion can be made about the branching content or frequency. The same is true for the DSC results. The main melting peak appears at the same temperature for both samples. Only the shoulder towards lower melting temperatures indicates a higher degree of branching for LDPE 5.

The HPLC elugrams of the two samples are compared in Fig. 14c. The highly branched LDPE 5 exhibits a very broad elugram with broad offset tailing and a peak elution volume of 5.33 mL. On the contrary, LT079 4 displays a rather narrow elugram with a sharp offset tailing. The differences in the elution profiles are solely due to differences in the degree of branching considering that both samples exhibit very narrow molar mass dispersities. The differences in their offset tailing can be ascribed to differences in LCB. Meunier *et al.* reported similar observations although a different column type was used.¹⁷ As has been discussed before, for high molar masses (>20 kg mol⁻¹) elution in HPLC is directly linked to branching. Early elution indicates high degrees of branching while late elution is due to rather linear structures. To confirm the differences in branching, Mark-Houwink plots of the two samples were compared to a linear reference of comparable molar mass. For the plots of the samples, a direct correlation between the intrinsic viscosity and molar mass is observed in accordance with eqn (2), that in comparison to the linear reference can be translated into a branching ratio g' , see eqn (6).

$$g' = \left[\frac{[\eta]_{\text{Br}}}{[\eta]_{\text{Li}}} \right]_M \quad (6)$$

It could be seen clearly that LDPE 5 exhibits a higher degree of LCB when compared to LT079 4 as indicated by the larger deviation from the linear plot towards lower $[\eta]$.

In another application, the microstructure for selected MMF-based library samples, *i.e.* LT660 4, LT079 2 and LDPE 1 with a comparable total branching of 11.1, 10.7 and 10.2/1000C, respectively, having different molar masses were compared as presented in Fig. 15. According to the CRYSTAF results in Fig. 15a, LT660 4 with a molar mass of 51.1 kg mol⁻¹ exhibits a broad multimodal crystallization profile with peak crystallization temperatures of approximately 34, 42 and 60 °C which can be attributed to branched species of different architectures. In comparison, LT079 2 and LDPE 1 having molar masses of 206.3 and 523.2 kg mol⁻¹ exhibit narrow crystallization profiles with peak crystallization temperatures of ~61.8

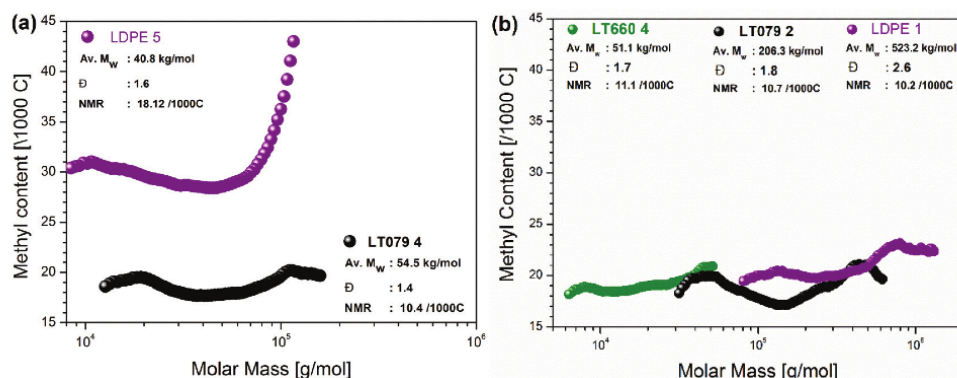


Fig. 13 SEC-IR plots describing methyl content distributions of selected MMF fractions with different degrees of branching but similar molar masses (a) and different molar masses but similar methyl contents (b) as a function of molar mass.

CHAPETR 4

Paper

View Article Online

Polymer Chemistry

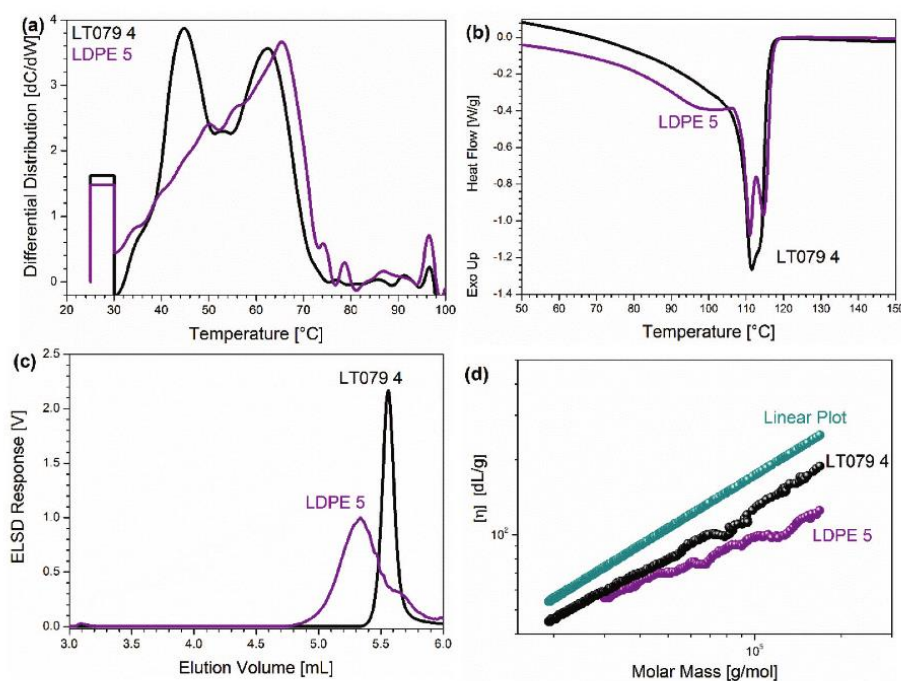


Fig. 14 Comparison of two library samples (LT079 4 and LDPE 5) with similar molar masses but different branching frequencies obtained by pMMF. Analysis by CRISTAF (a), DSC melting (b), HPLC elution (c) and M-H conformation plots (d).

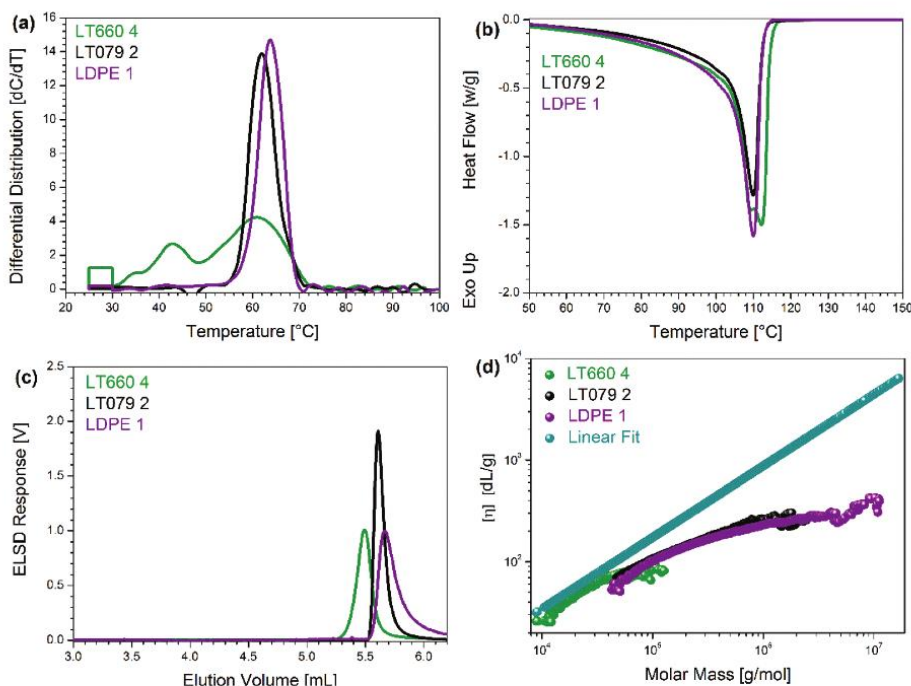


Fig. 15 Comparison of MMF-based library samples with similar branching frequencies but different molar masses as analysed by CRISTAF (a), DSC melting (b), HPLC elution (c) and M-H distribution plots (d).

CHAPETR 4

View Article Online

Polymer Chemistry

Paper

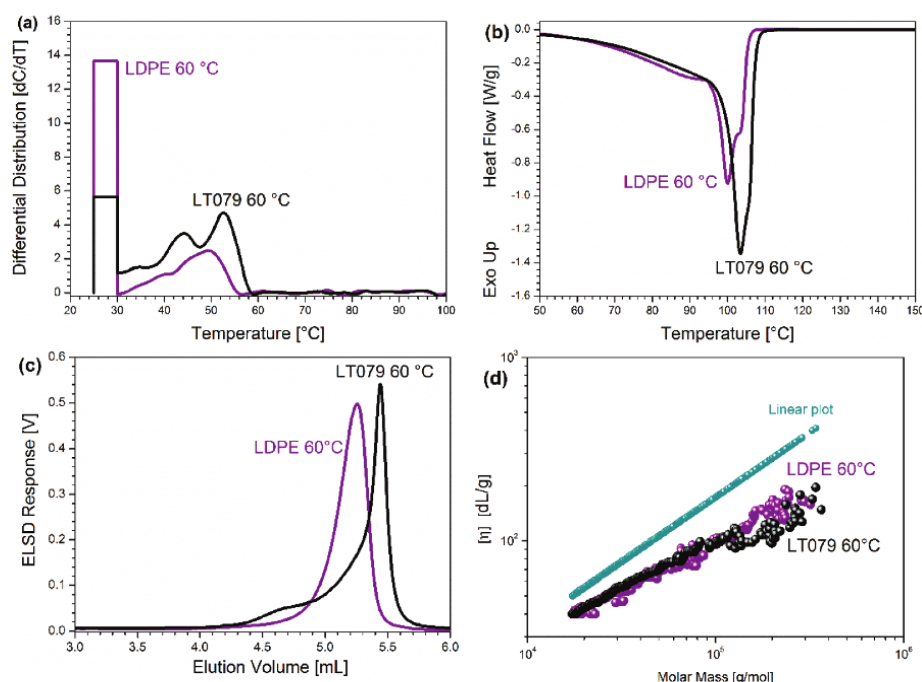


Fig. 16 Comparison of TREF-based library samples with different branching frequencies but similar molar masses as analysed by CRYSTAF (a), DSC melting (b), HPLC elution (c) and M-H distribution plots (d).

and ~ 63.7 °C, respectively. Different from these results, the DSC melting curves of the three samples look quite similar and do not indicate significant differences in branching. This leads to the preliminary conclusion that at lower molar masses CRYSTAF crystallization is significantly more influenced by molar mass compared to DSC melting. This finding, however, must be confirmed in future investigations. The HPLC behavior of the samples also seems to be influenced by the molar mass. The lowest molar mass sample LT660 4 with a molar mass of 51.1 kg mol^{-1} elutes first. This molar mass effect is somehow surprising since previous investigations indicated that for molar masses $>20 \text{ kg mol}^{-1}$ the molar mass influence on elution vanishes. On the other hand, even at the same average branching content, the ratio between SCB and LCB will influence the HPLC elution behavior. The differences in branching are clearly seen in the Mark-Houwink plots in Fig. 15d. Although all three samples follow the same trend, sample LT660 4 shows a high similarity with the linear reference in the low molar mass part of the distribution. This indicates that the sample has a significant amount of SCB while the other two samples with higher molar masses seem to be largely long chain branched. The fact that samples LT079 2 and LDPE 1 show the same conformation plots confirms the CRYSTAF and DSC results.

In the last application, the two library samples LT079 60 °C and LDPE 60 °C, having different branching contents of 11.2 and 14.0/1000C but similar molar masses of 32 and

30 kg mol^{-1} , respectively, were investigated. Again, the samples were compared using CRYSTAF, DSC, HPLC and the Mark-Houwink plots, see Fig. 16. In agreement with the higher branching content, sample LDPE 60 °C exhibits a significantly higher soluble part in CRYSTAF, see Fig. 16a. Due to the low molar mass, this highly branched material does not crystallize at ambient temperature or higher. As seen before in DSC, sample LDPE 60 °C shows a slightly lower melting temperature of the main peak and a shoulder at lower melting temperatures indicating some highly branched material (seen as the soluble part in CRYSTAF). In HPLC, sample LDPE 60 °C elutes earlier due to its higher branching. Interestingly, sample LT079 60 °C elutes later (lower branching content) but exhibits a small early eluting peak that indicates higher branching and might correspond to the soluble part seen in CRYSTAF. The Mark-Houwink plot in Fig. 16d shows similar trends for both samples. The fact that at higher molar masses the curve for sample LDPE 60 °C is closer to the linear reference might indicate that this sample has a higher ratio of SCB/LCB compared to sample LT079 60 °C.

Conclusion

Despite being a homopolymer, low density polyethylene (LDPE) exhibits a complex molecular structure that is determined by multiple molar mass and branching distributions.

CHAPETR 4

View Article Online

Paper

Polymer Chemistry

The present study convincingly shows that for a comprehensive microstructural analysis of LDPE, multiple preparative fractionation methods must be combined with multiple advanced analysis techniques. Preparative temperature rising elution fractionation (pTREF) and preparative molar mass fractionation (pMMF) produce libraries of fractions (samples) that are different regarding branching and molar mass, respectively. These LDPE sample libraries constitute samples that have comparable molar masses and different branching structures or *vice versa* have comparable branching but different molar masses. Cross-fractionation of these library samples with advanced analytical techniques provides in-depth information on the molecular heterogeneity of these samples as compared to bulk sample analysis.

Conflicts of interest

There are no conflicts to declare.

Acknowledgements

The authors gratefully acknowledge SASOL (South Africa) for providing the LDPE samples. The investigation of a number of samples using triple detector SEC was conducted by Kristina Pflug (Technical University, Darmstadt, Germany) which is gratefully acknowledged. PSEB acknowledges the financial support of his research by SASOL (South Africa).

References

- 1 P. S. Eselem Bungu and H. Pasch, *Polym. Chem.*, 2017, **8**, 4565–4575.
- 2 H. Pasch, *Polym. Adv. Technol.*, 2015, **26**, 771–784.
- 3 B. Monrabal, L. Romero, N. Mayo and J. Sancho-Tello, *Macromol. Symp.*, 2009, **282**, 14–24.
- 4 Y. Xue, S. Bo and X. Ji, *Chin. J. Polym. Sci.*, 2015, **33**, 1000–1008.
- 5 S. Cheruthazhekatt, T. F. J. Pijpers, G. W. Harding, V. B. F. Mathot and H. Pasch, *Macromolecules*, 2012, **45**, 2025–2034.
- 6 A. Ndiripo, D. Joubert and H. Pasch, *J. Polym. Sci., Part A: Polym. Chem.*, 2016, **54**, 962–975.
- 7 M. Busch, *Macromol. Theory Simul.*, 2001, **10**, 408–429.
- 8 A. J. Van Reenen, R. Brull, U. M. Wahner, H. G. Raubenheimer, R. D. Sanderson and H. Pasch, *J. Polym. Sci., Part A: Polym. Chem.*, 2000, **38**, 4110–4118.
- 9 C. Gabriel, *Einfluss der molekularen Struktur auf das viskoelastische Verhalten von Polyethylenschmelzen*, Shaker, Aachen, 2001.
- 10 V. Karimkhani, F. Afshar-Taromi, S. Pourmahdian and F. J. Stadler, *Polym. Chem.*, 2013, **4**, 3774.
- 11 M. Ahmadi, F. Rezaei, S. M. M. Mortazavi, M. Entezam and F. J. Stadler, *Polymer*, 2017, **112**, 43–52.
- 12 W. W. Yau, *Polymer*, 2007, **48**, 2362–2370.
- 13 S. Podzimek, *Light scattering, size exclusion chromatography, and asymmetric flow field flow fractionation: powerful tools for the characterization of polymers, proteins, and nanoparticles*, Wiley, Hoboken, NJ, 2011.
- 14 B. Monrabal and P. del Hierro, *Anal. Bioanal. Chem.*, 2011, **399**, 1557–1561.
- 15 B. Monrabal, J. Sancho-Tello, N. Mayo and L. Romero, *Macromol. Symp.*, 2007, **257**, 71–79.
- 16 M. J. Phiri, S. Cheruthazhekatt, A. Dimeska and H. Pasch, *J. Polym. Sci., Part A: Polym. Chem.*, 2015, **53**, 863–874.
- 17 D. Meunier, T. M. Stikich Jr., D. Gillespie and P. B. Smith, *Macromol. Symp.*, 2007, **257**, 56–70.
- 18 C. L. P. Shan, W. A. deGroot, L. G. Hazlitt and D. Gillespie, *Polymer*, 2005, **46**, 11755–11767.
- 19 S. Cheruthazhekatt, D. D. Robertson, M. Brand, A. van Reenen and H. Pasch, *Anal. Chem.*, 2013, **85**, 7019–7023.
- 20 R. Brüll, N. Luruli, H. Pasch, H. G. Raubenheimer, E. R. Sadiku, R. Sanderson, A. J. van Reenen and U. M. Wahner, *E-Polym.*, 2003, **3**, 785–793.
- 21 S. Cheruthazhekatt, T. F. J. Pijpers, V. B. F. Mathot and H. Pasch, *Macromol. Symp.*, 2013, **330**, 22–29.
- 22 H. Pasch and M. I. Malik, *Advanced Separation Techniques for Polyolefins*, Springer International Publishing, Cham, 2014.
- 23 T. Macko, R. Brüll, R. G. Alamo, F. J. Stadler and S. Losio, *Anal. Bioanal. Chem.*, 2011, **399**, 1547–1556.
- 24 J. K. er Jørgensen, A. Larsen and I. Helland, *E-Polym.*, 2010, **10**, 1596–1612.
- 25 Y. Xue, S. Bo and X. Ji, *J. Polym. Res.*, 2015, **22**, 1–10.
- 26 O. Sperber and W. Kaminsky, *Macromolecules*, 2003, **36**, 9014–9019.
- 27 A. M. Striegel and M. R. Krejsa, *J. Polym. Sci., Part B: Polym. Phys.*, 2000, **38**, 3120–3135.
- 28 A. Ndiripo and H. Pasch, *Anal. Bioanal. Chem.*, 2015, **407**, 6493–6503.
- 29 M. Zhang, D. T. Lynch and S. E. Wanke, *J. Appl. Polym. Sci.*, 2000, **75**, 960–967.
- 30 R. Brüll, H. Pasch, H. G. Raubenheimer, R. Sanderson, A. J. van Reenen and U. M. Wahner, *Macromol. Chem. Phys.*, 2001, **202**, 1281–1288.
- 31 Y. Xue, S. Bo, *et al.*, *Chin. J. Polym. Sci.*, 2015, **33**, 508–522.
- 32 D. E. Axelson, G. C. Levy and L. Mandelkern, *Macromolecules*, 1979, **12**, 41–52.
- 33 F. A. Bovey, F. C. Schilling, F. L. McCrackin and H. L. Wagner, *Macromolecules*, 1976, **9**, 76–80.
- 34 W.-J. Wang, S. Kharchenko, K. Migler and S. Zhu, *Polymer*, 2004, **45**, 6495–6505.
- 35 T. Pathaweaisariyakul, K. Narkchamnan, B. Thitisak, W. Rungswang and W. W. Yau, *Polymer*, 2016, **107**, 122–129.

CHAPETR 4

[View Article Online](#)

Polymer Chemistry

Paper

- 36 W. W. Yau, *Macromol. Symp.*, 2007, **257**, 29–45.
- 37 M. Wagner, K. Reiche, A. Blume and P. Garidel, *Pharm. Dev. Technol.*, 2013, **18**, 963–970.
- 38 Y. Xue, S. Bo and X. Ji, *J. Polym. Res.*, 2016, **23**, 131.
- 39 T. Usami and S. Takayama, *Macromolecules*, 1984, **17**, 1756–1761.
- 40 T. Usami and S. Takayama, *Polym. J.*, 1984, **16**, 731–738.

5 Combination of Preparative and Two-Dimensional Chromatographic Fractionation with Thermal Analysis for Branching Analysis of Polyethylene

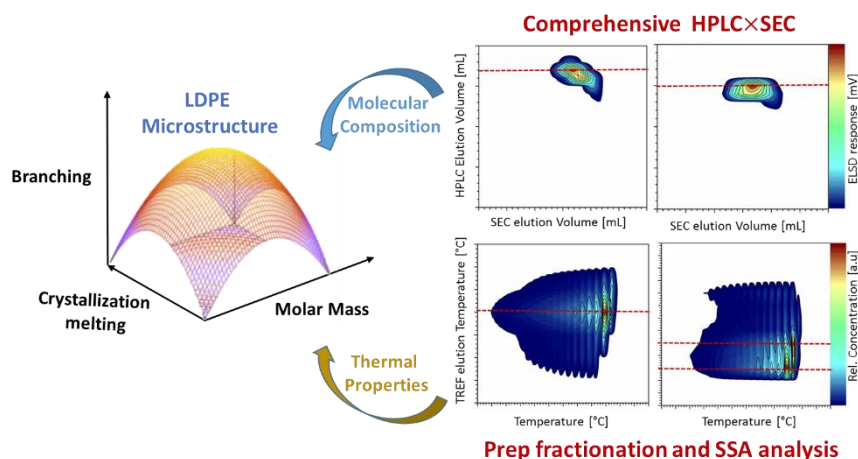


Figure 11: Multiple preparative fractionation of LDPE provides molar mass and branching fractions that were analysed regarding their thermal properties

Using the multiple preparative fractionation concept presented in Chapters 3 and 4, fractions of a representative sample of low density polyethylene (LDPE) were analysed by DSC and subsequently successive self-nucleation and annealing (SSA) to evaluate the effect of molar mass and branching on the thermo-physical behaviour, being the most relevant molecular property that influences the processing behaviour of the material.

Microstructural information for the LDPE fractions was obtained by combining pTREF/pMMF data with the SSA data to obtain two-dimensional plots relating branching and molar mass to crystal size distribution. From the TREF-SSA 2D contour plot, it was observed that two species with distinctively different crystal size/peak crystallization co-elute in TREF. Complementarily, the MMF-SSA 2D contour plot revealed that the branched species have predominantly high molar masses, while the more linear components exhibit lower molar masses. The fractions were analysed by HPLC, followed by comprehensive 2D-LC analysis. For some fractions, the 2D plots revealed co-elution of branched and linear components. In a similar way, the 2D plots confirmed higher degrees of branching for the higher molar mass fractions. These results were in agreement with the results reported for SSA.

More detailed information of this work has been published (P. S. Eselem Bungu, K. Pflug and H. Pasch, *Polymer. Chemistry*, 2018, 9, 3142–3157.) and can be found in this chapter.



Cite this: *Polym. Chem.*, 2018, **9**, 3142

Combination of preparative and two-dimensional chromatographic fractionation with thermal analysis for the branching analysis of polyethylene†

Paul S. Eselem Bungu,^a Kristina Pflug^b and Harald Pasch^{b*}

Low density polyethylene (LDPE) or, more generally, branched polyethylene exhibits excellent processing properties thanks to its complex molecular structure. The branches on the polymer backbone are distributed by location and size and these molecular properties determine the crystalline/amorphous morphology of the crystalline, semi-crystalline and amorphous components. In the present study, the molecular complexity of branched PE is correlated to its thermal properties and morphology. The study follows the multiple fractionation protocol established on a representative LDPE resin, whereby, narrowly dispersed branched fractions having broad molar mass distributions are generated using preparative temperature rising elution fractionation (pTREF). Alternatively, broadly branched fractions having narrow molar mass dispersities are obtained via preparative molar mass fractionation (pMMF). The molecular structure of the fractions and the bulk resin are investigated using solution crystallization analysis by laser light scattering (SCALLS), differential scanning calorimetry (DSC) and successive self-nucleation and annealing fractionation (SSA) to describe the thermal properties and the morphology of the different molecular species. Since these techniques are biased towards the analysis of the crystallisable components, solvent gradient high performance liquid chromatography (HPLC) is used as a complementary technique to account for both the crystalline and amorphous components. A comprehensive two-dimensional liquid chromatography technique coupling HPLC and size exclusion chromatography (SEC) is used to investigate the bivariate distributions of branching and molar mass. SEC-MALLS and SEC-IR5 are used to determine long chain branching and total branching of the fractions and the bulk resin.

Received 5th April 2018,
Accepted 17th May 2018
DOI: 10.1039/c8py00522b
rsc.li/polymers

Introduction

Free radical polymerization (FRP) is a typical industrial process for the production of low density polyethylene (LDPE), which is referred to more generally as branched polyethylene (PE). Different from metallocene-catalysed ethylene polymerization to produce PE with narrow molar mass dispersities, free radical polymerization generates polymer chains with broad branching and molar mass distributions. Despite the inferior mechanical properties of branched PE in comparison to the linear counterparts, these materials exhibit superior processing abilities originating from enhanced flow properties, in addition to improved clarity and stiffness which are induced

by low molar mass and highly branched components that act as internal plasticizers.¹

Polyethylenes exhibit complex molecular structures with respect to molar mass and topology. Their molecular complexity has attracted considerable research interest in the recent past. Structure-property relationships were established as a relevant tool to optimize end-use properties.^{2–4} The mechanism and kinetics for the large-scale polymerization of branched PE have been established.^{5–7} The consensus is that branched PE exhibits short chain (SCB) and long chain branching (LCB). The different branching types are formed via intramolecular backbiting and intermolecular chain transfer reactions (*i.e.* the insertion of macromers into the growing chain), respectively,^{6,7} and have been confirmed through detailed ¹³C NMR studies.^{8–13} For commercial branched PE, the *n*-butyl branch (C₄), which is formed by backwards backbiting of growing chains, constitutes the principal form of SCB which is co-existing with smaller amounts of methyl (C₁), ethyl (C₂) and amyl (C₅) branches in trifunctional branching units.¹⁴ Alternatively, *n*-hexyl (C₆) and longer branches (C₆₊) are

^aDepartment of Chemistry and Polymer Science, University of Stellenbosch, PO Box X1, 7602 Matieland, South Africa. E-mail: hpasch@sun.ac.za

^bTechnical Chemistry III, Technical University Darmstadt, Alarich-Weiss-Straße 8, 64287 Darmstadt, Germany

†Electronic supplementary information (ESI) available. See DOI: 10.1039/c8py00522b

CHAPTER 5

[View Article Online](#)

Polymer Chemistry

Paper

referred to as LCB based on ^{13}C NMR measurements.^{12,13} Even though NMR cannot predict the precise length of an LCB, rheological measurements have suggested that these branches are long enough to enhance chain entanglements and induce side chain crystallization.^{2,15} Recognizing that polymer chains are statistically distributed with respect to molecular size, branches at polymer backbones are also randomly distributed in size and location. The microstructural complexity of branched PE may result in the formation of multiple phase materials categorised into amorphous (densely branched), semi-crystalline (sparsely branched) and crystalline (low branched) regions. The size and number of these regions are determined not only by the number of branches but also by their size distributions. Therefore, branching measurements using ^{13}C NMR are valuable by providing average information on bulk samples but do not provide branching distributions.

Several well-established fractionation techniques such as temperature rising elution fractionation (TREF),^{16,17} crystallization analysis fractionation (CRYSTAF),^{16,18,19} crystallization elution fractionation (CEF),^{16,20,21} solution crystallization by laser light scattering (SCALLS)^{22–24} and differential scanning calorimetry (DSC)^{25–27} have been used for branching distribution analysis in complex polyolefins. Typically, these techniques are crystallization-based and provide branching distribution information of the crystallizable components. It is assumed that polymer chains with similar distributions in the crystallizable ethylene sequences (similar degree of branching) will co-crystallize, irrespective of their molecular size.^{28,29} By correlating the branching content to the crystallization temperature, the polymer crystallinity distribution can be directly linked to the branching distribution.^{30,31} A comprehensive structural characterization of branched PE (LDPE) using TREF and CRYSTAF was published previously.³²

A decade ago, Shan *et al.* introduced turbidity fractionation techniques also known as TFA (turbidity fractionation analysis) to evaluate SCB distributions in linear low density polyethylene.²² This method was modified by van Reenen (solution crystallization analysis by laser light scattering, SCALLS) and others in recent years to study the crystallization kinetics of different types of polyolefins and polymer blends.^{23,24,33} Experimentally, polymer solutions are subjected to controlled heating and cooling cycles to provide dissolution and crystallization as a function of temperature. Unlike CRYSTAF that measures the changes in polymer concentration as crystallization occurs, SCALLS observes the changes in turbidity as the polymer crystallizes or dissolves. One drawback in SCALLS over CRYSTAF is that the soluble components are unaccounted for and, therefore, the method can only be used for rather qualitative purposes.

Thermal fractionation by successive self-nucleation and annealing (SSA) has also been used for SCB evaluation in polyethylene.^{34,35} Just as CRYSTAF and DSC provide distributions of crystallizable sequences, SSA yields information on the crystal sizes distribution, which reflects the crystallizable methylene sequence length (CMSL) distribution for low temperature components. The longer the methylene sequence

length, the larger is the crystal size and thus, the higher is the melting temperature. At a certain point, the crystal size becomes smaller than the methylene sequence length (MSL) and must be calculated from the melting temperature using the method introduced by Keating and others.^{36,37} Unfortunately, all these fractionation techniques (A) suffer from co-crystallization effects and (B) are limited to characterizing the crystallizable components. It is important to note, however, that the molecular structure of branched PE is composed of materials in the crystalline and amorphous phases. In order to develop comprehensive structure–property relationships in LDPE, it is essential to obtain structural information on all components irrespective of crystallinity. In this case, crystallization-based techniques must be combined with other advanced techniques that are not based on crystallization such as high-temperature high performance liquid chromatography (HT-HPLC). HPLC fractionation of polyolefins is based on interactions of linear ethylene sequences (LES) with the stationary phase and can provide structural information for both the crystalline and amorphous components.^{4,16,38}

Recently, the concept of multiple preparative fractionations of polyolefins by pTREF and preparative molar mass fractionation (pMMF) was introduced and cross-fractionation by combining pTREF/pMMF with size exclusion chromatography (SEC) and CRYSTAF was established.³² However, the individual fractions still exhibited distributions with regard to molar mass and branching. Therefore, two-dimensional liquid chromatography (2D-LC) was introduced to map and correlate branching to molar mass in these fractions. Fractionation according to branching or chemical composition was conducted in the first dimension using HPLC, followed by molar mass fractionation in the second dimension using SEC, to provide bivariate distributions.^{16,39} In recent years, the combination of crystallization- and chromatography-based fractionation techniques along with ^{13}C NMR have proven to be a valuable tool in providing detailed structural information on complex polyolefins.^{14,32}

In a previous study, it was highlighted that fractions generated using the multiple fractionation concept were heterogeneously distributed with respect to molar mass (TREF fractions) and branching (MMF fractions).³² The current work will focus on investigating the microstructure of such fractions with advanced techniques such as DSC, SSA, HPLC, and 2D-LC. To enhance molar mass analysis, SEC will be coupled to a MALLS and an infrared detector (IR5) for quantitative LCB and total branching analysis.

Experimental

Materials and methods

1,2,4-Trichlorobenzene and 1-decanol used in the study were obtained from Sigma Aldrich. Except for its use as an eluent in HPLC, the TCB was distilled before use. The branched PE sample was provided by SASOL South Africa, while two linear PEs with narrow ($\bar{D} = 3.4$) and broad ($\bar{D} = 10.1$) MMDs were

CHAPTER 5

[View Article Online](#)

Paper

Polymer Chemistry

Table 1 Molecular properties of linear and branched polyethylene

Sample	M_w^a [kg mol ⁻¹]	M_n^a [kg mol ⁻¹]	D^a	T_d^b [°C]	T_c^b [°C]	T_c^c [°C]	T_c^d [°C]	T_m^d [°C]
Branched PE	264.9	25.2	10.5	77.2	63.1	63.0	98.6	111.2
Linear PE 1	56.6	16.2	3.4	95.3	83.1	85.0	111.9	134.6
Linear PE 2	328.2	32.6	10.1	—	—	84.6	118.3	133.7

^a As determined by SEC-MALLS. ^b Dissolution (T_d) and crystallization temperature (T_c) as determined by SCALLS. ^c As determined from CRYSTAF.^d As determined from DSC.

purchased from the American Polymer Standards Corporation. Table 1 summarizes the molecular properties of the linear and branched samples.

Solution crystallization analysis by laser light scattering (SCALLS). SCALLS analysis was performed using an instrument build in-house. A general scheme for the SCALLS setup and the detailed description with respect to its layout can be found in previous literature.^{23,24} SCALLS results were obtained by dissolving 20 mg of the analyte in 20 mL of TCB in a quartz tube placed into a four-port aluminium block and mounted on a magnetic heater stirrer. The heating coil is connected to an external temperature controller for controlled heating and cooling. The samples were then analyzed during the heating and cooling steps at constant stirring (500 rpm) and the dissolution and crystallization profiles were recorded at a cooling and heating rate of 0.5 °C min⁻¹ and 1 °C min⁻¹, respectively.

Differential scanning calorimetry (DSC). The thermal properties of the samples were determined using a TA Instruments Q100 DSC system, calibrated with indium metal standard. Calibration was done according to standard procedures and the melting and crystallization temperatures were measured under the same experimental conditions of heating and cooling at a scanning rate of 10 °C min⁻¹ in a temperature ranging between 10–200 °C. The samples were subjected to three temperature cycles, with the first cycle (first heating) being used to erase the sample thermal history. The crystallization and melting temperatures reported in Table 1 were recorded during the first cooling and second heating cycles. After each cycle, the temperature was kept isothermal for 2 min. The measurements were conducted in a nitrogen atmosphere at a purge gas flow rate of 50 mL min⁻¹. All measurements were conducted in triplicate.

Successive self-nucleation and annealing fractionation (SSA). The thermal fractionation (SSA) experiments for all samples were conducted using the TA DSC Q100 instrument, calibrated with standard indium and the furnace was purged with nitrogen during each analysis. The SSA fractionations of the samples (5.4 mg) were achieved according to the following protocol. In the first step, the sample thermal history was erased by heating and cooling the sample at a scanning rate of 10 °C min⁻¹ between 0 and 200 °C. Before cooling, the sample was held isothermally for 5 min. The sample was subjected to a second heating to a selected first self-seeding temperature (T_{s1}) based on the region published by Cavallo and others^{34,40} and then held isothermally for 5 min before cooling at a rate of 10 °C min⁻¹. In the third cycle, the sample was heated to a

self-seeding temperature (T_{s2}), which is lower than T_{s1} by 5 °C and kept isothermally for 5 min before cooling at the same rate. The previous cycles were repeated at every 5 °C step until 30 °C. At the final step, the sample was heated at a rate of 10 °C min⁻¹ from 0–200 °C to obtain multiple melting endotherms.

SEC-triple detector system. Long chain branching analyses were obtained using a high-temperature PolymerChar GPC-IR system equipped with an IR5 detector (Polymer Char Laboratories Ltd, Valencia, Spain) in hyphenation with a Wyatt Dawn Heleos II LS detector (Wyatt Technology Corporation, Santa Barbara, USA) and an online Visco H502 viscometer detector (Polymer Char Laboratories Ltd, Valencia, Spain). A column set of three Shodex UT 806 M columns and one Shodex UT 807 column (each 300 mm × 80 mm i.d.) and a Shodex UT-G guard column (50 mm × 8.0 mm i.d.) (Showa Denko K.K., Kanagawa, Japan) operating at 150 °C was used. The average particle sizes of all columns were 30 µm. The eluent 1,2,4-trichlorobenzene (TCB) stabilized with 2,6-di-*tert*-butyl-4-methylphenol (BHT, 0.0125%) was used at a flow rate of 1 mL min⁻¹. All samples (~2 mg) were dissolved in TCB (2 mL) for 1–2 hours and 0.2 mL of the solutions were injected. The MALLS data were processed with the Astra software version 6.1.6.5 (Wyatt Technology, Santa Barbara, USA) and a dn/dc value of -0.1040 mL g⁻¹ was used for all the samples. The MALLS data were analysed using a first order Zimm plot and assuming monodisperse polymer fractions after SEC. The molar mass dependency on branching frequencies was determined by the IR5 detector calibrated with six ethylene-1-octene copolymers with varying comonomer contents ranging between 2.6 and 46/100C.

High-temperature high-performance liquid chromatography (HT-HPLC). HT-HPLC chromatograms were obtained using a solvent gradient interactive chromatographic system (SGIC) constructed by Polymer Char (Valencia, Spain). The instrument is composed of an autosampler (which is a separate unit connected to the injector with a heated transfer line), two separate ovens, switching valves and two pumps which are equipped with vacuum degassers (Agilent, Waldbronn, Germany). For solvent gradient elution in HPLC, a high-pressure binary gradient pump was used. An evaporative light scattering detector (ELSD, model PL-ELS 1000, Polymer Laboratories, Church Stretton, England) was used with the following parameters: a gas flow rate of 1.5 SLM, 160 °C nebulizer temperature and an evaporation temperature of 270 °C. All samples were fractionated using a 100 × 4.6 mm i.d. Hypercarb column

CHAPTER 5

(Hypercarb®, Thermo Scientific, Dreieich, Germany) packed with porous graphite particles (particle diameter: 5 μm ; pore size: 250 Å and surface area: 120 $\text{m}^2 \text{g}^{-1}$). The column temperature was maintained at 160 $^{\circ}\text{C}$ in the column oven. The mobile phase flow rate during analysis was 0.5 mL min^{-1} . To achieve separation, a linear gradient was applied from 100 vol% 1-decanol to 100 vol% TCB within 10 min after sample injection. The conditions were held for 20 min before re-establishing 1-decanol to 100 vol%. Samples were injected at a concentration of 1–1.2 mg mL^{-1} , using 20 μL of each sample solution during analysis.

High-temperature two-dimensional liquid chromatography (HT-2D-LC). The bivariate fractionation data in HT-2D-LC were obtained by coupling HT-HPLC and HT-SEC using an electronically controlled eight-port valve system (VICI Valco instrument, Houston, Texas, USA), equipped with two 100 μL sample loops. The sample (12 mg) was dissolved in decanol (4 mL) and the samples were injected into the first dimension column using a 110 μL sample loop, using the same gradient reported for HPLC, a flow rate of 0.05 mL min^{-1} was used for the first dimension. In the second dimension, all samples were fractionated using a 100 \times 10 mm i.d. PL Rapide column (Polymer Laboratories, Church Stretton, UK) having an average particle diameter of 6 μm . The column was placed in the top oven and kept at 160 $^{\circ}\text{C}$, with a mobile phase flow rate of 2.75 mL min^{-1} . Data were collected using an evaporating light scattering detector with a similar setting as reported for HPLC.

Results and discussion

Bulk analysis

In the first part of this study, the comprehensive microstructural analysis of branched PE using the multiple fractionation concept was presented.³² The present investigation focusses on the correlation of microstructural parameters and thermal properties of branched and linear PE using SEC, CRYSTAF, DSC, HPLC and SEC-MALLS. After investigating some bulk properties, the main part of the study addresses the preparative fractionation of branched PE by pTREF and pMMF into fraction libraries with narrow branching and molar mass dispersities, respectively. The molar mass distributions and the CRYSTAF curves of the fractions, as well as the cross-fractionation plots, were reported in the first part of this study.³²

For the comprehensive analysis of the molecular complexity of branched PE, it is not only important to have molar mass and branching information from SEC and NMR experiments. As the size and the molecular topology also influence the solubility and the crystallinity of the material, dissolution and crystallization (in solution and in the melt) experiments can add to the correlation of these physical properties to molecular parameters. Such experiments can be conducted using SCALLS and DSC as is shown for the bulk samples in Fig. 1.

As branching decreases crystallinity, distinct differences between linear and branched PE are obtained when conducting DSC and SCALLS experiments. As is seen in the SCALLS

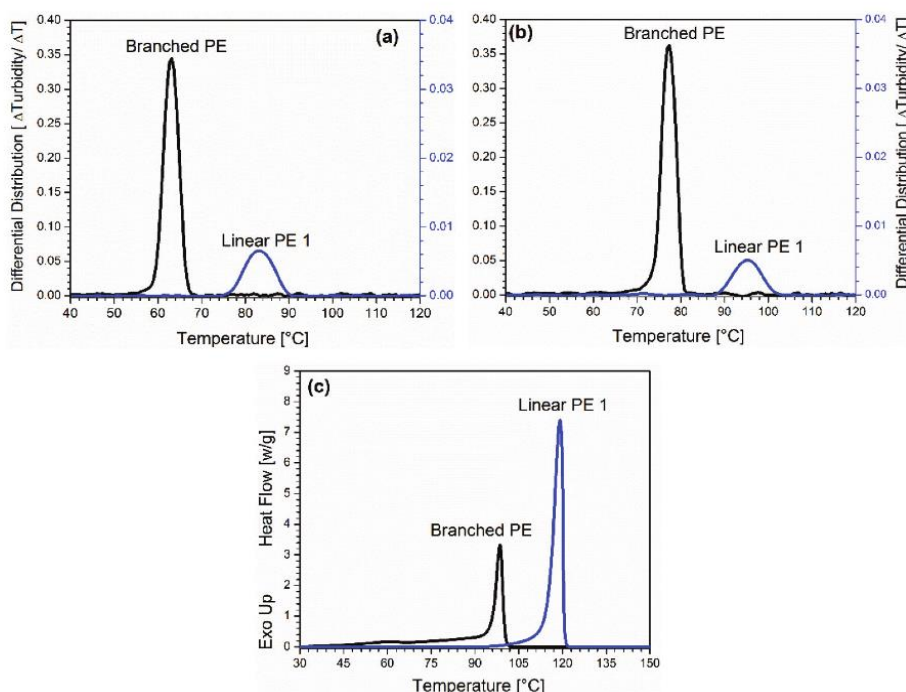


Fig. 1 Comparison of branched and linear PE obtained by (a) SCALLS crystallization, (b) SCALLS dissolution and (c) DSC crystallization.

CHAPTER 5

View Article Online

Paper

Polymer Chemistry

crystallization experiments, a broad unimodal crystallization profile with low peak intensity is reported for the linear PE around ~ 84 °C. In contrast, the branched PE exhibits unimodal but narrow crystallization profile around 63 °C. As an advantage compared to CRYSTAF, SCALLS provides also the possibility to investigate the dissolution behaviour of the sample during the heating cycle. For the linear PE, a peak dissolution temperature at around 95 °C is observed, while for branched PE this temperature is around 77 °C. The dissolution temperatures obtained in these experiments are very similar to the ones that were reported by Shan *et al.*²²

The peak intensity in SCALLS provides some extra information on the crystallization behaviour of branched vs. linear PE. Shan *et al.* suggested that turbidity is dependent on the size and number of lamellar crystals formed.²² Peak intensity in SCALLS is induced by a reduction in light transmission through the sample due to the formation of smaller or larger crystals upon crystallization. The higher peak intensity observed for branched PE is assumed to be due to the formation of many but predominantly smaller crystal sizes while linear PE forms larger but fewer crystals and, therefore, exhibits higher light transmission.

The solid-state properties of the linear and branched PEs was equally investigated using DSC as presented in Fig. 1c. Both samples display unimodal crystallization profiles with peak temperatures at 111.9 and 98.6 °C, which are typical crystallization temperatures for linear and branched PEs, respectively, provided that the molar mass effect is minimal. The thermal fractionation data are presented in Fig. 2. The SSA technique is used to examine the chain heterogeneity of the present complex samples. As clearly shown in Fig. 2a, the SSA-DSC plot for the branched PE displays a complex melting endotherm with more than 10 peaks and melting temperatures ranging from 55 to 120 °C. The peak intensity of these individual peak increases with an increase in temperature. The individual melting peaks, which are referred to as seeds, are representing groups of polymer chains with almost similar crystallizable methylene sequences lengths (CMSL), *i.e.* similar

thermodynamic stabilities, and are indicative of the topological heterogeneity of the sample. The linear PE exhibits a rather narrow melting endotherm at 135 °C that after peak deconvolution can be assigned to three melting peaks at 118, 123, and 135 °C, as shown in Fig. S1 in the ESI.† The number of peaks and the peak intensity distributions qualitatively distinguish the topological structures of the two homopolymers. As expected, the linear PE exhibits mostly very long crystallisable methylene sequences while the branched PE shows a broad distribution of rather short crystallisable methylene sequences. For a more subtle evaluation of structural differences, Keating *et al.* introduced three statistical terms (the arithmetic mean, \bar{L}_n , the weighted mean, \bar{L}_w , and the broadness index, $\bar{L}_w/\bar{L}_n = I$) in describing the lamellar thickness distribution (LD) (*i.e.*, crystal size distribution CSD) of polyethylene.

Here, L (nm) is the lamellar thickness with the melting temperature, T_m (°K), defined by the relationship in eqn (1). This equation was reported by Müller *et al.* and references therein²⁸ and is based on the thermodynamic analysis of random copolymers with methylene ($-\text{CH}_2-$) molar fractions (X) described by Flory.⁷ In this case, $T_m^\circ = 418$ °K, the temperature for an infinitely thick linear polyethylene, $\sigma = 0.07$ J m⁻², the lamellar surface energy, $\Delta H_v = 288 \times 10^6$ J m⁻³, the enthalpy of fusion for infinitely thick lamellae.

$$L(\text{nm}) = \frac{2\sigma T_m}{\Delta H_v(T_m^\circ - T_m)} \quad (1)$$

Based on this method, broadness indexes or dispersities of 1.08 and 1.03 were calculated for the branched and linear PE, respectively (see Table 2).^{29,36} It is however important to note that L (nm) is a mirror image of the MSL for polymers with shorter methylene sequences, exhibiting melting at lower temperatures.³⁷ For polymer chains with very long methylene sequences, *i.e.* chains melting at much higher temperatures, crystal thickening start to occur, while the crystal size remains unchanged, resulting in a more compact crystal packing. In such a case, the calculated lamellar thickness or crystal size does not reflect the corresponding MSL of the polymer chain.

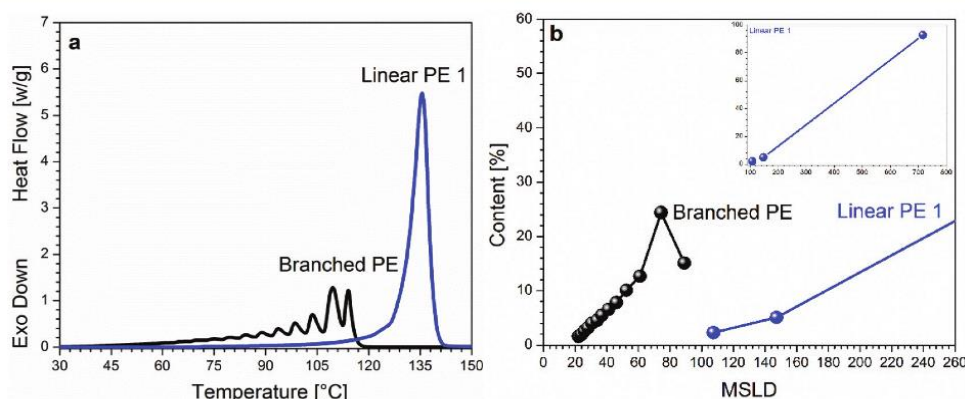


Fig. 2 SSA melting endotherms of branched and linear PE (a) and comparison of MSLD of the branched PE to the linear counterpart (b).

CHAPTER 5

View Article Online

Polymer Chemistry

Paper

Table 2 Summary of molecular and thermal properties of branched and linear PE

Sample	T_c^a [°]	T_m^a [°]	X_c^b [%]	V_c^c [mL]	Lamellar thickness			Methylene sequences		
					\overline{L}_n^d (nm)	\overline{L}_w^d (nm)	I_l^d	\overline{C}_n^d	\overline{C}_w^d	I_c^d
TREF										
30 °C	76.1	84.3	12.3	3.87	2.67	2.71	1.02	26.38	27.59	1.05
60 °C	90.5	100.1	37.3	5.26	3.93	4.13	1.05	40.77	44.14	1.08
70 °C	95.5	108.6	42.2	5.39	4.36	4.63	1.06	52.54	57.49	1.09
80 °C	98.8	111.7	46.5	5.43	4.62	4.93	1.06	56.49	63.03	1.12
90 °C	101.8	113.7	47.8	5.45	4.90	5.30	1.07	61.90	69.29	1.12
Br. PE	98.6	111.2	42.2	5.48	4.60	4.91	1.07	58.10	65.43	1.13
Li. PE 1	111.9	134.6	77.8	5.75	2.10	2.16	1.03	674.09	707.54	1.05
MMF										
Fr. 1	96.8	109.2	41.3	5.67	4.71	5.01	1.06	58.10	64.18	1.11
Fr. 2	97.1	111.5	42.0	5.61	4.85	5.22	1.08	60.65	68.13	1.12
Fr. 3	98.1	112.3	42.0	5.59	4.90	5.30	1.08	61.52	69.64	1.13
Fr. 4	100.3	111.6; 114.4	41.6	5.57	4.70	5.15	1.10	59.85	68.00	1.14
Fr. 5	102.6	111; 114.6	39.8	5.34	4.72	5.15	1.09	58.67	67.57	1.15
Fr. 6	102.8	110.5; 114	41.0	5.15	4.51	4.92	1.09	55.27	63.76	1.15
Fr. 7	101.6	109.2	41.0	4.75	4.12	4.49	1.09	49.08	56.42	1.15

^a As determined by DSC. ^b ($\Delta H_m/\Delta H_{m,PE} \times 100$), $\Delta H_{m,PE} = 293 \text{ J g}^{-1}$. ^c As determined by HPLC. ^d As determined from SSA.

This, therefore, explains why the reported \overline{L}_n and \overline{L}_w for the linear PE are smaller than the corresponding values of the branched PE, as well as the closeness in their broadness indexes as presented in Table 2. Due to this limitation, the methylene molar fractions (X), which are related to the MSL through eqn (2), were assigned to the peak melting temperatures using the equation derived from the calibration curve reported by Keating and others.^{36,37,41} In the current case, the methylene sequence length distribution (MSLD) plots (see Fig. 2b) were measured from the derived equation by Zhang *et al.* in eqn (3) who used a similar fractionation method.²⁹

$$\text{MSL} = \frac{2X}{1-X} = \frac{2}{e^{[\frac{142.2}{T_m} - 0.3451]} - 1} \quad (2)$$

$$\ln(X) = 0.3451 - \frac{142.2}{T_m}; \quad r^2 = 0.9997 \quad (3)$$

where $X = 0.900$ for $n\text{-C}_{20}\text{H}_{42}$.

Here, the statistical terms \overline{C}_n and \overline{C}_w , the broadness index, $I_c = \overline{C}_w/\overline{C}_n$ were recalculated based on the derived MSL *i.e.* number of CH_2 groups. Broadness indexes of 1.05 and 1.13 were reported for the linear and branched PE as shown in Table 2. Interestingly, respective \overline{C}_n and \overline{C}_w values of 674 and 707 were reported for the linear PE indicating a more linear structure with longer methylene sequences and higher homogeneity. In comparison, \overline{C}_n value of 58 and \overline{C}_w values of 65 were reported for the branched PE, which is ascribed to a more branched topology with shorter methylene sequences and higher heterogeneity. This, therefore, confirms the point that lamellar thickness is smaller for chains with longer methylene sequences.

Generally, the DSC heat flow is directly dependent on the size of crystallites formed and the specific heat capacity. Therefore, a branched material exhibiting broad branching distribution will produce a variation of lamellar crystal sizes

and subsequently a decrease in the heat of fusion with decreasing crystal size. With this in mind, the peak area for each SSA seed was converted to percentage weight fraction (content %) using the correction method proposed by Zhang and co-workers.^{35,40,41} Presented in Fig. 2b are the MSLD plots for the two samples, expressing the distribution of the seed content (%) as a function of MSL and displaying seeds with methylene sequences of $\text{C}_{20}\text{--C}_{90}$ for the branched PE and $\text{C}_{108}\text{--C}_{714}$ for the linear PE.

Experimentally, quantitative branching information can be calculated from ^{13}C NMR spectroscopy data as was previously reported.³² In a similar way, the conformation plots are used to evaluate LCB of SEC fractions as a function of molar mass. The contraction effect induced by LCB is observed by comparing linear and branched molecules of the same molar mass using the relationship in eqn (4).^{12,42,43} In the current study, the variation of LCB and the total branching content (total branching) expressed per thousand carbon (/1000C) are presented in Fig. 3 as a function of molar mass. The LCB data were calculated from the contracting factor after integrating eqn (5) and (6) to obtain eqn (7).^{11,12,31,44,43} The branching contents were determined using an IR5 detector coupled to SEC and calibrated with a series of ethylene-1-octene copolymer standards with varying comonomer contents and has a recommended standard error of ± 1 .

Fig. 3a presents the branching content dependency on molar mass plots for the linear and branched PE. As clearly seen, the linear PE exhibits very low branching at every given molar mass with a maximum branching frequency of 2.3/1000C, represented by the dotted line. It should be noted that the error on the linear PE is rather high due to its very low methyl content. In contrast, the branched PE displays a higher degree of branching but displays a decrease in the branching content from 30 to 15/1000C as molar mass increases. This could be because the set polymerization temperature and

CHAPTER 5

View Article Online

Paper

Polymer Chemistry

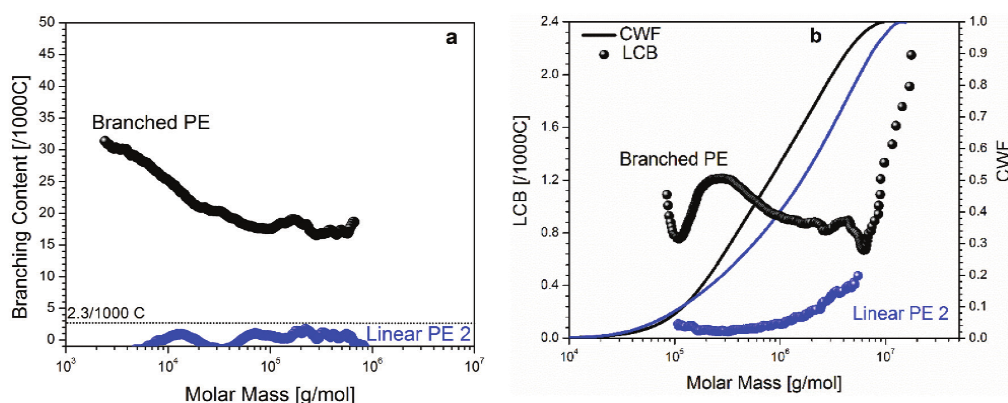


Fig. 3 Branching distribution plots comparing (a) branching frequency and (b) LCB frequency as a function of molar mass for the branched PE and the linear PE.

pressure to a greater extent promote chain growth reaction pathways, but suppress the intramolecular chain transfer reactions resulting in a decrease in branching as molar mass increases.⁴² Alternatively, the plots in Fig. 3b, present the LCB distribution for the branched and linear PE expressed as a function of molar mass. As expected, no material is observed below 10^5 g mol^{-1} due to the detection limit of the MALLS detector. The branched PE displays a variation in LCB as molar mass increases. However, the branched PE displays a higher LCB content at every given molar mass when compared to the linear PE. The linear PE indicates an increase in LCB as molar mass increases, most noticeable at the higher molar mass region. Although this may appear strange, similar results were reported by Gabriel and others.^{15,43,44} From their findings, it was indicated that a sparse level of LCB is also formed in metallocene-catalysed polymerized polyethylene.

$$R_g = 0.029M^{0.57} \quad (4)$$

where intercept $K = 0.029$ and the slope $a = 0.57$.⁴⁵

$$g = \left[\frac{\langle R_g^2 \rangle_{\text{Br}}}{\langle R_g^2 \rangle_{\text{Li}}} \right]_M \quad (5)$$

$$g = \left[\left(1 + \frac{m}{7} \right)^{1/2} + \frac{4m}{9\pi} \right]^{-1/2} \quad (6)$$

$$\frac{\text{LCB}}{1000\text{C}} = \lambda = Rm \times \frac{1000}{M} \quad (7)$$

where, $m = \text{LCBf}$, long chain branching per molecule, $R = 14$, the factor of repeated molar mass units.

Even though qualitative and quantitative branching information is obtainable when conducting bulk sample analyses, this approach is limited to providing average information. In addition, minor components will be left undetected. To obtain in-depth structural information on the heterogeneous nature of branched PE, the resin was fractionated preparatively into narrowly distributed branched fractions using pTREF and nar-

rowly dispersed molar mass fractions using pMMF as was previously reported.³² A detailed microstructural analysis of the fractions using a combination of advanced analytical techniques will be presented in the next section.

Branching analysis of pTREF and pMMF fractions

For a comprehensive structural analysis, detailed microstructural investigation on pTREF and pMMF fractions was conducted using SEC, CRYSTAF and ^{13}C NMR as previously reported.³² Quantitative analytical data on the pTREF and pMMF fractions, as well as the molar mass based on recovered material, calculated from the TREF/MMF-SEC data, are reporting. A bulk molar mass of 339 kg mol^{-1} is reported for the branched PE based on polystyrene calibration. Relative molar masses (Rel. M_w) of 319 and 307 kg mol^{-1} calculated from TREF and MMF recovered material, respectively, were reported, which are comparable to the bulk M_w .

In the current study, the molecular complexity of the fractions is investigated by combining thermal and chromatographic fractionation techniques. IR5 and MALLS detectors will be coupled to SEC, for branching distribution information of the eluting fractions as a function of molar mass. The plots in Fig. 4 compare the variation in the branching content of the TREF and MMF fractions as a function of molar mass. As clearly demonstrated, the linear PE exhibits a very low branching content and the dotted line around 2.3/1000C indicates the upper branching limit. It should be noted, that all fractions of the branched PE exhibit branching far beyond this line indicating a higher branching structure/topology. As can be seen in Fig. 4a, the TREF fractions display a variation in the branching vs. molar mass distribution plots and show a decreasing trend in the branching content as the TREF fractionation temperature increases from 30–90 °C. This is expected since TREF fractionates by crystallizability, which is a function of branching (SCB and LCB). The fact that the fractions do not exhibit a pronounced molar mass dependency of the branching content confirms that TREF fractionation is

CHAPTER 5

View Article Online

Polymer Chemistry

Paper

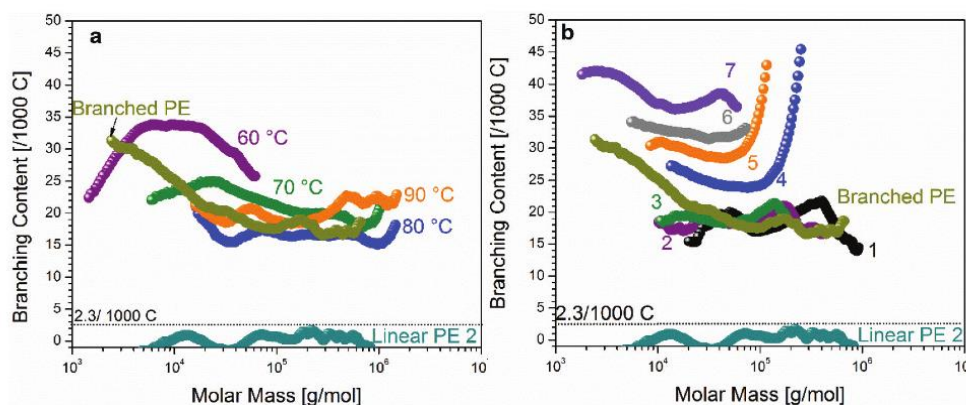


Fig. 4 SEC – IR5 plots expressing the branching content (methyl content) variation as a function of molar mass. The plots compare the (a) TREF fractions, (b) MMF fractions of the branched PE to the linear PE.

dominated by branching and not molar mass. The MMF fractions display branching and molar mass distribution plots that lie along the plot of the bulk resin as shown in Fig. 4b. Interestingly, the branching content of the MMF fractions increases with an increase in the fraction number from 1 to 7 (decreasing molar mass, see Table 3). This can be explained by the fact that the relative SCB content increases with decreasing molar mass.

The average branching contents (/1000C) of the fractions measured by SEC – IR5 are shown in Table 3 indicating complex branching structures of the TREF and MMF fractions.

Presented in Fig. 5 are conformation plots of the bulk branched resin and the fractions. From the Zimm–Stockmayer

relation in eqn (4), a linear relationship between the radius of gyration (R_g) and molar mass is observed for the ideal linear reference PE (see Fig. 5a and b). From previous literature^{2,16,17} it was reported that LCB enhances chain entanglement, which leads to a greater contraction of the branched molecules, and therefore, a reduction in size. For linear and branched molecules of the same molar mass, larger and smaller R_g are observed, respectively. The effect of LCB is indicated by the deviation of the plots of branched fractions from the plots of the linear reference. As is seen in Fig. 5a and b, conformation plots of the TREF and MMF fractions are compared to the ideal linear reference.

The fractions deviate from the linear plots towards lower R_g values, indicating that all TREF and MMF fractions exhibit some degree of branching.

When comparing the low and the high molar mass portions of the conformation plots, see zoomed parts in Fig. 5a (labelled a1 and a2), remarkable differences between the fractions are seen. In the lower molar mass region, branching in the fractions increases with an increase in the TREF fractionation temperature. The 70 °C TREF fraction is very close to the linear reference and may be due to SCB. In the higher molar mass region, LCB is more pronounced as indicated by Fig. 5a2.

As expected, a decrease in the degree of LCB of the fractions is seen with an increase in the TREF fractionation temperature.

Using this approach, very selective information about branching in the low and high molar mass regions can be obtained for the TREF fractions. The conformation plots of the MMF fractions are presented in Fig. 5b. MMF is a molar mass sensitive technique and, therefore, branching in these fractions are expected to follow a more random trend. In the lower molar mass region, the plots of fractions 4 and 5 lie parallel to but lower compared the linear plot. This behaviour is characteristic for samples with SCB. At the higher molar mass end, fraction 5 deviates strongest from the linear plot indicating the

Table 3 Summary of molar mass and branching data of the bulk and fractions of the branched PE

Sample name	Yield ^a [mg]	Yield ^a [%]	M_w^b [kg mol ⁻¹]	M_n^a [kg mol ⁻¹]	\bar{P}^b	Br (SEC) [/1000C] ^c
TREF						
30	0.07	2.45	25.4	2.4	10.4	102.6
60	0.25	8.47	17.5	6.2	2.8	31.7
70	0.43	14.77	235.7	42.7	5.5	21.4
80	1.64	56.03	388.7	89.6	4.3	16.9
90	0.49	16.65	385.5	78.4	4.9	20.5
130	0.05	1.63	—	—	—	—
Branched PE	3.00	100.0	338.9	37.2	9.1	22.0
Recovery	2.93	97.67	—	—	—	—
MMF						
1	0.90	32.28	579.9	130	4.4	18.6
2	0.73	26.29	278.8	77.2	3.6	19.5
3	0.60	21.56	165.5	60.1	2.8	20.0
4	0.17	5.99	103.8	41.0	2.5	30.9
5	0.14	5.14	55.7	25.2	2.2	34.7
6	0.10	3.53	29.8	16.4	1.8	33.6
7	0.15	5.22	20.1	7.3	2.7	38.3
Branched PE	3.00	100.0	338.9	37.2	9.1	22.0
Recovery	2.79	93.0	—	—	—	—

^a As determined by TREF and MMF. ^b As determined by SEC. ^c As determined SEC – IR5.

CHAPTER 5

Paper

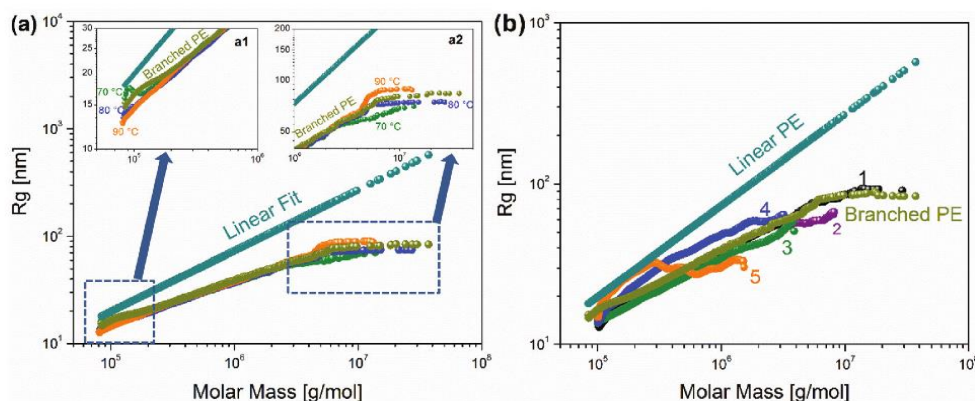
View Article Online
Polymer Chemistry

Fig. 5 Conformation plots comparing (a) the TREF fractions and (b) the MMF fractions of the branched to the linear PE.

highest degree of LCB. It is clear that in particular fractions 4 and 5 are highly heterogeneous with regard to SCB and LCB. MMF fractions 1, 2 and 3 are the higher molar mass fractions with fraction 3 having the lowest slope in the conformation plot and, therefore, the highest LCB.

The crystallization exotherms of the fractions are presented in Fig. S2 in the ESI.† As observed with the TREF fractions in Fig. S2a,† all the fractions (except the 30 °C fraction) exhibit unimodal crystallization profiles with peak crystallization temperatures increasing with an increase in the TREF elution temperature, indicating a decrease in branching. All fractions exhibit crystallization below 111.9 °C which corresponds to the crystallization temperature of the linear PE. Similar plots showing the crystallization of the MMF fractions are given in Fig. S2b.† With the exception of fractions 6 and 7 that show

broad onset tailing, all fractions display unimodality. In addition, the peak crystallization temperatures are observed to increase with a decrease in the fraction molar mass (increasing MMF fraction number, see Table 2 for more details). The melt endotherms are given in Fig. 6. In the case of the TREF fractions (see Fig. 6a), the 30 and 60 °C TREF fractions display multiple peaks, which indicate complex branching structures. In contrast, the higher temperature TREF fractions (*i.e.* fractions between 70 and 90 °C) display monomodal melting profiles. The peak melting temperatures increase with increasing TREF temperatures (decrease in branching). The melt endotherms showing the molar mass effect on melting temperature are presented in Fig. 6b. As clearly seen, the melt endotherms of fractions 4 to 7 display bimodal melting peaks, which may represent structurally different species of similar

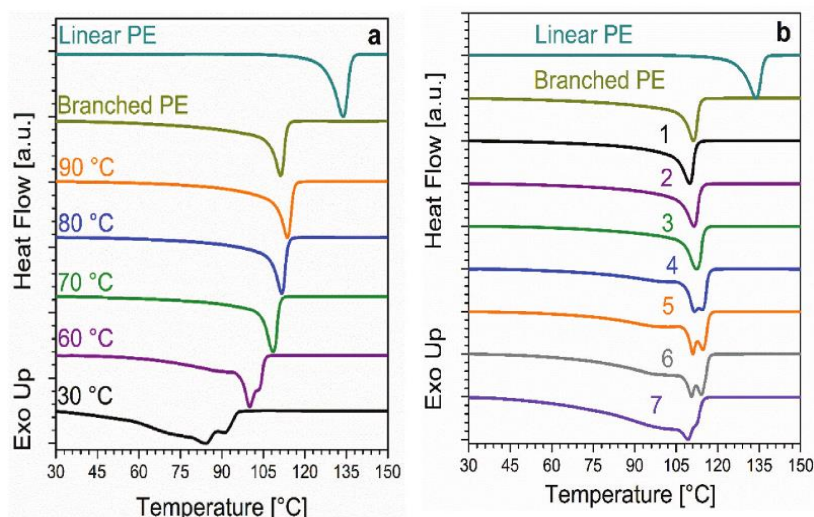


Fig. 6 DSC melting endotherms of (a) TREF fractions and (b) MMF fractions. Linear PE 1 was used as the linear reference.

CHAPTER 5

View Article Online

Polymer Chemistry

Paper

molar masses. On the other hand, unimodal but narrow melt endotherms are reported for fractions 1 to 3. Even though higher in molar mass, these fractions display lower peak melting temperatures indicating a more branched structure with greater homogeneity. A general decrease in the peak melting temperatures is observed as the fraction molar masses decrease (*i.e.* MMF fraction numbers increase). However, no major differences of the fractions' crystallinities are observed as shown in Table 2. Similar results were previously reported with CRYSTAF whereby all MMF fractions display comparable peak crystallization temperatures, indicating similar crystallizabilities even though they differ in composition.³² For all the fractions derived from pTREF or pMMF, the results clearly indicate that none of the fractions contains linear components.

Thermal fractionation by SSA was conducted on the individual fractions as presented in Fig. S3 in the ESI.[†] After SSA fractionation, the fractions display melt endotherms with multiple peaks, having distinct shapes and peak distributions. Also, as the fractions become increasingly branched, *i.e.* at decreasing TREF temperatures, the number of peaks increases and the peak temperature for the peak with the highest peak area decreases (see Fig. S3a[†]). The SSA melt endotherms of the MMF fractions are presented in Fig. S3b.[†] As is seen, the thermograms broaden with increasing number of peaks as the

MMF fraction number increases (*i.e.* molar mass decreases, see Table 2). The peaks with the highest peak area in the SSA-DSC plots of the MMF fraction series display peak temperatures between 112.5 and 114 °C, except for the fraction with highest molar mass (fraction 1) and lowest molar mass (fraction 7), that display peak temperatures at 109 and 103 °C, respectively. Though these peak temperatures vary within a small temperature window of about 1.5 °C, it is interesting to note that the peak temperature of the peak with the highest area increases slightly with an increase in the fraction molar mass (*i.e.* decrease in the fraction number from 6 to 2). Similar observations were made by CRYSTAF, whereby a small change in the peak crystallization temperature was reported.^{32,48} To our surprise, fraction 4 to 6 display seeds with peak melting temperatures around 117 °C as indicated by the circle in Fig. S3b,[†] which is ascribed to low molar mass chains with longer methylene sequences/higher linearity. These peaks are completely absent in the higher molar mass fractions as well as the higher temperature TREF fractions. These peaks, therefore, could account for the bimodal nature of the melt endotherms and the displayed higher melting temperatures of these fractions when compared to the higher molar mass fractions (1 to 3) as shown in Table 2 and Fig. 6b.

The MSLD plots of the fractions and bulk resins are presented in Fig. 7. As stated earlier, these plots express the vari-

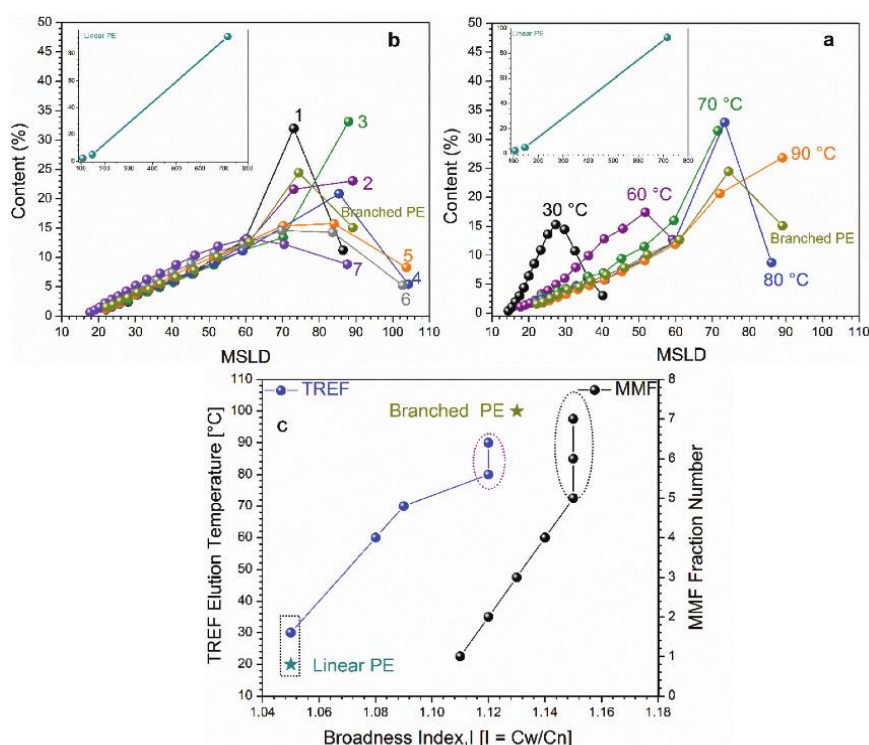


Fig. 7 Plots comparing the MSLD of (a) TREF fractions and (b) MMF fractions of the branched PE to the linear PE 1. (c) Compares the broadness index (*I*) distribution of the TREF and MMF fractions.

CHAPTER 5

View Article Online

Paper

Polymer Chemistry

ation in the crystal size as a function of MSL. Fig. 7a displays the MSLD plots of the TREF fractions. As previously reported, three main fraction components constitute the branched PE after TREF fractionation, see fractions eluting at 30, 60 and 70–130 °C.⁴⁸ The highly branched 30 and 60 °C fractions, which are the lower molar mass components, composed of polymer chains with crystallisable methylene sequences ranging between C₁₄–C₄₀ and C₁₈–C₆₀, respectively. The seeds representing the largest population of these fractions exhibit fraction contents of 14 and 16%, which composed of molecules with average crystallisable methylene sequences of approximately C₂₇ and C₅₀, respectively, and are ascribed to highly branched structures.

In comparison, the higher temperature TREF fractions, which consist of the 70, 80 and 90 °C fractions, have molar masses above 200 kg mol^{−1} (see Table 3). The seeds representing the larger populations in these fractions display content of 30, 31 and 26%, and constitute chains with crystallisable methylene sequences of ~C₇₀, C₇₄ and C₉₀. Interestingly, the fractionation temperatures of the 30, 70 and 90 °C fractions are numerically the same as the MSL of the seeds with the highest peak area (*i.e.* the seed with highest peak area for the 70 °C fractions display MSL of ~C₇₀). In the case of the 80 and 60 °C fractions, the MSL for the seeds with the highest peak area is lower than their fractionation temperature. However, the fractionation temperatures for these fractions are numerically the same as the MSL of the seeds with the highest peak melting temperature, which is the last peak on their respective SSA plots (*i.e.* the last seeds of the 60 and 80 °C fractions display MS of ~C₆₀, and C₈₀, respectively). Therefore, SSA is a suitable technique for predicting the precise TREF elution temperatures needed for the fractionation of polyolefins with complex microstructure. This observation was previously reported and was introduced in the work of Xue *et al.*³⁴

Plots of MSLD *versus* crystal size content of the MMF fractions are given in Fig. 7b. For chains with MSL up C₆₀, a linear increase in the seed content is observed with an increase in the methylene sequences. In the case of the MMF fractions, a

linear increase in the seed content is seen with an increase in the MSL for chains with methylene sequences of up C₆₀ as indicated in the area defined by the rectangular box. For chains with higher methylene sequences (>C₆₀), varying content amounts are observed. The seeds with the highest contents are reported for fractions 1 and 3, which display contents of 32 and 33% corresponding to chains with MSL of C₇₃ and C₈₈, respectively. It is important to note that the MSL for seed with the highest population of fraction 1 (pMMF) and the 80 °C fraction (pTREF) is C₇₃. These two fractions constitute the main component of their respective fraction series.

Some seeds with contents of ~5, 8 and 5% are observed for fractions 4, 5 and 6 with peak melting temperatures around 117 °C, see the red cycle in Fig. 8b. These peaks are composed of chains with methylene sequences of about C₁₀₃, which are attributed to chains with lower molar masses and branching contents (higher crystallinity). Such chains are absent in the highest temperature TREF fractions and, therefore, highlight the effect of co-crystallization/co-elution occurring in the TREF process.

Presented in Fig. 7c are plots describing the effect of TREF elution temperature/MMF fraction number on the broadness indexes. As clearly seen, the TREF fractions show a linear increase in broadness indexes as TREF temperature increases to 80 °C and remain constant for higher TREF temperatures. The linear PE shows a very low broadness index of 1.05. In the case of the MMF fractions, a linear increase in the broadness index with an increase in the MMF fraction number (decrease in molar mass) from fraction 1 to 5 is observed, while fractions 5–7 display similar broadness indexes of 1.15. However, all the MMF fractions display MSL heterogeneities as expressed by the high broadness indexes ranging from 1.11 to 1.15, as compared to 1.05 to 1.12 of the TREF fractions. This observation further confirms that MMF fractions are more homogenous in molar mass but very broad in their branching distributions.

To gain further insight into the molecular heterogeneity of the fractions, the TREF and MMF data were combined with the SSA data to generate two-dimensional (2D) plots as deployed

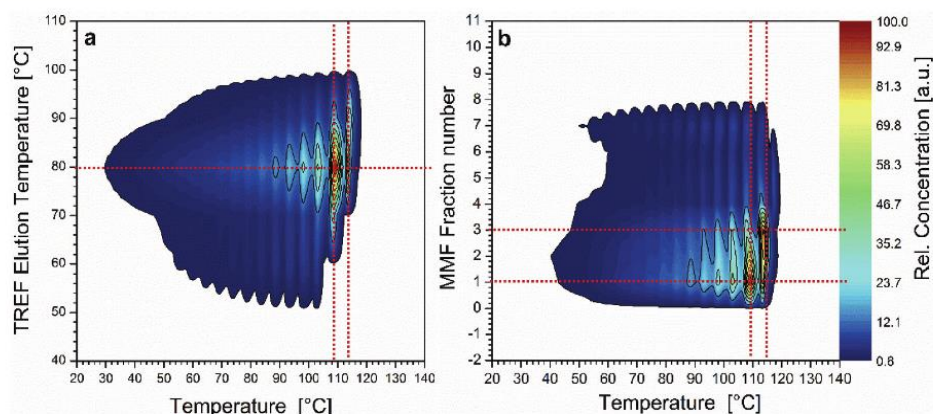


Fig. 8 2D contour plots obtained by combining (a) TREF-SSA and (b) MMF-SSA of branched PE.

CHAPTER 5

View Article Online

Polymer Chemistry

Paper

in Fig. 8. Each point on the contour plot presented in Fig. 8a relates the melting temperature at which a population of lamellar crystals with similar crystallisable methylene sequences (CMS) will co-elute in TREF, being a reflection of their branching contents (see Table 2). It clearly indicates that increasing TREF temperatures correlate to longer CMS. Two main groups of crystals exhibit melting temperatures at ~ 110 °C and ~ 114 °C. They elute at TREF temperatures ranging from 70 to 90 °C, the main components being observed at 80 °C TREF temperature. It is important to note that these fractions represent the highest molar mass components of the bulk resins (>200 kg mol $^{-1}$).

In Fig. 8b, the MMF fraction number directly reflects the molar mass as shown in Table 3 and in previous literature.^{32,48} Similar to the TREF fractions, two main populations of lamellar crystals exhibit melting temperatures at ~ 110 °C and ~ 114 °C. These two distinctive groups of crystals belong to fractions 1 and 3, respectively. Considering the fact that pMMF fractionation is dominated by molar mass, this dependency shows an interesting correlation between crystal size and molar mass. The fact that different crystal sizes (corresponding to different molar masses) elute in the same TREF temperature range highlights the co-crystallization/co-elution effect when using crystallization-based techniques, and therefore, the necessity of multiple preparative fractionation protocols for an in-depth microstructural analysis of complex polyolefins like LDPE.

HPLC and two-dimensional chromatographic analysis

As mentioned previously, thermal fractionation is crystallization-based and, therefore, can only characterize the crystallizable components. To account for all components including the amorphous fractions, the crystallization-based techniques are complemented with solvent gradient HPLC, which uses 1-decanol/TCB as eluent and porous spherical graphite as the stationary phase. Detailed descriptions of the separation in HPLC was previously reported.^{16,32}

For a sound interpretation of the HPLC data, it is important to note that molecules with a linear uninterrupted ethylene sequence backbones are strongly retained on the stationary phase, while the retention time for branched molecules decreases as a function of the degree of branching.^{4,49} The individual HPLC elugrams of the fractions and the bulk PE resins are presented in Fig. S4 in the ESI.† The linear PE displays a unimodal and narrow elution peak at 5.75 mL, which is typical for molecules with very long linear ethylene sequences. The branched PE and the fractions display elugrams at elution volumes between 3.87 and 5.48 mL (TREF fractions) and 4.75 and 5.67 mL (MMF fractions), which are below the elution volume presented for the linear PE. The decrease in elution volume is caused by branching and lower molar masses. Fig. S4a in the ESI† shows the individual elugrams of the TREF fractions. The peak elution volumes decrease and the peaks broaden as the TREF elution temperature decreases from 90 to 30 °C.

The peak broadening is due to an increase in structural heterogeneity, while the decreasing peak elution volume is ascribed to increasing degrees of branching. In comparison, the elugrams for the MMF fractions are given in Fig. S4b.† A steady increase in the peak elution volumes is observed for fractions 7 to 1 which corresponds to increases in molar mass. Some fractions display broad elugrams, which are indicative of structural heterogeneity. For fractions 3 to 1 the peak elution volumes increased only slightly and the elugrams become increasingly narrow. This is because at very high molar masses all macromolecules elute at the same elution volume.

For an in-depth structural investigation, the branched and linear PE were fractionated using 2D chromatography. In this technique, the HPLC column in the first dimension is in hyphenation with the SEC column in the second dimension. The polymers are fractionated firstly by branching, followed by subsequent fractionation of the HPLC fractions according to their hydrodynamic sizes to yield molar mass information, see the 2D contour plots in Fig. 9. The dotted line at HPLC elution volume of 5.6 mL separates the elution areas of the linear and branched components. Above this line (at higher elution volume) molecules elute which constitute the linear backbone (at 5.7 mL). Below this line branched components elute, which for the linear sample exhibit a molar mass bimodality. One has to consider, however, that to a certain extent elution peaks overlap and, therefore, there is no strict separation between the linear and branched elution areas.

In comparison to the linear PE, the branched PE presented in Fig. 9b constitutes mostly branched components that exhibit HPLC elution below 5.6 mL. Only a minute amount of less than 0.5% is observed above this line. The rectangular box labelled 1 indicates that the linear PE exhibits predominantly linear species as compared to the branched PE. Similarly, from the rectangular box labelled as 2, it could be seen that the bulk molar mass distributions of the linear and branched samples are rather similar.

The 2D-LC analyses of selected TREF fractions of the branched sample are presented in Fig. 10. As has been shown in previous investigations, branching decreases with increasing TREF elution temperature. At the same time, lower molar masses correspond to lower TREF elution temperatures. As can be seen in Fig. 10c and d, the TREF fractions eluting at 80 and 90 °C, respectively, produce 2D plots that are very similar to the 2D plot of the bulk sample. These are the majority fractions determining the molecular composition of the bulk sample. This is in good agreement with the previous analytical data. Compared to these fractions, the TREF fractions eluting at 70 and 60 °C, respectively, indicate decreasing molar masses and increasing branching, see Fig. 10b and a. As can be seen clearly, the 60 °C TREF fraction has the lowest molar mass (highest SEC elution volume) and the highest degree of branching which confirms the NMR results (not shown here) and the SSA results (for the shortest crystallizable methylene sequences). In a similar way, the pMMF fractions were analyzed by 2D-LC, see Fig. 11. In this case, MMF fraction 3 is rather identical to the bulk sample. Fractions 2 and 1 exhibit

CHAPTER 5

[View Article Online](#)

Paper

Polymer Chemistry

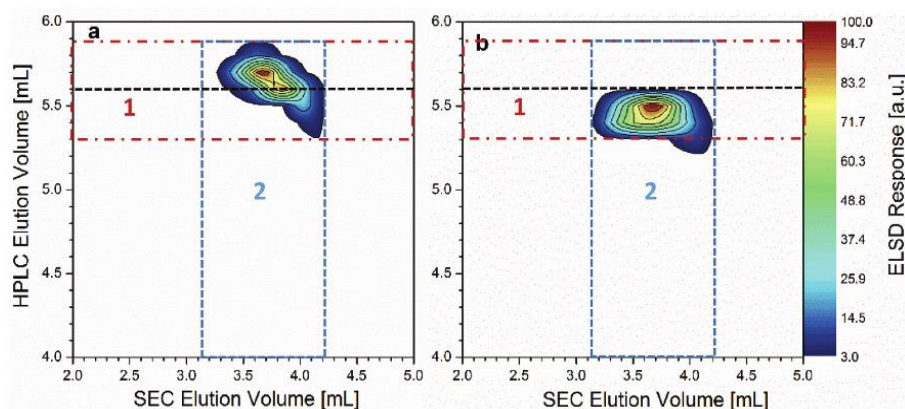


Fig. 9 2D contour plots correlating branching to molar mass of (a) linear PE 1 and (b) branched PE.

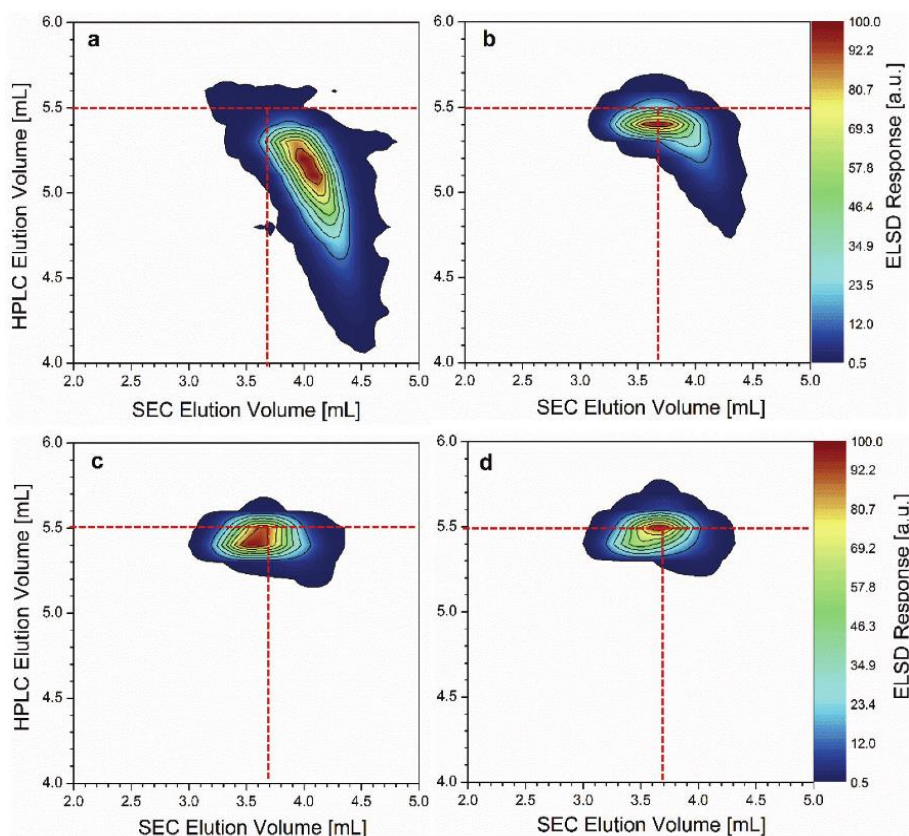


Fig. 10 2D contour plots of the TREF fractions of branched PE. The plots labeled (a) to (d) correspond to TREF fractions 60 to 90 °C. The dotted line indicates the peak elution volumes of the bulk sample analysis of branched PE.

increasing molar masses as is signified by the decreasing SEC elution volumes see Fig. 11b and a, respectively. At the same time, the fractions have slightly different degrees of branching as can be seen from the different HPLC elution volumes. Fraction 1 displays a lower HPLC peak elution volume at

5.4 mL indicating a higher degree of branching in comparison to fractions 2 and 3 with an HPLC elution volume of 5.5 mL. This result correlates well with the SSA results reported in Fig. 8b, where a higher amount of linear structures was reported for fraction 3. Following the same logic, fractions 4, 5

CHAPTER 5

View Article Online

Polymer Chemistry

Paper

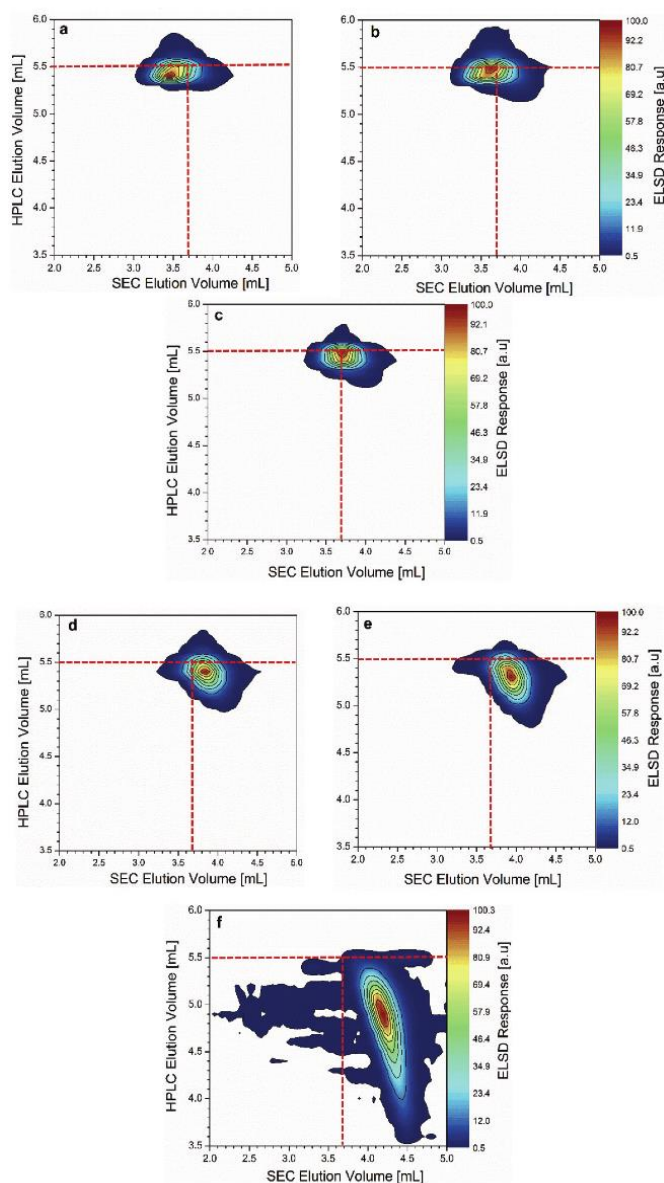


Fig. 11 2D contour plots of the MMF fractions of branched PE. The plots labeled (a) to (f) correspond to MMF fractions 1, 2, 3, 4, 5 and 7. Fraction 6 was omitted due to insufficient amount of material. The dotted line indicates the peak elution volumes of the bulk sample analysis of branched PE.

and 7 have lower molar masses and increased degrees of branching. Fraction 7 has the lowest molar mass and the highest degree of branching and is very similar to the 60 °C TREF fraction; compare Fig. 10a and 11f.

Conclusion

The microstructural complexity of branched polyethylene (*e.g.* LDPE) originates from the broad molar mass and branching distributions. Here, the branches at the polymer backbone are

distributed with respect to their locations and sizes. The size and number of branches incorporated significantly affect chain crystallinity and the crystalline morphology. Therefore, to understand the molecular structure, representative branched and linear PEs were used to establish relationships between molecular structure, crystallization and melting behaviour, and crystal size/morphology. The morphology of the bulk resins was investigated in solution and melt using SCALLS, DSC and SSA, which subsequently followed the analyses of preparative fractions. Fractions with narrow molar mass and branching dispersities were generated from the

CHAPTER 5

View Article Online

Paper

Polymer Chemistry

branched resin using pMMF and pTREF, respectively. Molar mass characterization using SEC was enhanced with a MALLS and IR5 detectors, to provide long chain branching (LCB) and total branching information as a function of molar mass. SCALLS and DSC are crystallization-based methods, which are limited to analyzing the crystallizable components. As a complementary method, HPLC was used to analyze the fractions, to account for both the crystalline and amorphous components. Since polymer properties are influenced by both branching and molar mass, cross-fractionation experiments were conducted of the bulk resins and fractions thereof, using 2D-LC. This technique coupling HPLC and SEC provides bivariate distribution plots, thereby, providing the interrelationships between branching and molar mass.

The TREF/MMF-SSA analyses have clearly shown the correlation between crystal size and molar mass, which highlight the effect of co-crystallization and co-elution in TREF.

The combination of TREF/MMF-SSA and 2D-LC has shown that the relatively highly linear components and the extremely highly branched components of the branched PE exist in small amounts.

Conflicts of interest

There are no conflicts of interest to declare.

Acknowledgements

The authors would like to thank Sasol (South Africa) for providing the LDPE sample and supporting the research financially.

References

- 1 E. H. Immergut and H. F. Mark, in *Plasticization and Plasticizer Processes*, ed. N. A. J. Platzer, American Chemical Society, Washington, D.C., 1965, vol. 48, pp. 1–26.
- 2 W. W. Yau, *Polymer*, 2007, **48**, 2362–2370.
- 3 A. Krumme, M. Basiura, T. Pijpers, G. Vanden Poel, L. C. Heinz, R. Bruell and V. B. F. Mathot, *Mater. Sci.*, 2011, **17**, 260–265.
- 4 H. Pasch and M. I. Malik, *Advanced Separation Techniques for Polyolefins*, Springer International Publishing, Cham, 2014.
- 5 D. B. Malpass, *Introduction to Industrial Polyethylene: Properties, Catalysts, and Processes*, John Wiley & Sons, Inc., Hoboken, NJ, USA, 2010.
- 6 M. Busch, *Macromol. Theory Simul.*, 2001, **10**, 408–429.
- 7 P. J. Flory, *Principles of polymer chemistry*, Cornell Univ. Press, Ithaca, NY, 19. print., 2006.
- 8 D. E. Axelson, G. C. Levy and L. Mandelkern, *Macromolecules*, 1979, **12**, 41–52.
- 9 D. C. Bugada and A. Rudin, *Eur. Polym. J.*, 1987, **23**, 809–818.
- 10 M. E. A. Cudby and A. Bunn, *Polymer*, 1976, **17**, 345–347.
- 11 H. N. Cheng, *Polym. Bull.*, 1986, **16**, 445–452.
- 12 F. A. Bovey, F. C. Schilling, F. L. McCrackin and H. L. Wagner, *Macromolecules*, 1976, **9**, 76–80.
- 13 J. N. Hay, P. J. Mills and R. Ognjanovic, *Polymer*, 1986, **27**, 677–680.
- 14 Y. Xue, Y. Fan, S. Bo and X. Ji, *Chin. J. Polym. Sci.*, 2015, **33**, 508–522.
- 15 C. Gabriel, *Einfluss der molekularen Struktur auf das viskoelastische Verhalten von Polyethylenschmelzen*, Shaker, Aachen, 2001.
- 16 H. Pasch, *Polym. Adv. Technol.*, 2015, **26**, 771–784.
- 17 A. Ndiripo and H. Pasch, *Anal. Bioanal. Chem.*, 2015, **407**, 6493–6503.
- 18 S. Cheruthazhekatt and H. Pasch, *Anal. Bioanal. Chem.*, 2014, **406**, 2999–3007.
- 19 S. Anantawaraskul, J. B. P. Soares and P. M. Wood-Adams, in *Polymer Analysis Polymer Theory*, Springer Berlin Heidelberg, Berlin, Heidelberg, 2005, vol. 182, pp. 1–54.
- 20 B. Monrabal, L. Romero, N. Mayo and J. Sancho-Tello, *Macromol. Symp.*, 2009, **282**, 14–24.
- 21 B. Monrabal, J. Sancho-Tello, N. Mayo and L. Romero, *Macromol. Symp.*, 2007, **257**, 71–79.
- 22 C. L. P. Shan, W. A. deGroot, L. G. Hazlitt and D. Gillespie, *Polymer*, 2005, **46**, 11755–11767.
- 23 S. Cheruthazhekatt, D. D. Robertson, M. Brand, A. van Reenen and H. Pasch, *Anal. Chem.*, 2013, **85**, 7019–7023.
- 24 D. D. Robertson, R. Neppalli and A. J. van Reenen, *Polym. Test.*, 2014, **40**, 79–87.
- 25 A. Prasad, *Polym. Eng. Sci.*, 1998, **38**, 1716–1728.
- 26 T. S. Motsoeneng, A. S. Luyt and A. J. van Reenen, *J. Appl. Polym. Sci.*, 2014, **131**, 466–476.
- 27 M. Zhang, D. T. Lynch and S. E. Wanke, *J. Appl. Polym. Sci.*, 2000, **75**, 960–967.
- 28 A. J. Müller and M. L. Arnal, *Prog. Polym. Sci.*, 2005, **30**, 559–603.
- 29 M. Zhang and S. E. Wanke, *Polym. Eng. Sci.*, 2003, **43**, 1878–1888.
- 30 R. Brüll, N. Luruli, H. Pasch, H. G. Raubenheimer, E. R. Sadiku, R. Sanderson, A. J. van Reenen and U. M. Wahner, *e-Polym.*, 2003, **3**, 785–793.
- 31 A. J. Van Reenen, R. Brüll, U. M. Wahner, H. G. Raubenheimer, R. D. Sanderson and H. Pasch, *J. Polym. Sci., Part A: Polym. Chem.*, 2000, **38**, 4110–4118.
- 32 P. S. Eselem Bungu and H. Pasch, *Polym. Chem.*, 2017, **8**, 4565–4575.
- 33 I. Amer, A. van Reenen and M. Brand, *Polym. Int.*, 2015, **64**, 466–476.
- 34 Y. Xue, S. Bo and X. Ji, *Chin. J. Polym. Sci.*, 2015, **33**, 1000–1008.
- 35 Y. Xue, S. Bo and X. Ji, *J. Polym. Res.*, 2015, **22**, 1–10.
- 36 M. Keating, I.-H. Lee and C. S. Wong, *Thermochim. Acta*, 1996, **284**, 47–56.
- 37 F. Zhang, J. Liu, Q. Fu, H. Huang, Z. Hu, S. Yao, X. Cai and T. He, *J. Polym. Sci., Part B: Polym. Phys.*, 2002, **40**, 813–821.

CHAPTER 5

[View Article Online](#)

Polymer Chemistry

Paper

- 38 T. Macko, R. Brüll, R. G. Alamo, F. J. Stadler and S. Losio, *Anal. Bioanal. Chem.*, 2011, **399**, 1547–1556.
- 39 S. Cheruthazhekatt, T. F. J. Pijpers, G. W. Harding, V. B. F. Mathot and H. Pasch, *Macromolecules*, 2012, **45**, 2025–2034.
- 40 D. Cavallo, A. T. Lorenzo and A. J. Müller, *J. Polym. Sci., Part B: Polym. Phys.*, 2016, **54**, 2200–2209.
- 41 F. Zhang, Q. Fu, T. Lü, H. Huang and T. He, *Polymer*, 2002, **43**, 1031–1034.
- 42 G. Luft, R. Kämpf and H. Seidl, *Makromol. Chem.*, 1982, **108**, 203–217.
- 43 V. Karimkhani, F. Afshar-Taromi, S. Pourmahdian and F. J. Stadler, *Polym. Chem.*, 2013, **4**, 3774.
- 44 P. M. Wood-Adams, J. M. Dealy, A. W. DeGroot and O. D. Redwine, *Macromolecules*, 2000, **33**, 7489–7499.
- 45 M. Wagner, K. Reiche, A. Blume and P. Garidel, *Pharm. Dev. Technol.*, 2013, **18**, 963–970.
- 46 S. Podzimek, *Light scattering, size exclusion chromatography, and asymmetric flow field flow fractionation: powerful tools for the characterization of polymers, proteins, and nanoparticles*, Wiley, Hoboken, NJ, 2011.
- 47 W.-J. Wang, S. Kharchenko, K. Migler and S. Zhu, *Polymer*, 2004, **45**, 6495–6505.
- 48 P. S. Eselem Bungu and H. Pasch, *Polym. Chem.*, 2018, **9**, 1116–1131.
- 49 T. Macko, R. Brüll, R. G. Alamo, F. J. Stadler and S. Losio, *Anal. Bioanal. Chem.*, 2011, **399**, 1547–1556.

CHAPTER 5

Electronic Supplementary Material (ESI) for Polymer Chemistry.
This journal is © The Royal Society of Chemistry 2018

Combination of Preparative and Two-Dimensional Chromatographic Fractionation with Thermal Analysis for the Branching Analysis of Polyethylene

Paul S. Eselem Bungu,^a Kristina Pflug^b and Harald Pasch^{*a}

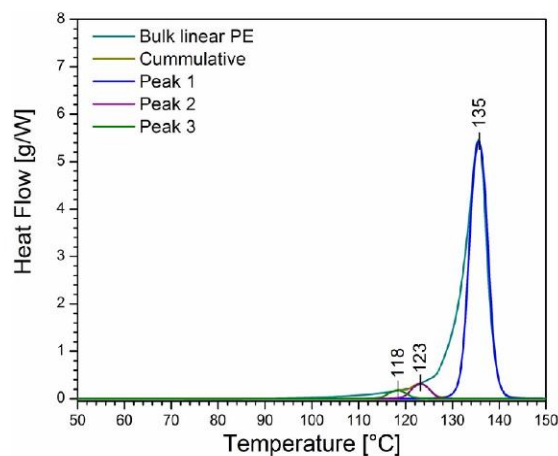


Figure S1: Peak Deconvolution of the SSA plot of linear PE 1, showing additional peaks at 118 and 123 °C

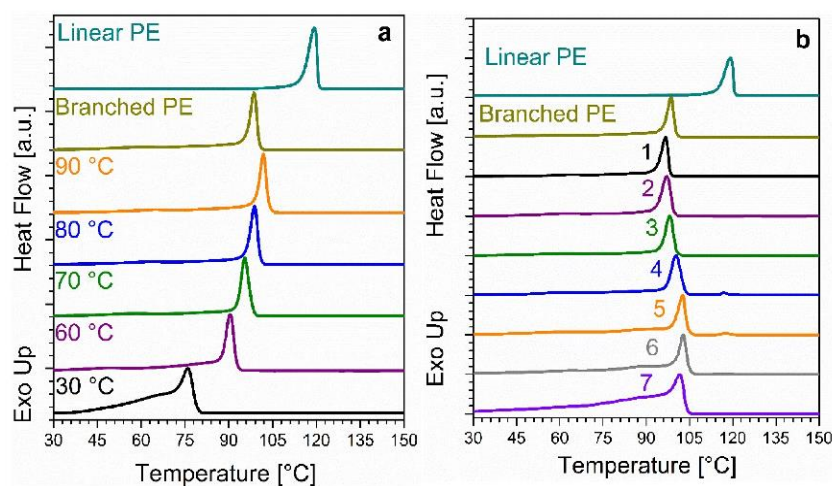


Figure S2: DSC crystallization exotherms of (a) TREF fractions and (b) MMF fractions. Linear PE 1 was used as the linear reference.

CHAPTER 5

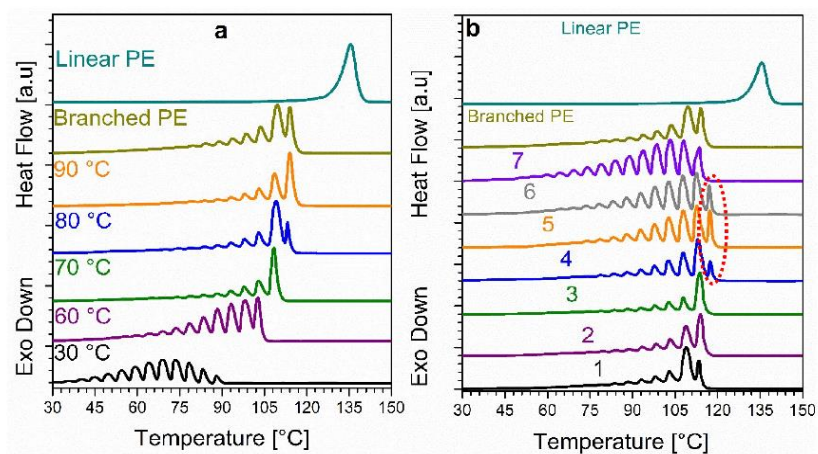


Figure S3: DSC melting endotherms obtained after thermal fractionation by SSA, (a) TREF fractions and (b) MMF fractions. Linear PE 1 was used as the linear reference.

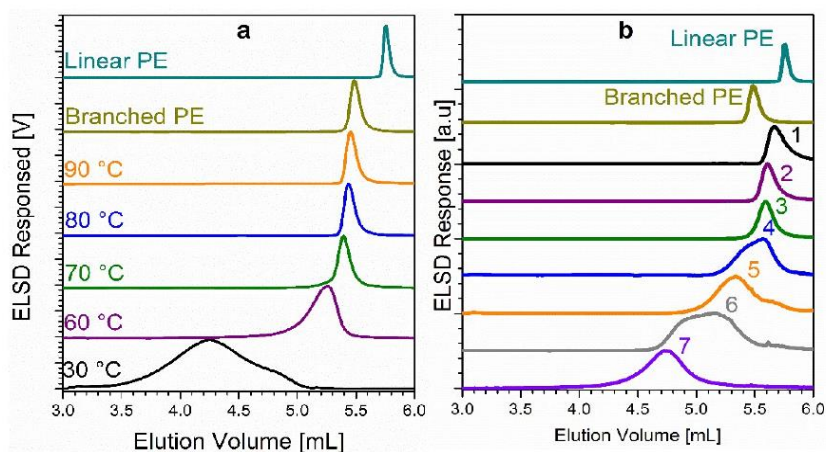


Figure S4: Individual HPLC elugrams of (a) TREF fractions and (b) MMF fractions of branched PE as compared to the linear and branched bulk samples. Linear PE 1 was used as the linear reference.

6 Comprehensive Analysis of Novel Grafted Polyethylene Using Multiple Fractionation Methods

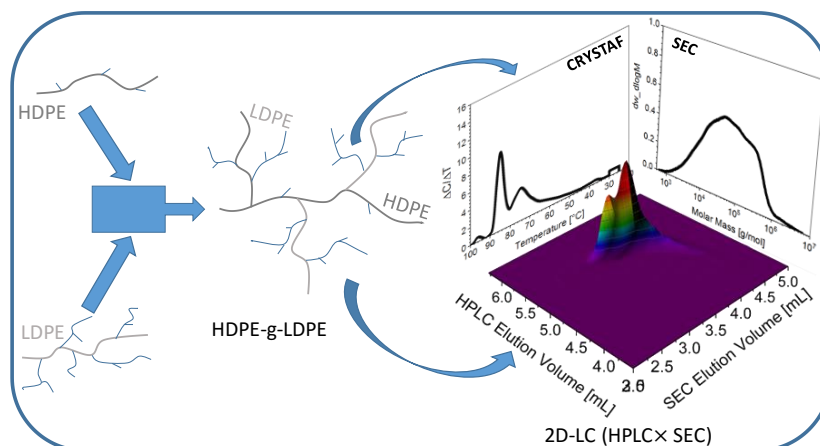


Figure 12: Chain heterogeneity in novel grafted polyethylene

In this chapter, the analysis of novel polymers, produced by grafting low density polyethylene (LDPE) onto a high density polyethylene (HDPE) backbone (HDPE-g-LDPE) were analysed and compared to the reference linear (HDPE) and branched (LDPE) homopolymers. The molecular structures of the bulk resins were investigated using SEC, CRYSTAF, HPLC, DSC, SEC-MALLS and ^{13}C NMR. The results revealed that the molecular structure of the grafted samples is heterogeneous, constituting a mixture of non-grafted LDPE, non-grafted HDPE and the grafted materials. The SEC results indicated a complex mixture of different molar mass species, while CRYSTAF, HPLC and DSC showed a complex mixture of branched, linear and grafted components in the bulk materials.

^{13}C NMR results revealed that the grafted samples constitute predominantly n-butyl groups as short chain branches and a small amount of long chain branching (LCB). The presence of LCB was confirmed by SEC-MALLS, and the results revealed that different grafting products had different levels of LCB.

For a comprehensive evaluation, the grafted samples and the reference LDPE were fractionated by pTREF. The results confirmed the different compositions of the samples with one sample containing a higher amount of non-grafted HDPE, indicating a lower degree of grafting and, therefore, lower conversion.



The fractions were also analysed by 2D-LC (HPLC \times SEC), which provided comprehensive 2D plots showing the interrelationship between the branched/grafted/linear components and molar mass.

The detailed results of this work has been published (P. S. Eselem Bungu, K. Pflug, M. Busch and H. Pasch, *Polym. Chem.*, 2018, 9, 5051–5065) and can be found in this chapter.



Cite this: DOI: 10.1039/c8py01122b

Comprehensive analysis of novel grafted polyethylenes using multidimensional fractionation methods†

Paul S. Eselem Bungu, ^a Kristina Pflug,^b Markus Busch^b and Harald Pasch ^{*,a}

Advanced polyolefins exhibit sophisticated molecular structures with unique processing and applications properties. One way of tailor-making novel polyolefin structures is through novel polymerization processes or modifying existing structures through functionalization or grafting. The latter approach is taken in the present work where novel grafted polyethylenes (HDPE-*g*-LDPE) were prepared. To elucidate the molecular heterogeneity of these novel materials in terms of branching and molar mass, a comprehensive multidimensional analytical approach was developed. Advanced analytical techniques such as CRYSTAF, DSC, HPLC, SEC and NMR were used for bulk sample analysis and first indications for the presence of non-grafted LDPE and HDPE along with the graft polymer HDPE-*g*-LDPE were obtained. For a more detailed study of the materials' heterogeneity, the samples were fractionated by preparative TREF to obtain fractions which were further analyzed regarding branching, molar mass and crystallinity. Different components including the non-grafted LDPE, HDPE and the grafted HDPE-*g*-LDPE were identified by crystallization-based, spectroscopic and chromatographic methods. The compositions of the different TREF fractions were estimated and fractions were identified that predominantly consist of HDPE-*g*-LDPE. The bulk samples and their corresponding TREF fractions were analyzed by 2D-LC (HPLC × SEC) to provide comprehensive two-dimensional pictures demonstrating the relationship between molar mass and branching.

Received 1st August 2018,
Accepted 14th September 2018
DOI: 10.1039/c8py01122b
rsc.li/polymers

Introduction

Advanced polyolefins such as polyethylene (PE), polypropylene (PP), polyolefin copolymers and blends have constantly been replacing traditional materials like alloys, ceramics and even glasses in applications such as in household appliances, automobile body parts, interior décor for cars and aircraft, *etc.* This is owing to the fact that these thermoplastics are affordable and possess competitive properties like high toughness and hardness in addition to high environmental stability. Additional advantages include their high resistance to thermo-oxidative degradation and excellent recyclability.

Despite all these positive attributes, high-density polyethylene (HDPE) particularly at very high molar masses may exhibit poor processability, which may limit some of its applications.^{1,2} Some properties of HDPE can be enhanced by intro-

ducing functional groups (polar or non-polar) at the backbone of the polymer chain, thereby altering the molecular architecture. Long chain branching (LCB) for example, impacts rheological properties and, therefore, enhances processability and influences materials' crystallinity without necessarily affecting the structural strength. Branching can further improve properties such as ductility and transparency.³ Copolymerization, polymer grafting and controlled radical polymerization are some processes known to yield new thermoplastic polyolefin materials with finely tuned properties, thereby, producing alternative classes of materials with improved properties.^{4–9}

In the current study, novel grafted polyethylenes are produced by grafting branched homopolymer chains (low-density polyethylene, LDPE) onto linear homopolymer backbones (HDPE) to yield grafted polyethylene of the type HDPE-*g*-LDPE that is schematically presented in Fig. 1. Presumably, these novel grafted polyethylenes may inherit the intrinsic properties of the individual constituents along with unique properties derived from the synergistic action of both components.

Besides changing the polymer architecture, microstructural parameters such as compositional distribution, the degree of branching/grafting, molecular size *etc.*, are equally changed. As a result of these structural changes, different physical pro-

^aDepartment of Chemistry and Polymer Science, University of Stellenbosch, PO Box X1, 7602 Matieland, South Africa. E-mail: hpasch@sun.ac.za

^bErnst-Berl-Institute of Technical Chemistry, Technical University Darmstadt, Alarich-Weiss-Straße 8, 64287 Darmstadt, Germany

†Electronic supplementary information (ESI) available. See DOI: 10.1039/c8py01122b

CHAPTER 6

View Article Online

Paper

Polymer Chemistry

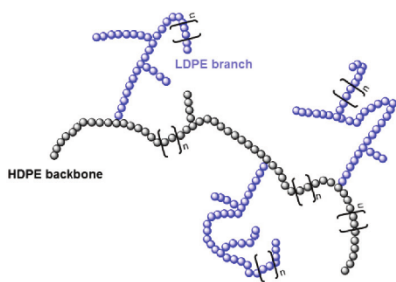


Fig. 1 Schematic representation of grafted polyethylene.

erties including novel crystallization and flow behaviors are obtained. Therefore, it is of utmost importance to conduct a thorough microstructural investigation of the molecular composition of these novel grafted polyethylenes. This will enable correlating microstructural parameters and physical properties to develop structure–property relationships.

To unravel the microstructure of these polymers, a series of established analytical techniques are available. The molecular size of the polymers is typically determined by size exclusion chromatography (SEC). SEC coupled to either a refractive index (RI) or an infrared (IR) detector alongside light scattering (LS) and viscometer detectors in a triple detector mode (SEC-RI-LS-Vis or SEC 3D) is a powerful tool for the determination of the polymer size and LCB.^{10,11} Branching distribution information can be obtained by crystallization analysis fractionation (CRYSTAF),^{12,13} which measures polymer crystallization from a dilute solution, and differential scanning calorimetry (DSC),¹⁴ which analyses the polymer crystallization and melting behavior. These two techniques (CRYSTAF and DSC) are crystallization-based, hence are limited to the crystallizable components of the materials.

High-temperature high-performance liquid chromatography (HPLC), developed by Macko, Pasch and others^{13,15–17} is capable of analyzing both the crystalline and the amorphous components of complex polyolefins. Thermal fractionation by successive self-nucleation and annealing (SSA)^{18–20} may be used to fractionate these samples. This technique fractionates by segregating molecules according to their crystallizable methylene sequences (CMS) providing detailed insight regarding the polymer heterogeneity. In addition, cross-fractionation such as HPLC \times SEC can be conducted to achieve separation firstly by branching, then by molecular size using high-temperature two-dimensional liquid chromatography (2D-LC).^{15,20,21} The importance of polymer fractionation on a preparative scale using techniques such as temperature rising elution fractionation (TREF), molar mass fractionation (MMF) and solvent gradient elution fractionation has been highlighted in previous reports.^{16,17,19–22} These techniques provide material in mg to g scale with different structural compositions (pTREF) or different molar masses (pMMF) that can be analyzed further using offline techniques. Spectroscopic techniques such as ¹³C NMR spectroscopy have been used as a quick tool to determine

average branching as well as the branch types. By NMR definition, branches ranging from 1 carbon atom (methyl) to 5 carbon atoms (*n*-amyl) are termed short chain branches (SCB), while *n*-hexyl (6 carbon atoms) and longer branches are termed long chain branches (LCB). Because of poor resolution in ¹³C NMR, branches longer than amyl branches cannot be differentiated and quantified as LCBs of different lengths. Hence, for a detailed LCB analysis NMR must be incorporated into a complex analytical protocol including triple detector SEC (RI-LS-VIS) and other analyses. It is the aim of the present study to combine a number of different analytical techniques and to provide a unique tool for the comprehensive microstructural characterization of these novel grafted polymers.

Experimental

Materials

The novel grafted polymers, gc115 and gc100, of the form HDPE-*g*-LDPE and the reference linear (HDPE) and branched (LDPE) homopolymers used in this report were laboratory products, and were produced in a combination of a continuously stirred tank reactor (CSTR) inline with a tube reactor under high-pressure conditions.^{23,24} 1-Decanol and 1,2,4-trichlorobenzene (TCB) (Sigma-Aldrich, South Africa) used in all the analyses were used as received.

Physical properties of the samples are summarized in Table 1. For a better comparison, the experimental conditions for the preparation of gc115 and gc100 were the same. However, the LDPE polymerizations (2nd step) were conducted at tube reactor temperatures of 115 (gc115) and 100 °C (gc100), respectively. The reference materials HDPE and LDPE were produced under similar experimental conditions. The experimental conditions for the polymerizations are given in Table 2.

High-temperature size exclusion chromatography (HT-SEC). The samples were analysed using a PL 220 high-temperature chromatograph (Polymer Laboratories, Church Stretton, UK) equipped with a differential refractive index (RI) detector, three PLgel Olexis columns (300 mm \times 7.5 mm i.d.) and a PLgel Olexis guard column (50 \times 7.5 mm i.d.) (Polymer Laboratories now Agilent, Church Stretton, UK) operating at 150 °C. The eluent 1,2,4-trichlorobenzene (TCB) stabilized with 2,6-di-*tert*-butyl-4-methylphenol (BHT, 0.0125%) was used at a flow rate of 1 mL min^{−1}. All samples (~2 mg) were dissolved in TCB (2 mL)

Table 1 Summary of the physical properties of the grafted polymers and the reference materials

Sample name	M_w^a (kg mol ^{−1})	D^a	M_w^b (kg mol ^{−1})	D^b	T_c (°C)	T_m (°C)	X_c^c (%)
gc115	145.7	8.2	119.7	14.5	117.9	129.6	63.1
gc100	314.8	9.8	488.8	19.9	112.3	125.5	60.9
LDPE	792.5	17.0	2573.9	18.1	106.3	117.1	51.7
HDPE	209.1	17.7	—	—	119.0	133.1	75.5

^a Determined by HT-SEC-RI, polystyrene equivalents. ^b Determined by HT-SEC-LS. ^c $X_c = (\Delta H_m / \Delta H_m^{PE} \times 100)$, $\Delta H_m^{PE} = 294 \text{ J g}^{-1}$.

CHAPTER 6

View Article Online

Polymer Chemistry

Paper

Table 2 Summary of the experimental parameters for homopolymerization (LDPE and HDPE) and polymer grafting (gc100 and gc115)

Sample	Catalyst ($\times 10^{-2}$ mol ppm)	MMAO (mol ppm)	Initiator ^a	Initiator (mol ppm)	T_{CSTR} (°C)	T_{TUBE} (°C)	Conversion (%)	Polymerization in
LDPE	—	—	DEDPH	1.67	201	185	1.82	Tube
gc100	1.88	40	TBPA	1.25	170	100	1.49	CSTR and tube
gc115	1.88	40	TBPA	1.25	170	115	1.07	CSTR and tube
HDPE	1.88	40	—	—	169	118	0.82	CSTR

^a Diethyl-diphenyl-hexane (DEDPH), *tert*-butylperoxyacetate (TBPA), co-catalyst (MMAO), catalyst (DOC).

for 1–2 hours and 200 μL of the solutions were injected. Linear polystyrene standards (Polymer Laboratories now Agilent, Church Stretton, UK) with narrow MMD were used for calibration. The molar mass values reported for LDPE and the linear PE (HDPE) in Table 1 are polystyrene equivalents. All measurements were performed in triplicate.

GPC-triple detector system (GPC-IR-MALLS-vis). Long chain branching analyses were obtained using a high-temperature Polymer Char GPC-IR system (Polymer Char, Valencia, Spain) equipped with an IR5 detector in hyphenation with a Wyatt Dawn Heleos II LS detector and an online Visco H502 viscometer detector, three Shodex UT 806 M columns, one Shodex UT 807 column and a Shodex UT-G guard column. The average particle sizes of all columns were 30 μm . The experimental conditions were the same as stated for HT-SEC. The MALLS data were processed with the Astra software version 6.1.6.5 (Wyatt Technology, Santa Barbara, USA) and a dn/dc value of $-0.1040 \text{ mL g}^{-1}$ was used for all the samples. The MALLS data were analysed using a first order Zimm plot assuming monodisperse polymer fractions after SEC. The molar mass dependent SCB frequencies were determined by the IR5 detector calibrated with ethylene-1-octene-copolymers of varying comonomer contents.

Crystallization analysis fractionation (CRYSTAF). Crystallization from solution was monitored using a 200 Polymer Char (Valencia, Spain) CRYSTAF instrument. Each analyte ($\sim 20 \text{ mg}$) was simultaneously dissolved in TCB (35 mL) in five stainless steel reactors with stirring at 160 °C. After the samples were completely dissolved ($\sim 150 \text{ min}$), the temperature of the reactor was reduced to 100 °C and stabilized for 60 min. The crystallization step was conducted by slowly reducing the solution temperature to 30 °C at a linear cooling rate of $0.1 \text{ }^\circ\text{C min}^{-1}$ to minimize the effect of co-crystallization. During the cooling stage, the solution concentration was measured as a function of temperature using an infrared detector and the results were recorded.

Differential scanning calorimetry (DSC). The thermal properties of the samples were determined using a TA Instruments Q100 DSC system (TA Instruments, New Castle, USA), calibrated with indium metal standard. Calibration was done according to standard procedures and the melting and crystallization temperatures were measured under the same experimental conditions of heating and cooling at a scanning rate of $10 \text{ }^\circ\text{C min}^{-1}$ at a temperature ranging between 10–200 °C. The samples were subjected to three temperature cycles, with the first cycle (first heating) being used to erase

the sample thermal history. The crystallization and melting temperatures reported in Table 1 were recorded during the first cooling and second heating cycles.

After each cycle, the temperature was kept isothermal for 2 min. The measurements were conducted in a nitrogen atmosphere at a purge gas flow rate of 50 mL min^{-1} . All measurements were conducted in triplicate.

Carbon-13 nuclear magnetic resonance spectroscopy (^{13}C NMR). The ^{13}C NMR analyses of the samples and fractions were carried out using a 600 MHz Varian Unity Inova NMR spectrometer at a resonance frequency of 150 MHz. All samples ($\sim 60 \text{ mg}$) were dissolved in deuterated 1,1,2,2-tetrachloroethane- d_2 (TCE- d_2) ($95.5 \pm \text{atom\% D}$, Sigma-Aldrich, South Africa). TCE- d_2 was also used as an internal reference (74.3 ppm), and the analyses were performed at 120 °C.

High-temperature high-performance liquid chromatography (HT-HPLC). HT-HPLC chromatograms were obtained using a solvent gradient interactive chromatographic system (SGIC) constructed by Polymer Char (Valencia, Spain). The instrument is composed of an autosampler (which is a separate unit connected to the injector with a heated transfer line), two separate ovens, switching valves and two pumps which are equipped with vacuum degassers (Agilent, Waldbronn, Germany). For solvent gradient elution in HPLC, a high-pressure binary gradient pump was used. An evaporative light scattering detector (ELSD, model PL-ELS 1000, Polymer Laboratories, Church Stretton, England) was used with the following parameters: a gas flow rate of 1.5 SLM, 160 °C nebulizer temperature and an evaporation temperature of 270 °C. All samples were fractionated using a $100 \times 4.6 \text{ mm i.d.}$ Hypercarb column (Thermo Scientific, Dreieich, Germany) packed with porous graphite particles (particle diameter: 5 μm ; pore size: 250 Å and surface area: $120 \text{ m}^2 \text{ g}^{-1}$). The column temperature was maintained at 160 °C in the column oven. The mobile phase flow rate during analysis was 0.5 mL min^{-1} . To achieve separation, a linear gradient was applied from 100% 1-decanol to 100% TCB within 10 min after sample injection. The conditions were held for 20 min before re-establishing 1-decanol to 100 vol%. Samples were injected at a concentration of $1\text{--}1.2 \text{ mg mL}^{-1}$, using 20 μL of each sample solution during analysis.

Preparative temperature rising elution fractionation (pTREF). Preparative TREF was carried out using an instrument build in-house. A dilute solution ($\sim 1 \text{ wt\%}$) was made by dissolving the sample (3.0 g) in xylene (300 mL) in a glass reactor at 130 °C.

CHAPTER 6

View Article Online

Paper

Polymer Chemistry

Irganox 1010 (2% w/w) (Ciba Speciality Chemicals, Switzerland) was added as a stabilizer to prevent thermo-oxidative degradation of the sample during the fractionation. The reactor was quickly immersed into a temperature-controlled oil bath and filled with a crystallization support (sea sand). The oil bath, the support, and the reactor were preheated and maintained at 130 °C to prevent the uncontrolled recrystallization of the sample. To ensure a controlled crystallization under the TREF conditions, the oil bath was cooled to ambient temperature (~25 °C) at a rate of 1 °C per hour. The polymer-coated sand was transferred into a stainless steel column which was placed in a modified GC oven for elution. A continuous flow of preheated xylene was used to elute the polymer fractions as the oven temperature was raised at predetermined intervals. The eluted solutions (~500 mL) were dried by evaporating the eluent using a rotary evaporator at a vacuum pressure of 30–40 mbar and the fractions were precipitated with acetone. The fractions were then completely dried under vacuum to a constant weight. The fractionation process was conducted in triplicate.

Ethylene polymerization and polymer grafting. The ethylene polymerizations were carried out in a high-pressure polymerization set-up, consisting of a 100 mL continuous stirred tank autoclave (CSTR) in series with a 3 m long tubular reactor (high-pressure capillary in heat exchanger). While the HDPE is produced catalytically in the CSTR, the LDPE is produced by free radical polymerization in the tubular reactor. The samples were produced within as part of a joined project of The Dow Chemical Company and the Technical University of Darmstadt.^{6,23–27}

The concept of the metallocene catalysed polymerizations is described in literature and the grafting process was presented previously.^{6,25–27}

A detailed description of the experimental procedure can be found in the studies by Becker²³ and Bauer.²⁴

In a first step, the HDPE was produced using a metallocene catalyst in the CSTR. Then, the mixture was directly transferred into the tubular reactor and peroxide was added inline. The peroxide quenches the catalyst and initiates the polymerization of ethylene to LDPE. The free radical polymerization producing the LDPE leads to transfer reactions of the radical functionality. If the radical functionality is transferred to an HDPE molecule, grafted HDPE-g-LDPE is produced. However, the mixture is also assumed to contain non-grafted LDPE and pure HDPE.

While the grafted samples were produced in the dual reactor system using both initiator systems, the LDPE and the HDPE reference were synthesised using only the corresponding initiator system within the dual reactor set-up. The polymerization parameters are summarized in Table 2.

Results and discussion

Bulk sample analysis

Typically, knowledge regarding polyolefin microstructure is difficult to obtain and can be unravelled only through the com-

bination of different analytical techniques.¹⁵ Molecular size and topology (chemical composition or branching) are the two main parameters that govern the properties of the present samples. In polyolefin characterization, molecular size distribution information is achieved *via* coupling SEC to either RI or IR detectors.^{28,29} For detailed LCB characterization as a function of molecular size, advanced detectors like MALLS or online viscometers are deployed.^{30,31} On the other hand, branching analysis of polyolefins can be achieved by observing changes in the polymer crystallizability as a function of temperature. In this report, SEC-RI will be used to determine molar mass distributions, while CRYSTAF and DSC will be used to investigate crystallizability and branching.^{32,33} Information regarding the branching types as well as the branching content of the polymers will be achieved by ¹³C NMR spectroscopy.³⁴

The microstructural characterization of the two novel grafted polymers gc115 and gc100 and their linear (HDPE) and branched (LDPE) references listed in Table 1 is achieved firstly by studying the molecular size (molar mass) using the SEC-RI system. As can be seen in Fig. 2a, all samples exhibit bimodal distributions with molar mass peak maxima at 8.4 and 272.1 kg mol⁻¹ (HDPE), 9.3 and 107.1 kg mol⁻¹ (gc115), 32.7 and 1162.6 kg mol⁻¹ (gc100) and 31.7 and 1487.7 kg mol⁻¹ (LDPE). As clearly seen in Table 2, all the samples exhibit broad molar mass distributions (MMD) as indicated by their high molar mass dispersities (*D*). Thus, the molar mass peak maxima of the grafted polymers are at similar or smaller masses than those of the respective homopolymers. Although, this seems contradicting at first sight, the reason for that can presumably be found in the free radical kinetics of the ethylene polymerization. The transfer of a radical from a growing LDPE chain to an HDPE macromolecule performs the grafting of LDPE on an HDPE backbone. If the formed secondary radical propagates, a grafted polymer chain is formed. However, the secondary radical can also undergo a β -scission reaction and thus segment the HDPE macromolecule. Thus,

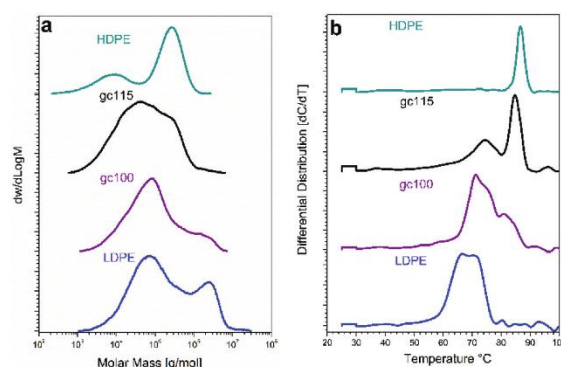


Fig. 2 Plots showing the compositional differences of the grafted samples and the reference materials. (a) Molar mass distribution plots as determined by SEC-RI, (b) CRYSTAF crystallization curves.

CHAPTER 6

View Article Online

Polymer Chemistry

Paper

these two competing reactions might lead to a grafted polymer exhibiting an intermediate molar mass.

Considering that crystallinity is determined by the polymer microstructure, CRYSTAF experiments were conducted on all the samples. CRYSTAF fractionates polymer molecules from dilute solutions according to crystallizability at temperatures ranging from 100 to 30 °C. As stated in previous works and the references therein^{16,17,22,35} polyethylene molecules that crystallize between 90 and 80 °C are highly linear (highly crystalline), while the crystallization temperature of the branched polymer varies between 80 and 30 °C depending on the degree of branching or comonomer content. Highly branched fractions with non-crystallizable backbones stay in solution and are observed as a rectangular peak below 30 °C (soluble fraction).

The CRYSTAF results for the individual samples are shown in Fig. 2b. As expected, the HDPE exhibits unimodal and narrow crystallization profile around 86 °C, indicating high crystallinity. In contrast, the crystallization profiles of the grafted polymers as well as of the LDPE reference are complex and differ in shape. The three samples exhibit characteristic bimodalities, indicating molecular species having distinctively different architectures. In gc115 the grafted polymer and/or some ungrafted LDPE were observed at 74.5 °C. The peak at 84.5 °C constitutes mainly the non-grafted HDPE. In a similar way, sample gc100 constitutes mainly the grafted HDPE and/or ungrafted LDPE as indicated by the main peak at 71.3 °C.

A small amount of non-grafted or slightly grafted HDPE backbone is observed around 80.9 °C. LDPE, on the other hand, exhibits two crystallization peaks at 66.7 and 70.3 °C that is ascribed to branched species with different degrees of branching. The absence of crystallization above 80 °C clearly indicates the absence of HDPE.

Another powerful technique used to characterize polymer branching and crystallinity is DSC. Different from CRYSTAF, DSC measures polymer melting and crystallization behavior in their solid state. In Fig. 3a, the DSC curves of the four samples

were recorded from the second heating cycle at temperatures ranging from 10–200 °C, at a heating rate of 10 °C min⁻¹ is reported. All samples exhibit melting endotherms between 90 and 140 °C. As clearly seen, the HDPE exhibits a narrow melting endotherm at 133 °C, indicating a linear structure. LDPE displays a unimodal melting profile at 117 °C, which clearly indicates a branched structure. Different from the reference materials, the grafted polymers exhibit distinct bimodal melting profiles, indicating molecular species that differ in composition.

As compared to CRYSTAF and DSC, solvent gradient HPLC fractionates polyethylenes according to their linear ethylene sequence lengths. As has been highlighted by several authors,^{15,16,35,36} branched PE is separated from the linear counterparts *via* the adsorption/desorption mechanism using a mixture of poor (adsorption promoting) solvent (1-decanol) and good (desorption promoting) solvent (TCB) in a gradient mode. In this type of separation, linear polyethylenes are strongly retained on the Hypercarb stationary phase and are eluted at 100% TCB. Branched PEs are retained to a lesser extent, and elute at variable 1-decanol-to-TCB ratios depending on the degree of branching. For a typical branched polymer, the elution volume is directly related to the branching content. In Fig. 3b, the typical elution profile of an 1-octene/ethylene copolymer (13.8 mol% 1-octene, LLDPE) is shown with elugram with peak elution volume around 4.7 mL indicating a higher degree of branching. As is seen, the HDPE, LDPE and gc100 display unimodal and narrow elugrams. The late elution volume of 5.66 mL for HDPE indicates a linear backbone. This observation corresponds well with the CRYSTAF and DSC results shown in Fig. 2b and 3a, respectively. LDPE and gc100 elute earlier at elution volumes of 5.48 and 5.53 mL, respectively, indicating different degrees of branching. In comparison, gc115 exhibits a characteristic bimodality expressing distinct elution peaks at 5.58 and 5.71 mL. The first peak is assigned to the grafted HDPE and/or the ungrafted LDPE backbone, while the second peak is assigned to non-grafted HDPE backbone. Although clear bimodality was observed with the CRYSTAF and DSC results of gc100, it was clearly absent in the HPLC elugram. This might be an indication that this sample contains rather low amounts of non-grafted HDPE and the bimodality seen in DSC is due to different branched components. Branched polyethylene may exhibit a trifunctional or tetrafunctional branching architecture, *i.e.* may constitute different types of branching. For a detailed branching analysis, the samples were analyzed by ¹³C NMR spectroscopy. The individual ¹³C NMR spectra of the grafted polymers and the reference PEs are given in Fig. 4. The peaks were assigned according to previous reports and literature therein.^{16,37} The branching contents (branch per 1000 carbons) of the different branch types were calculated as previously reported^{16,37–39} and the results are reported in Table 3.

The reference HDPE exhibits small amounts of methyl (0.11 per 1000 C) butyl (0.22 per 1000 C) branches, respectively. The predominant type of SCB for all samples was the *n*-butyl branch, which was reported as 3.23, 2.87, 0.66 and 0.22 per

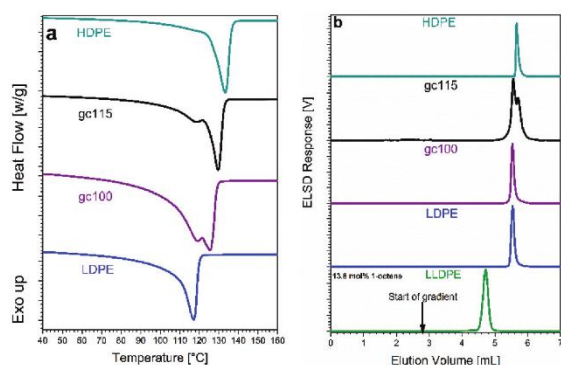


Fig. 3 DSC melting endotherms and HPLC elugrams of the grafted polymers and the reference materials. (a) DSC plots were recorded at a temperature ranging from 10–200 °C at a heating rate of 10 °C min⁻¹. (b) HPLC elugrams were recorded using solvent gradient elution from 100% decanol to 100% TCB at 160 °C.

CHAPTER 6

Paper

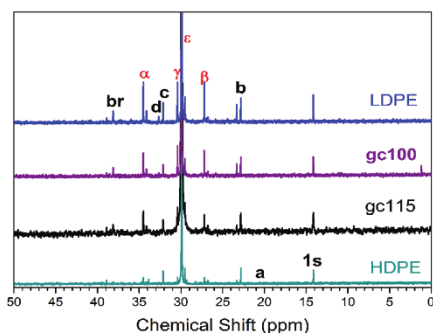
View Article Online
Polymer Chemistry

Fig. 4 ^{13}C NMR spectra for the grafted polymers and reference branched and linear PE recorded in TCE- d_2 at 120 °C. The chemical shift was corrected using the TCE- d_2 peak as the internal standard.

1000 C for LDPE, gc100, gc115, and HDPE, respectively. When comparing the total branching contents, as expected LDPE scored the highest (7.67 per 1000 C) degree of branching, while the lowest score (1.64 per 1000 C) was recorded for gc115. Branching in HDPE is very low and is mainly due to a small amount of SCB.

Currently, SEC coupled to either an online viscometer (VIS) or a light scattering (LS) detector is widely used to measure the molecules' intrinsic viscosity ($[\eta]$) and radius of gyration (R_g) in solution, respectively.

By comparing $[\eta]$ or R_g of a branched molecule to that of a linear reference of the same molar mass, LCB information is obtained.^{11,16,30,40,41} In triple detector SEC, the intrinsic viscosities of the eluting SEC fractions are measured as a function of molar mass (obtained by the MALLS detector). Molar mass and $[\eta]$ are correlated through the Mark-Houwink (M-H) relationship shown in eqn (1).⁴¹ For an ideal linear reference material, a M-H exponent (α) and M-H coefficient (K) of 0.703 and 5.3×10^{-2} were used, respectively.

$$[\eta] = 5.3 \times 10^{-2} M^{0.703} \quad (1)$$

$$g' = \left[\frac{\langle R_g^2 \rangle_{\text{Br}}}{\langle R_g^2 \rangle_{\text{Li}}} \right]_M \quad (2)$$

Table 3 Detailed branching information of the grafted and reference PEs as recorded by ^{13}C NMR spectroscopy

Branch type	Chemical shift (δ) (ppm) ^{16,17}		Branching content (per 1000 C)			
	δ_{ex}	δ_{Li}	LDPE	gc100	gc115	HDPE
Methyl (a)	21.03	21.03	—	—	—	0.11
Butyl (b)	23.32	23.32	3.23	2.87	0.66	0.22
Amyl (c)	32.65	23.64	0.21	0	0	0
LCB (d)	32.14	32.16	4.22	2.63	0.99	0.07
SCB	—	—	3.44	2.86	0.66	0.33
Total	—	—	7.67	5.50	1.64	0.40

Polym. Chem.

This journal is © The Royal Society of Chemistry 2018

$$g' = \left[\frac{[\eta]_{\text{Br}}}{[\eta]_{\text{Li}}} \right]_M \quad (3)$$

$$g' = g^\epsilon \quad (\text{where } 0.5 \leq \epsilon \leq 1.5) \quad (4)$$

According to the Zimm-Stockmayer relationship, the branching index, g , expressed in eqn (2) determines the impact of LCB on the size of molecules in solution. $\langle R_g \rangle$ represents the radius of gyration for the branched (Br) and linear (Li) molecules of the same molar mass. According to Flory's solution theory,^{42,43} $\langle R_g \rangle$ of molecules in solution is directly proportional to the cube root of the molecule's $[\eta]$. Therefore, the $[\eta]$ ratio of branched and linear molecules of the same molar mass may equally be used to measure the branching factor, g' , in accordance to eqn (3). Theoretically,¹⁰ g can be estimated from g' by deploying eqn (4). The structure factor, ϵ is related to the number of LCB units in the branched polymer. However, this conversion is often challenging since ϵ is assumed to depend on the molecular structure and varies between 0.5 and 1.5. Macromolecules with LCB are more compact in solution compared to their linear counterparts of the same molar mass due to enhanced entanglement. This effect results in the contraction of the branched molecule, thereby reducing the $[\eta]$. LCB is identified by the deviation of the M-H plot of a branched sample from a linear reference material of the same molar mass. The greater the deviation, the smaller the exponent, α , and therefore, the greater the degree of LCB.

According to the M-H plot in Fig. 5a, a direct linear relationship exist between $[\eta]$ and molar mass for an ideal linear reference material. The experimental plot for HDPE superimposes the ideal linear plot indicating a linear structure. However, a small amount of slightly branched material is observed at the low molar mass region, which is in agreement with the ^{13}C NMR results.

Upon comparing the behavior of LDPE to that of HDPE (linear plot), a clear deviation towards lower $[\eta]$ values is observed, indicating branching. Branching increases with increasing molar mass as would be expected for a randomly branched PE. A complex behavior is seen for the data of gc100 and gc115 (grafted PEs), indicating branching heterogeneity. Interesting, both gc110 and gc115 lie between LDPE and HDPE, indicating a sparsely branched structure.

In the case of gc100 all data points are below the linear/HDPE plots, indicating a more branched structure. A low amount of molecules with low degree of branching is observed at molar mass around 10^5 g mol^{-1} . This observation is in perfect agreement with the CRYSTAF, DSC and HPLC results. In comparison, gc115 shows molecules with varying architecture at different molar mass regions. At molar mass ranging between 10^4 and 10^5 g mol^{-1} linear macromolecules are present as indicated by the 'linear' behavior of the M-H plot. At molar mass around $2 \times 10^4 \text{ g mol}^{-1}$ and below, branched molecules seem to be present which might be due to non-grafted LDPE. An increasing degree of grafting (approaching the behavior of gc100) is seen at higher molar masses starting

CHAPTER 6

View Article Online

Polymer Chemistry

Paper

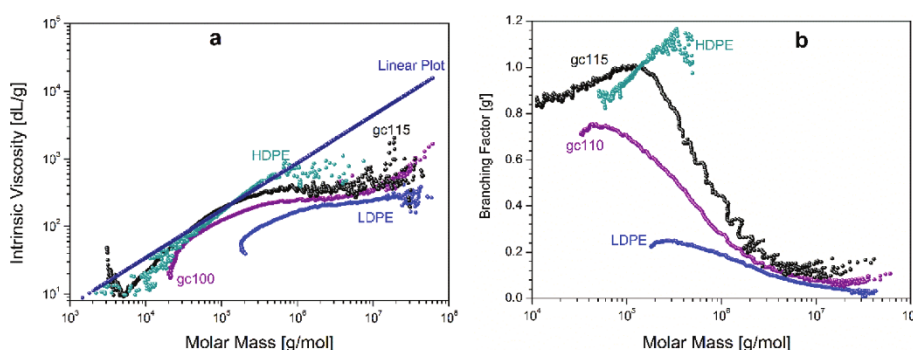


Fig. 5 SEC-viscometer measurements illustrating branching in the grafted polyethylenes while comparing them to the HDPE and LDPE reference materials. (a) Mark-Houwink plots presenting intrinsic viscosity as a function of molar mass. (b) Variation in the branching ratio as a function of molar mass.

at about $2 \times 10^5 \text{ g mol}^{-1}$. These components are tentatively assigned to the grafted PE.

The M-H data in Fig. 5a enabled to calculate the branching factor, g' . Fig. 5b illustrates the variation of g' as a function of molar mass for all the analytes. In this plot, the branching ratio is scaled from 1 to 0. Molecules with a ratio of 1 are considered to be linear. Depending on the degree of LCB, the ratio decreases as branching increases. Similar plots relating the branching index g (measured from $\langle R_g \rangle$) to molar mass are reported in the Fig S1a of the ESI.† Clearly, HDPE exhibits some branching in the lower molar mass region as indicated by a decrease in g' as molar mass decreases. At higher molar masses g' approaches 1.0. As clearly seen, LDPE exhibits high degrees of LCB throughout all molar masses with branching ratios between 0.3 and 0.02.

The branching ratio plot clearly shows the differences between gc115 and gc100. Grafting is much more pronounced for gc100 and linear (non-grafted) molecules are not seen. In contrast, gc115 contains a significant amount of linear species. It is worth mentioning that at very high molar masses the branching structure of the grafted samples seems to be very similar to LDPE, which can be explained by the very high degree of grafting of the corresponding molecules. Plots of branching index (g) versus branching factor (g') is reported in Fig. S1b of the ESI.† This plot highlights the topological differences between the different samples in comparison to the branched PE.

The bulk sample analyses of gc100, gc115 and the reference polymers were performed using a range of analytical techniques. As clearly, observed, only one-dimensional information with regard to molar mass and branching was obtained from the different techniques.

The bulk sample results provided proof for the success of the grafting reaction as non-grafted LDPE, non-grafted HDPE and grafted PE could be detected and tentatively assigned. For a more comprehensive analysis of the molecular complexity of the grafted samples and for being able to correlate branching to molar mass and provide more subtle molecular details, pre-

parative fractionation such as TREF is required. This technique provides fractions that have different crystallizabilities, which are directly related to different degrees of branching. Such TREF fractions are still heterogeneous regarding molar mass and branching and will be analyzed by a number of advanced analytical methods to obtain two-dimensional branching and molar mass information.

Analyses of TREF fractions

Temperature rising elution fractionation (TREF) on a preparative scale is frequently used to fractionate polyolefins into fractions of similar crystallizability (corresponding to similar chemical compositions) in mg to g amounts. These fractions can be analyzed further using offline techniques to obtain chemical composition, branching and molar mass information. All branched samples of the present study were fractionated according to a procedure that was described previously.¹⁶

A total of eight fractions per sample were collected at 30, 60, 70, 80, 90, 100, 110 and 130 °C and the wt% distribution is expressed as a function of TREF elution temperature, see Fig. 6. According to literature,^{15–17,22,44,45} the fractions eluting at 30 °C constitute mainly highly branched components of low molar masses, while fractions obtained at 100 and 130 °C represent highly linear components that have a high degree of crystallinity. In the present case, it is assumed that TREF fractionates in the order of increasing crystallinity (decreasing branching) with increasing elution temperature. Comparing the fractions obtained between 100 and 130 °C for the three samples, an amount of 42.8 wt% is observed for gc115 as compared to 18.2 and 6 wt% for gc100 and LDPE, respectively. In contrast, 48.9 wt% of gc115 was obtained at 80 and 90 °C eluting temperatures, compared to 74.8 and 83.5 wt% for gc100 and LDPE, respectively. When comparing branching in gc100 and gc115, it is very clear that gc100 contains a higher amount of branched components. Sample gc115 contains a higher amount of components eluting at 100 and 110 °C that exhibit a lower branching structure. In this sample, a certain amount

CHAPTER 6

View Article Online

Paper

Polymer Chemistry

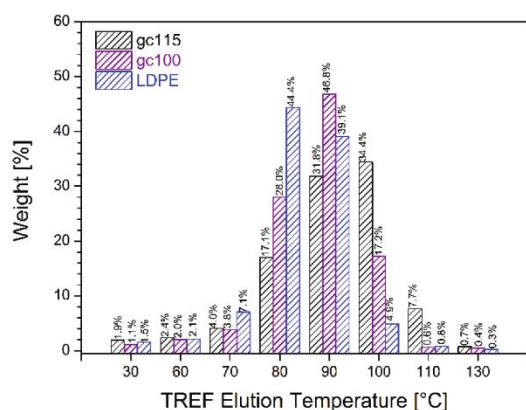


Fig. 6 Preparative TREF fractionation of gc100, gc115 and LDPE. The fractions were obtained by eluting the crystallized samples with xylene at temperatures ranging from 30 to 130 °C.

of material (7.7 wt%) elutes at 110 °C that is likely to be non-grafted HDPE. This finding is in agreement with the analytical results on the bulk samples. In comparison, the amount of non-grafted HDPE in sample gc100 is very low as indicated by the low amount of material eluting at 110 and 130 °C TREF temperatures. For the fractions eluting between 30 and 70 °C, no major difference in the weight amount was observed for all three samples. Due to limited amounts of materials obtained for the 30, 60, 110 and 130 °C fractions, further analyses of these fractions focused on specific methods while a more extended screening was done only for the majority fractions eluting at 80, 90 and 100 °C. In a first step, the TREF fractions were analysed by HT-SEC, see Fig. 7 and Table 4.

Table 4 reports polystyrene equivalent molar masses as determined by standard SEC-RI experiments. Here, one has to keep in mind that these molar masses are only indicative since the different TREF fractions have different degrees of branching. At higher degrees of branching the hydrodynamic

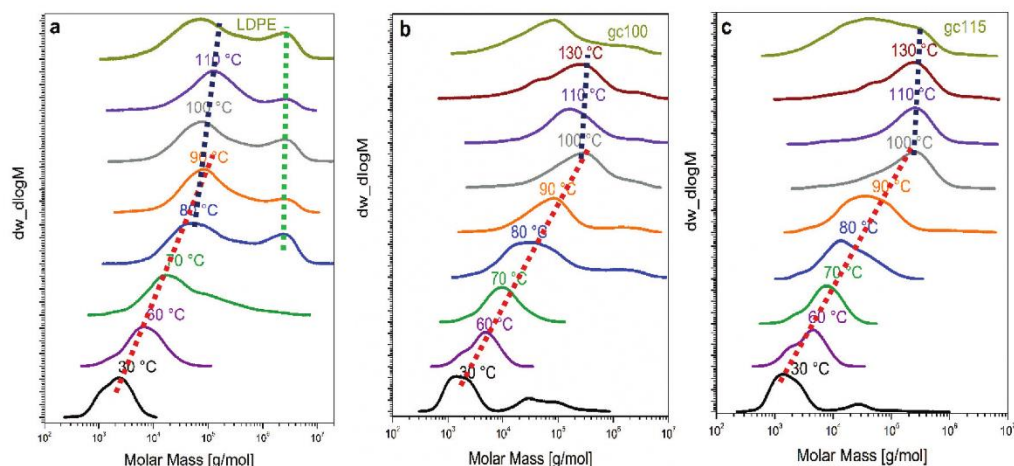


Fig. 7 Molar mass distribution curves comparing the TREF fractions to their respective bulk samples. (a) LDPE, (b) gc100 and (c) gc115.

Table 4 Molar mass parameters and CRYSTAF crystallization temperatures for the bulk materials and TREF fractions. Molar mass information was measured by a SEC-IR system in TCB at 150 °C. Molar masses are polystyrene equivalents

TREF fraction	LDPE				gc100				gc115			
	M_w (kg mol^{-1})	M_n (kg mol^{-1})	\bar{D}	T_c (°C)	M_w (kg mol^{-1})	M_n (kg mol^{-1})	\bar{D}	T_c (°C)	M_w (kg mol^{-1})	M_n (kg mol^{-1})	\bar{D}	T_c (°C)
Bulk	792.5	46.8	17.0	70.8	314.8	32.1	9.8	71.3	145.5	17.7	8.2	84.8
30	2.4	1.7	1.5	—	26.9	2.2	12.5	—	10.7	1.6	6.5	—
60	9.3	5.0	1.9	60.5	5.2	3.5	1.5	52.1	4.6	3.1	1.5	52.7
70	143.1	15.9	9.0	67.8	13.1	7.3	1.8	61.0	8.9	5.6	1.6	60.0
80	780.5	54.7	14.2	72.4	269.9	22.4	12.1	70.7	27.7	11.6	2.4	70.5
90	532.1	60.6	8.8	72.1	284.3	86.9	3.3	74.2	107.9	22.0	4.9	74.6
100	769.0	63.7	12.1	—	479.3	93.9	5.1	85.0	250.4	70.8	3.9	86.2
110	535.4	68.3	1.8	—	453.3	86.1	5.3	—	285.6	2.9	4.0	86.4
130	—	—	—	—	435.3	49.4	8.8	—	315.8	49.0	6.5	—

CHAPTER 6

View Article Online

Polymer Chemistry

Paper

volumes at given molar mass decrease. Fig. 7a reports the individual MMDs of the TREF fractions of LDPE. The 30, 60 and 70 °C fractions exhibit unimodal MMD curves that broaden with an increase in the TREF elution temperature.

Typical bimodal MMD curves similar to the MMD curve of the bulk LDPE sample were observed for the 80 to 130 °C fractions. These results indicate that with a decrease in branching (higher TREF temperature) molar masses increase. Apparently, this is not the case with the fractions between 90–130 °C, which do not show significant increases in molar masses with increasing TREF temperature. These SEC results indicate that the given polymerization process is quite complex and produces components with significant molar mass heterogeneities. With the exception of the 30 °C fractions that exhibit characteristic bimodal MMDs, all the other fractions of gc100 and gc115 exhibit unimodal MMD curves. The curves broaden and molar masses increase for fractions eluting at higher TREF temperatures, see Fig. 7b and c.

The 2D contour plots for the three samples were generated by cross-combining the TREF elution temperatures and the SEC elution data. The plots clearly demonstrate the compositional differences between the samples (see Fig. 8a–c). As can be seen, polymer elution from TREF is influenced by both the degree of branching and the molar mass. This observation is clearly illustrated by the pronounced tailing of the SEC curves

in the low molar mass regions as seen for the lower temperature TREF fractions.

Structurally, gc115 exhibits a pronounced bimodality with the contour plot in Fig. 8c showing two main peaks at 90 and 100 °C TREF temperatures. These peaks also exhibit SEC elution at 20.8 and 18.6 mL, corresponding to the lower and the higher molar mass components that can be assigned to the grafted and non-grafted HDPE, respectively. In comparison to gc115, the contour diagram of gc100 (see Fig. 8b) displays its main peak at 90 °C TREF temperature. The corresponding SEC elution volume of 19.8 mL indicates relatively high molar mass materials and can be attributed predominantly to the grafted polymer. The contour plot for LDPE is given in Fig. 8c. The main peak corresponds to the 80 °C TREF fraction. This fraction exhibits a molar mass bimodality with distinct molar mass species observed at 16.2 and 20.2 mL SEC elution volume.

The CRYSTAF results given in Fig. 9 also highlight the structural differences of the TREF fractions. As seen in Fig. 9a, the individual TREF fractions of LDPE between 70–100 °C exhibit unimodal crystallization profiles with peak crystallization temperatures at 60, 67, 72 and 71 °C, respectively.

As the TREF elution temperatures increase, the crystallization peaks broaden and the higher temperature fractions display shoulders at lower temperatures. This is due to co-

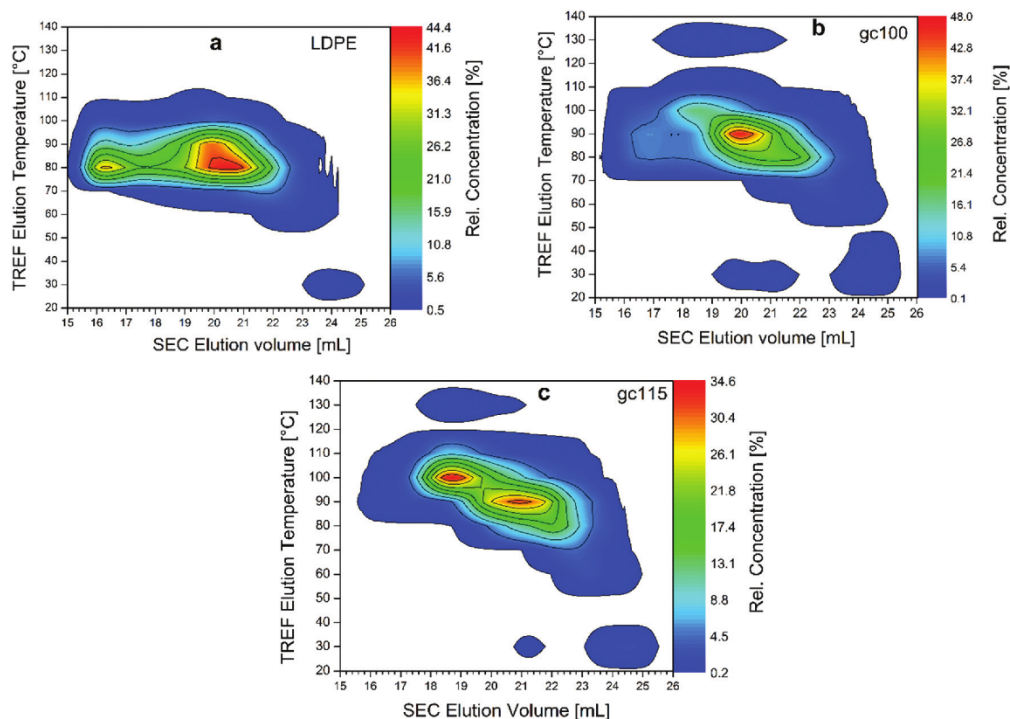


Fig. 8 2D plots illustrating TREF-SEC cross-fractionation of (a) LDPE, (b) gc100 and (c) gc115.

CHAPTER 6

View Article Online

Paper

Polymer Chemistry

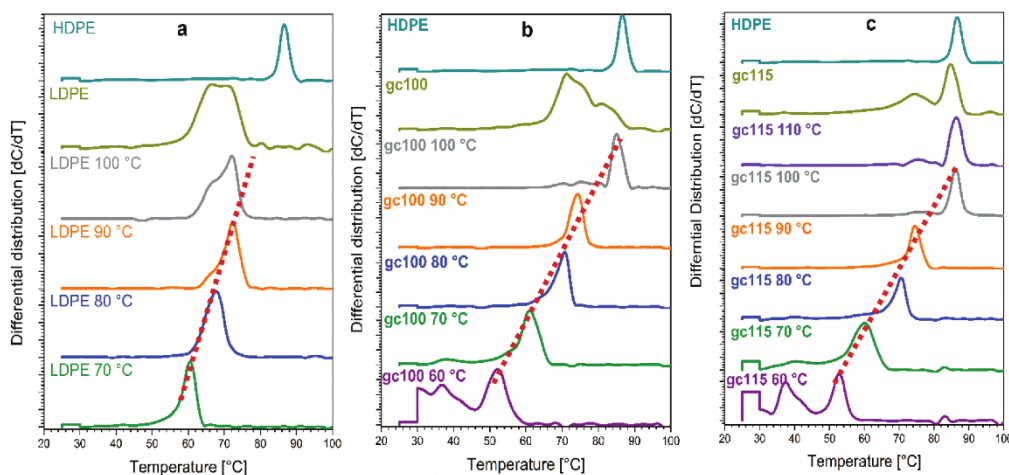


Fig. 9 CRYSTAF curves illustrating the crystallization behaviour observed for the TREF fractions at 30–100 °C temperature range. (a) LDPE, (b) gc110 and (c) gc115.

eluting species of similar crystallizabilities in TREF that are different regarding branching as indicated by CRYSTAF. No material was observed crystallizing above 75 °C, indicating the absence of linear macromolecules (*e.g.* HDPE). The crystallization behaviour for the individual TREF fractions of gc100 and gc115 are displayed in Fig. 9b and c.

The 60 °C fractions of gc100 and gc115 exhibit multimodalities in their crystallization profiles, which indicate that these fractions contain components with significant molar mass and/or branching heterogeneities. As SEC, however, indicates rather low molar mass dispersities, the observed behaviour is more likely due to different branching structures that co-elute in TREF. The fractions that elute at temperatures between 70–90 °C display characteristic unimodal profiles; peak crystallization temperatures increase from 60 to 72 °C. These crystallization curves show that TREF provides fractions with distinctively different degrees of branching that can be analysed further regarding the details of the branch microstructures. The fractions eluting at these TREF temperatures are tentatively assigned to the grafted polymers.

The 100 °C fraction of gc100 exhibits a narrow crystallization peak at 85 °C, while the 100 and 110 °C fractions of gc115 exhibit crystallization at 86 °C. These peaks are due to HDPE and serve as a clear indication of the presence of non-grafted HDPE in these samples.

In Fig. 10, the TREF fractions as analysed by CRYSTAF and the TREF and CRYSTAF data were combined to produce two-dimensional contour plots. These plots express the relationship between TREF elution temperatures and CRYSTAF crystallization temperatures. It is known that fractionation of branched polyolefins in TREF and in CRYSTAF produce different results. This is due to the fact that in TREF the sample is first crystallized and then re-dissolved in the elution process. In CRYSTAF, fractionation is based on only one-step,

which is crystallization from dilute solution (first step in TREF).

A correlation of TREF and CRYSTAF results for different samples can, therefore, provide additional unique information on the composition of the samples. According to Fig. 10a, LDPE exhibits a rather homogeneous contour diagram with some bimodality that indicates that the sample contains fractions with lower and higher degrees of branching corresponding to CRYSTAF temperatures of 60 and 74 °C, respectively. In contrast, the 2D plots for gc100 and gc115 (see Fig. 10b and c) are much more complex presenting a number of components with different crystallization temperatures. At the highest temperature of about 85 °C, non-grafted linear PE is identified.

The concentration of this component is significantly higher in sample gc115, which is in confirmation with previous analytical results. Further, different components are seen at crystallization temperatures of about 50, 60, 70 and 75 °C that are due to non-grafted LDPE and grafted PE. Tentatively, the components at crystallization temperatures of about 50 and 60 °C are assigned to non-grafted LDPE. These components correspond to the 60 and 70 °C TREF fractions which according to Fig. 6 make less than 10 wt% of the total samples. The species that are seen at crystallization temperatures of about 70 and 75 °C are then assigned to grafted PE fractions with different degrees of branching. These correspond to the 80 and 90 °C TREF fractions, which constitute about 49 and 75 wt% in gc115 and gc100, respectively. The average branching frequency (branching per 1000 C) of the 80, 90 and 100 °C TREF fractions of gc100 and gc115 were measured by ¹³C NMR spectroscopy and the results are reported in Table 5.

The branching of the TREF fractions decreases from 7.0 per 1000 C in the 80 °C TREF fraction, to 2.7 and 1.6 in the 90 and 100 °C TREF fractions of gc115, respectively. A similar trend

CHAPTER 6

View Article Online

Polymer Chemistry

Paper

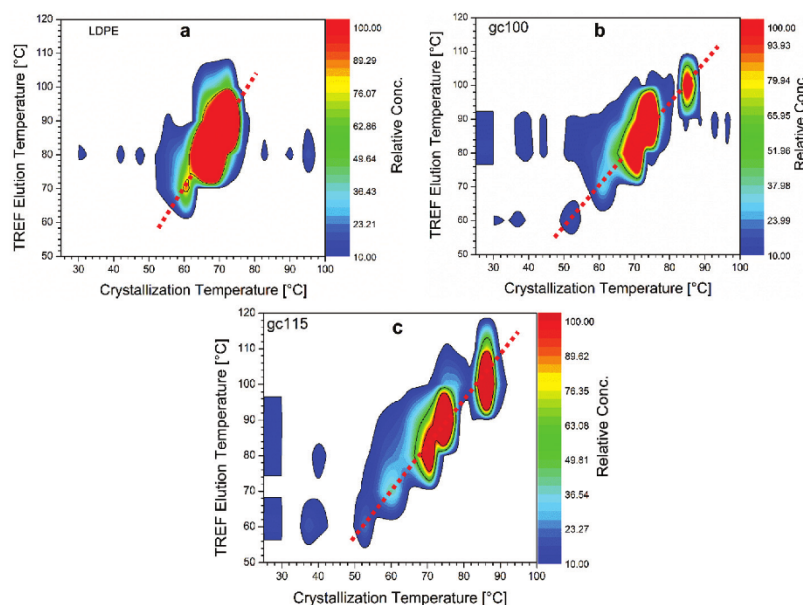


Fig. 10 TREF-CRYSTAF cross-fractionation plots showing the compositional differences between the three samples.

Table 5 Summary of the average number of branches per 1000 C in the TREF fractions of gc100 and gc115

TREF fraction	Sample name	Branching per 1000 C		
		SCB	LCB	Total
80 °C	gc100	3.18	2.62	5.80
	gc115	3.25	3.78	7.03
90 °C	gc100	3.10	1.45	4.55
	gc115	1.31	1.35	2.65
100 °C	gc100	1.10	0.62	1.72
	gc115	1.32	0.25	1.57
Bulk	gc100	2.87	2.63	5.50
	gc115	0.66	0.99	1.64

was observed for gc100, which reported 5.8, 4.6 and 1.7 per 1000 C for the 80, 90 and 100 °C TREF fractions, respectively. It is obvious from these results that the differences in the fractions' crystallizability is due to differences in the degree of branching.

When accounting for the contribution of the different branch types (SCB and LCB), it was observed that SCB constitutes a greater number of branch points in each fraction, when compared to the LCB. These results are in agreement with previous studies.^{30,34} Looking at the individual TREF fractions of the two grafted samples, it was observed that the 80 °C fraction of gc115 exhibits a higher degree of SCB (3.3 per 1000 C) and LCB (3.8 per 1000 C) compared to the 3.2 and 2.6 per 1000 C, SCB and LCB for gc100, respectively. On the other hand, a higher SCB and LCB frequency was reported for the 90 °C TREF fraction of gc100, when compared to gc115 (see Table 5).

Considering the fact that the relative amount of this fraction in gc100 compared to gc115 is significantly higher, it can be concluded that gc100 contains a significantly higher percentage of grafted PE.

Different from crystallization-based fractionation as in TREF and CRYSTAF, high-temperature solvent gradient HPLC fractionates polyolefins according to their linear ethylene sequence lengths. This technique was used to analyze the TREF fractions in addition to the crystallization-based methods. The individual chromatograms of the fractions are given in Fig. 11. In general, the peak elution volume in the elugrams increases with an increase in the TREF elution temperature, which can be attributed to an increase in longer linear ethylene sequences in the fractions (decrease in branching). As can be seen, the elugrams become narrower with increasing TREF elution temperature, indicating an increased structural homogeneity in the higher temperature fractions.

As seen in Fig. 11a for LDPE, the elugrams of all the fractions exhibit typical monomodal distributions except for the 30 °C fraction that exhibits two species eluting at 3.9 and 4.2 mL. All the TREF fractions of LDPE can be assigned to branched species since their elution volumes are lower than that of HDPE. The elution volumes decrease with decreasing TREF elution temperature indicating an increase in branching in the same order. For samples gc100 and gc115 a similar assignment can be obtained. The 100 °C TREF fractions in both cases can be assigned to non-grafted HDPE. The difference between the samples being that this TREF fraction makes 34 wt% of the total sample in gc115 and only 17 wt% in gc100.

For the 90 °C TREF fraction of gc100 a clear deviation from the behavior of HDPE is seen and, therefore, this fraction is

CHAPTER 6

Paper

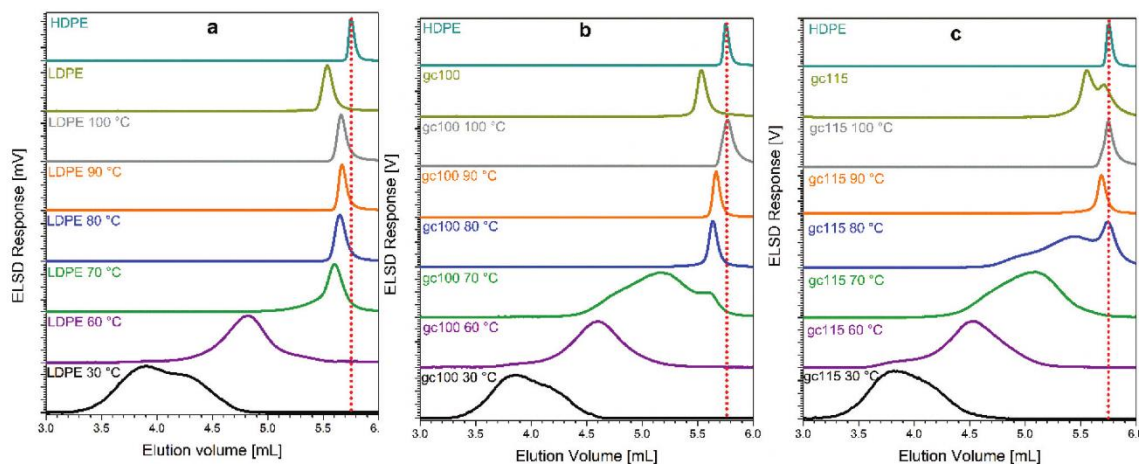
View Article Online
Polymer Chemistry

Fig. 11 HPLC elugrams of the individual TREF fractions of (a) LDPE, (b) gc100 and (c) gc115, obtained using 1-decanol/TCB as eluent at 160 °C.

assigned to grafted PE making 47 wt% of the total sample. The 80 °C TREF fraction of gc100 is further shifted to lower elution volumes indicating a grafted PE with a higher degree of branching.

This fraction makes 28 wt% of the total sample. Thus, it can be assumed that sample gc100 contains roughly 75 wt% of grafted PE. In contrast, the 90 °C TREF fraction of gc115 is only slightly shifted to lower elution volumes indicating a very low degree of branching. In the 80 °C TREF fraction of this sample a peak at higher elution volume is detected (see also total sample) that might be assigned tentatively to lower molar mass non-grafted HDPE. The total amount of the 80 and 90 °C TREF fractions of gc115 corresponding mainly to grafted PE is 49 wt%. Thus, the HPLC results confirm the previous finding that sample gc115 has a significantly lower amount of grafted components compared to gc100.

For a comprehensive microstructural analysis of gc100 and gc115, 2D chromatography separations were performed. In this technique, HPLC is coupled to SEC online, see Fig. 12. The HPLC fractions from the first dimension are subsequently analyzed by SEC in the second dimension to obtain molar mass information as a function of branching as illustrated in the 2D contour plots of the gc100 and gc115. Each point in the plots is directly related to the amount of material of a given molar mass and degree of branching.

To logically interpret these results, it is important to note that the least retained HPLC fractions eluting at a HPLC elution volume of around 4.5 mL exhibit shorter linear ethylene sequences due to a higher degree of branching, while the highly retained fractions eluting at around 5.5 mL contain macromolecules with longer linear ethylene sequences and lower branching. Similarly, the fractions eluting at around 3.0 mL on

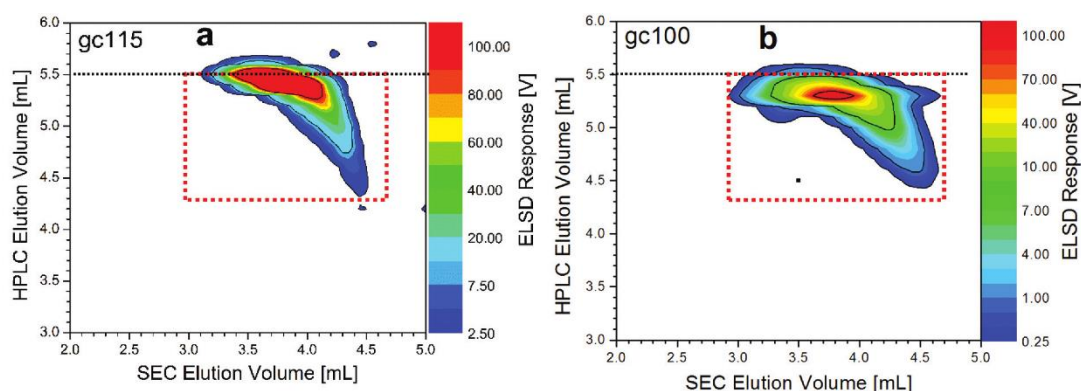


Fig. 12 2D-LC plots of samples gc115 (a) and gc100 (b). HPLC fractionation was conducted in solvent gradient conditions. 1st dimension HPLC, 2nd dimension SEC, detector ELSD.

CHAPTER 6

[View Article Online](#)

Polymer Chemistry

Paper

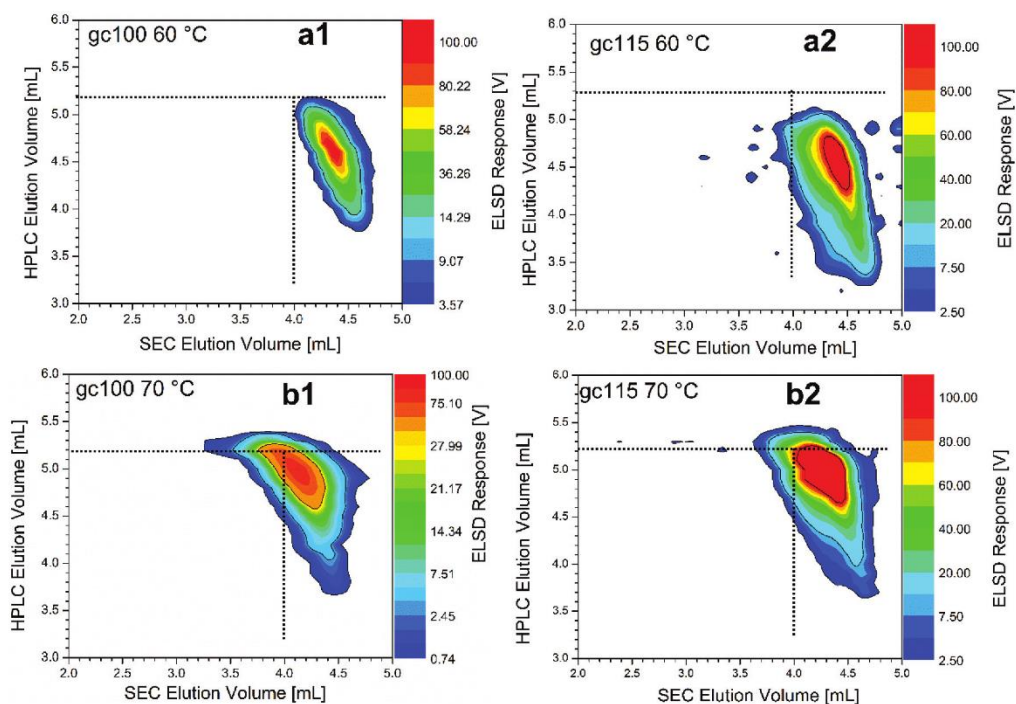


Fig. 13 Two-dimensional contour plots of the TREF fractions of gc115 and gc100. The plots labelled a1 and b1 and the plots labelled a2 and b2 correspond to TREF fractions at 60 and 70 °C of gc100 and gc115, respectively.

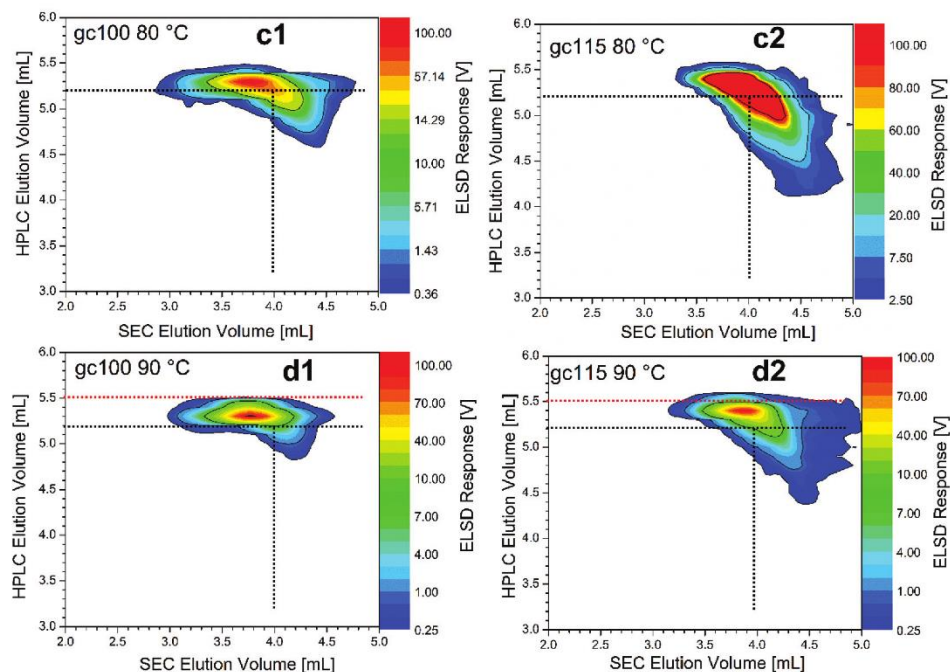


Fig. 14 Two-dimensional contour plots of the TREF fractions of gc115 and gc100. The plots labelled c1 and d1 and the plots labelled c2 and d2 correspond to TREF fractions at 80 and 90 °C of gc100 and gc115, respectively. Dotted red line indicates start of elution of HDPE.

CHAPTER 6

[View Article Online](#)

Paper

Polymer Chemistry

the SEC scale correspond to high molar masses while those eluting at around 4.5 mL have lower molar masses.

In Fig. 12 the dotted line at a HPLC elution volume of 5.5 mL indicates the start of the elution of non-grafted HDPE. Although separation in the 1st dimension is not perfect, it can be clearly seen that a significantly higher percentage of sample gc115 elutes beyond this line. Accordingly, a smaller percentage of this sample is branched material. Another interesting observation is that all branched material (see red box) elutes at higher SEC elution volume as compared to the non-grafted HDPE. This is in agreement with the assumption that the hydrodynamic volume of a branched molecule is smaller than that of a linear molecule having the same molar mass.

The 2D-LC separations of the TREF fractions eluting at 60 °C are presented in Fig. 13(a1) and (a2). These fractions have been tentatively assigned to non-grafted LDPE. Their elution ranges in the 1st and 2nd dimensions are indicated by dotted lines. As can be seen, these fractions elute at low HPLC elution volumes indicating highly branched structures and at high SEC elution volumes indicating small hydrodynamic volumes. In comparison to these fractions, the 70 °C TREF fractions elute at higher HPLC elution volumes and lower SEC elution volumes indicating lower degrees of branching and larger hydrodynamic volumes, respectively. Here it can be assumed that a transition from non-grafted LDPE to the grafted polymers HDPE-g-LDPE can be observed. Qualitatively, similar behavior is observed for sample gc115. Following this logic, the behavior of the TREF fractions eluting at 80 and 90 °C can be understood as well. As for gc100, the 2D-LC elution pattern is characteristic for the grafted polymer HDPE-g-LDPE with a higher molar mass compared to the 70 °C TREF fraction. The species eluting at lower HPLC elution volume and higher SEC elution volume might be due to some residual non-grafted LDPE, see Fig. 14(c1). These species are not seen in the 90 °C TREF fraction of gc100. Instead, the majority of the material elutes at low SEC, high HPLC elution volumes see Fig. 14(d1), and it is assumed that this material is rather pure grafted PE. In comparison, the fractions of sample gc115 seem to contain higher amounts of non-grafted LDPE as can be seen even in the 90 °C TREF fraction of gc115. Still, this fraction is also assigned to be mainly grafted PE. In all cases there is no or very little material eluting beyond a HPLC elution volume of 5.5 mL (dotted red line) indicating that these fractions do not contain non-grafted HDPE.

Conclusions

In the current work, the comprehensive multidimensional analysis of novel grafted polyethylenes (HDPE-g-LDPE) is presented. To elucidate the molecular heterogeneity in terms of branching and molar mass, these novel materials were characterized by advanced analytical techniques such as CRYSTAF, HPLC, SEC and NMR. The grafted polymers were compared to linear (HDPE) and branched (LDPE) reference materials. The bulk analysis revealed macromolecules with complex branch-

ing architectures, incorporating predominantly *n*-butyl short branches and long branches (C₆ and longer) distributed randomly across the polymer chains of variable molar masses. The large molar mass dispersities measured by SEC clearly highlight the complexity of these polymers. First indications for the presence of non-grafted LDPE and HDPE along with the graft polymer HDPE-g-LDPE were obtained.

For a more detailed study of the materials' heterogeneity, the samples were fractionated by preparative TREF to obtain fractions in mg to g amounts which were further analyzed regarding branching, molar mass and crystallinity. Different components including the non-grafted LDPE, HDPE and the grafted HDPE-g-LDPE were identified by crystallization-based (CRYSTAF, DSC), spectroscopic (¹³C-NMR) and chromatographic methods (SEC, HPLC, 2D-LC). The compositions of the different TREF fractions were estimated and fractions were identified that predominantly consist of HDPE-g-LDPE. It was found that sample gc100 had a significantly higher amount of true grafted polymer as compared to sample gc115.

The bulk samples and their corresponding TREF fractions were analyzed by 2D-LC (HPLC×SEC) to provide comprehensive two-dimensional pictures demonstrating the relationship between molar mass and branching. An alternative method starting with fractionating these materials by molar mass using preparative protocols to obtain homogenous molar mass fractions and then cross-fractionate these materials for branching analysis using online and offline techniques will be a matter of further reports.

Conflicts of interest

There are no conflicts to declare.

Acknowledgements

The authors would like to thank Elsa Malherbe and Dr. Jaco Brand, Central Analytical Facility (CAF) at Stellenbosch University for the NMR analyses. Special thanks go to the National Research Foundation of South Africa (NRF) for their financial support.

References

- 1 C. T. Love, G. Xian and V. M. Karbhari, *J. Appl. Polym. Sci.*, 2007, **104**, 331–338.
- 2 A. L. Andrady and M. A. Neal, *Philos. Trans. R. Soc., B*, 2009, **364**, 1977–1984.
- 3 M. J. Phiri, S. Cheruthazhekatt, A. Dimeska and H. Pasch, *J. Polym. Sci., Part A: Polym. Chem.*, 2015, **53**, 863–874.
- 4 Y. Inoue, T. Matsugi, N. Kashiwa and K. Matyjaszewski, *Macromolecules*, 2004, **37**, 3651–3658.
- 5 *High pressure process technology: fundamentals and applications*, ed. A. Bertucco and G. Vetter, Elsevier, Amsterdam, 1st edn, 2001.

CHAPTER 6

View Article Online

Polymer Chemistry

Paper

- 6 S. W. Ewart, T. W. Karjala and M. Demirors, *J. Polym. Sci., Part A: Polym. Chem.*, 2017, **55**, 861–866.
- 7 A. Ndiripo, *Comparative study on the molecular structure of ethylene/1-octane, ethylene/1-heptene and ethylene/1-pentene copolymers using advanced analytical methods*, Stellenbosch University, 2015.
- 8 T. Mori and N. Oi, Modified olefin copolymer, *US patent*, 7160950, 2007.
- 9 Y. Reyes and J. M. Asua, *Macromol. Rapid Commun.*, 2011, **32**, 63–67.
- 10 S. Podzimek, *Light scattering, size exclusion chromatography, and asymmetric flow field flow fractionation: powerful tools for the characterization of polymers, proteins, and nanoparticles*, Wiley, Hoboken, NJ, 2011.
- 11 W. W. Yau, *Polymer*, 2007, **48**, 2362–2370.
- 12 B. Monrabal, L. Romero, N. Mayo and J. Sancho-Tello, *Macromol. Symp.*, 2009, **282**, 14–24.
- 13 H. Pasch, M. I. Malik and T. Macko, in *Polymer Composites – Polyolefin Fractionation – Polymeric Peptidomimetics – Collagens*, ed. A. Abe, H.-H. Kausch, M. Möller and H. Pasch, Springer Berlin Heidelberg, Berlin, Heidelberg, 2012, vol. 251, pp. 77–140.
- 14 A. Prasad, *Polym. Eng. Sci.*, 1998, **38**, 1716–1728.
- 15 H. Pasch, *Polym. Adv. Technol.*, 2015, **26**, 771–784.
- 16 P. S. Eselem Bungu and H. Pasch, *Polym. Chem.*, 2017, **8**, 4565–4575.
- 17 P. S. Eselem Bungu and H. Pasch, *Polym. Chem.*, 2018, **9**, 1116–1131.
- 18 D. Cavallo, A. T. Lorenzo and A. J. Müller, *J. Polym. Sci., Part B: Polym. Phys.*, 2016, **54**, 2200–2209.
- 19 Y. Xue, S. Bo and X. Ji, *Chin. J. Polym. Sci.*, 2015, **33**, 1000–1008.
- 20 P. S. Eselem Bungu, K. Pflug and H. Pasch, *Polym. Chem.*, 2018, **9**, 3142–3157.
- 21 S. Cheruthazhekatt, T. F. J. Pijpers, V. B. F. Mathot and H. Pasch, *Macromol. Symp.*, 2013, **330**, 22–29.
- 22 A. Ndiripo, P. Eselem Bungu and H. Pasch, *Polym. Int.*, 2018, DOI: 10.1002/pi.5547.
- 23 T. Becker, *Erprobung eines Hochdruck-Hybrid-Verfahrens für Polymerisationen*, Masters Thesis, Technical University, Darmstadt, 2013.
- 24 C. Bauer, *Neue Verfahrensvarianten für die Hochdruck-Polyethylen-Synthese*, PhD Thesis, Technical University, Darmstadt, 2018.
- 25 M. Roth, *Neue Konzepte in der Hochdruck Polyethylensynthese*, PhD Thesis, Technical University Darmstadt, Darmstadt, 2010.
- 26 T. P. Karjala, S. W. Ewart, C. R. Eddy, A. E. Vigil, M. Demirors, S. Munjal and W. W. Yau, Process to Make Long Chain Branched (LCB), Block, or Interconnected Copolymers of Ethylene, *U.S. Patent and Trademark Office*, 8722817, 2014.
- 27 S. Ewart and K. Tom, *AIChE Annual Meeting*, Minneapolis, 2017.
- 28 W. W. Yau and D. Gillespie, *Polymer*, 2001, **42**, 8947–8958.
- 29 H. Pasch and M. I. Malik, *Advanced Separation Techniques for Polyolefins*, Springer International Publishing, Cham, 2014.
- 30 Y. Xue, S. Bo and X. Ji, *Chin. J. Polym. Res.*, 2015, **33**, 1000–1008.
- 31 P. Tackx and J. Tacx, *Polymer*, 1998, **39**, 3109–3113.
- 32 R. Brüll, H. Pasch, H. G. Raubenheimer, R. Sanderson, A. J. van Reenen and U. M. Wahner, *Macromol. Chem. Phys.*, 2001, **202**, 1281–1288.
- 33 B. Monrabal, L. Romero, N. Mayo and J. Sancho-Tello, *Macromol. Symp.*, 2009, **282**, 14–24.
- 34 Y. Xue, Y. Fan, S. Bo and X. Ji, *Chin. J. Polym. Sci.*, 2015, **33**, 508–522.
- 35 B. Monrabal, J. Sancho-Tello, N. Mayo and L. Romero, *Macromol. Symp.*, 2007, **257**, 71–79.
- 36 T. Macko, R. Brüll, R. G. Alamo, F. J. Stadler and S. Losio, *Anal. Bioanal. Chem.*, 2011, **399**, 1547–1556.
- 37 A. M. Striegel and M. R. Krejsa, *J. Polym. Sci., Part B: Polym. Phys.*, 2000, **38**, 3120–3135.
- 38 T. Usami and S. Takayama, *Macromolecules*, 1984, **17**, 1756–1761.
- 39 T. Usami and S. Takayama, *Polym. J.*, 1984, **16**, 731–738.
- 40 C. Gabriel, *Einfluss der molekularen Struktur auf das viskoelastische Verhalten von Polyethylenschmelzen*, Shaker, Aachen, 2001.
- 41 W.-J. Wang, S. Kharchenko, K. Migler and S. Zhu, *Polymer*, 2004, **45**, 6495–6505.
- 42 P. J. Flory, *Principles of polymer chemistry*, Cornell Univ. Press, Ithaca, NY, 19. print., 2006.
- 43 T. Macko, H. Pasch and J. F. Denayer, *J. Chromatogr. A*, 2003, **1002**, 55–62.
- 44 M. J. Phiri, S. Cheruthazhekatt, A. Dimeska and H. Pasch, *J. Polym. Sci., Part A: Polym. Chem.*, 2015, **53**, 863–874.
- 45 A. Ndiripo and H. Pasch, *Anal. Bioanal. Chem.*, 2015, **407**, 6493–6503.

CHAPTER 6

Electronic Supplementary Material (ESI) for Polymer Chemistry.
This journal is © The Royal Society of Chemistry 2018

Supporting Information

Comprehensive Analysis of Novel Grafted Polyethylenes Using Multidimensional Fractionation Methods

Paul S. Eselem Bungu^a, Kristina Pflug^b, Markus Busch^b and Harald Pasch^{*a}

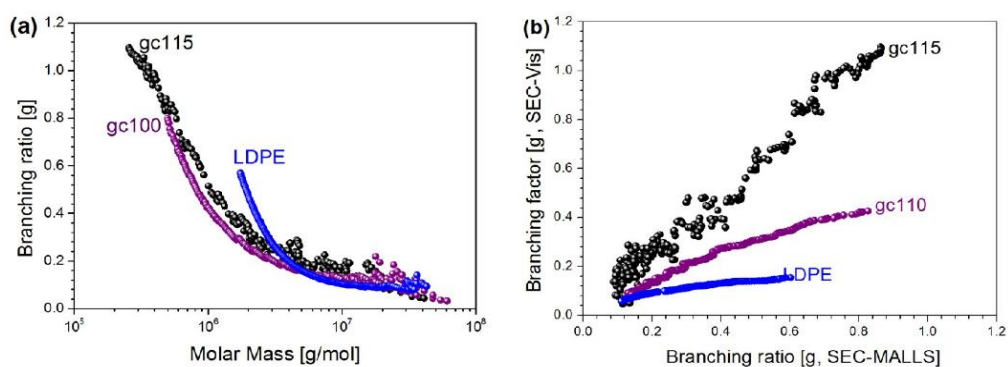


Figure S 1: plots showing showing in (a) the relationship between branching ratio (g) as a function of molar mass as determined by SEC-MALLS and (b) the relationship between g (calculated from) and g' (calculated from).

7 Concluding Remarks

Low density polyethylene (LDPE) is a branched polyolefin with a complex molecular structure that exhibits distributions in molar mass, short chain branching (SCB) and long chain branching (LCB). Several analytical techniques are in place for the characterization of polyolefins and related materials with regard to branching and molar mass. Until this day, however, no suitable technique exists, that is capable of addressing branching in LDPE, without the interference of molar mass effects. In the present study, selective fractionation and analysis techniques have been developed that address the distributions in molar mass and branching independent from each other and that enable the comprehensive microstructural analysis of LDPE.

In the first part of the study, a new approach to the comprehensive analysis of one of the most widely used material over the last 50 years-LDPE- is presented. Despite being a homopolymer, LDPE exhibits a complex molecular structure, combining molar mass distribution with short chain and long chain branching distributions. Bulk analysis on LDPE was conducted using established methods such as SEC-RI, CRYSTAF, DSC, HPLC and ^{13}C -NMR to provide molar mass and branching information. However, the correlation between these parameters could not be obtained using a single (one-dimensional) analytical approach. The only possible way of correlating molar mass with SCB and LCB information is through a multiple preparative fractionation protocol, which was described conceptually in this part of the study. It was demonstrated that selective preparative fractionations provide fractions with different molar masses and branching architectures. More specifically, preparative molar mass fractionation (pMMF) has shown to be rather insensitive to branching and can provide fractions with different molar masses but similar branching. Complementary, preparative temperature rising elution fractionation (pTREF) produces fractions with similar molar masses but different branching. These fractions were then analysed consecutively by a set of advanced analytical methods. By combining data obtained from the preparative fractionations with those of the analytical methods such as in pTREF/pMMF-SEC or pTREF/pMMF-CRYSTAF, two-dimensional diagrams that correlate branching and molar mass were constructed. By using this approach, the complex microstructure of branched polyethylene can be mapped and evaluated.

In the second part of the study, the applicability of the multiple preparative fractionation concept was investigated using three representative LDPE resins. Although being homopolymers, it was observed that the molecular structure of all resins was quite complex and they were displaying distinctively different molar mass and branching distributions. It was shown that the multiple fractionation concept is a powerful approach to generate sample libraries via pTREF and pMMF that constitute samples of

CONCLUDING REMARKS

comparable molar masses but different branching structures or alternatively have comparable branching but different molar masses. Cross-investigation of these library samples with advanced analytical techniques provided in-depth information on the molecular heterogeneity of preparative fractions (library samples) as compared to bulk sample analysis.

The sample library approach was exploited to investigate the effects of molar mass and branching on the microstructural properties independently. This was achieved by comparing the behaviour of selected fractions with similar branching but distinctively different molar masses using CRYSTAF, HPLC, DSC and SEC-Vis. In CRYSTAF, broad crystallization profiles and high amounts of soluble components were found for low molar mass fractions, while higher molar mass fractions displayed narrow crystallization profiles. These results proved a greater compositional heterogeneity for the lower molar mass components. In a similar way, results for fractions with varying branching contents but similar molar mass were obtained and it was found that all fractions displayed broad crystallization profiles.

In the third part of the study, multiple preparative fractionations were used in combination with thermal (DSC and SSA) and chromatographic (HPLC and 2D-LC) analysis techniques to address branching in LDPE. The dissolution/melting and crystallization behaviour in solution and in melt using SCALLS, DSC and SSA were compared to a reference linear PE. In order to relate this information to branching, a quantitative branching as a function of molar mass study was conducted using SEC-IR5 (methyl content distribution) and SEC-MALLS (for LCB distribution). Individual fractions generated by pTREF and pMMF were thermally fractionated using SSA and the crystal size distribution was correlated with the branching distribution. In addition, two-dimensional plots correlating the TREF fractionation temperature and the crystallization temperature (TREF-SSA), as well as molar mass and the crystallization temperature (MMF-SSA), were constructed for the first time. The TREF-SSA plot revealed co-elution of branched and higher molar mass components in the higher TREF temperature fractions. It was found that the results from thermal fractionation correlate well with those of the chromatographic analyses.

In the last part of the study, the multiple fractionation concept was used to investigate the molecular heterogeneity of novel grafted polymers that were produced by grafting LDPE onto a HDPE backbone. Bulk analysis of these materials displays a compositional heterogeneity in branching and molar mass. Following TREF fractionation, the amounts of non-grafted linear PE and grafted molecules were determined. ^{13}C NMR analysis of the fractions indicated that branching decreases with an increase in the TREF fractionation temperature. The cross-analysis of the TREF fractions with advanced analytical

CONCLUDING REMARKS

techniques for molecular structure and thermal properties linked molar mass, branching, crystallization and melting.

To conclude, in this research, it was demonstrated that the multiple fractionation concept is a powerful approach to generate sample libraries that may constitute materials of comparable molar masses and different branching structure or alternatively, comparable branching but different molar masses. Cross-analysis of the library samples with advanced analytical techniques provides in-depth information on the molecular heterogeneity of branched polyethylene. The present multidimensional approach can be adopted for other similarly complex polyolefin materials.